

Brane-Higgs-boson phenomenology in five-dimensional warped supersymmetryCharles Bouchart,¹ Alexander Knochel,² and Grégory Moreau¹¹*Laboratoire de Physique Théorique, CNRS and Université Paris-Sud 11, Bâtiment 210, F-91405 Orsay Cedex, France*²*Institut für Theoretische Physik, Universität Heidelberg, Philosophenweg 19, D-69120 Heidelberg, Germany*

(Received 11 June 2011; published 28 July 2011)

Constructing supersymmetric extensions of higher-dimensional models can have several motivations; it is, for instance, necessary in the context of string theories. Studying the supersymmetric version of the well-motivated model proposed by Randall and Sundrum, with the Higgs boson localized on the so-called TeV-brane, is not trivial since singularities appear in the Higgs couplings. Those are regularized by the contribution from the exchange of infinite towers of Kaluza-Klein (KK) scalar modes with Dirichlet-Dirichlet boundary conditions. Here we first derive the regularized four-dimensional (4D) effective Higgs couplings and induced sfermion mass matrices. A general method is provided for this regularization, based on the completeness relation. The sfermion masses must be obtained either from integrating out the mentioned KK towers or by treating their mixing effects, depending on the cases. We then use the obtained Higgs couplings and sfermion masses for some phenomenological applications. On one side, we show at the one-loop level how all quadratic divergences in the Higgs mass cancel out for any cutoff, due to 5D supersymmetry (SUSY) and to 5D anomaly cancellation; the analytical way followed here also allows a justification of the infinite KK summation required for the so-called KK regularization in 5D SUSY, which has motivated a rich literature. On the other side, we show that a certain pattern of SUSY breaking in the bulk would allow one to distinguish experimentally the minimal SUSY model à la Randall and Sundrum with bulk matter from the minimal 4D SUSY model, in the scenario where only superpartners were produced at the Large Hadron Collider. In this SUSY-breaking context, two of the discriminating tests developed make use of some different features arising in the squark or slepton mass spectrum. The other distinctive supersymmetric Randall-Sundrum feature is the possibly larger (even dominant) Higgs boson decay branching ratios into sleptons, compared to the 4D minimal supersymmetric standard model. In the same SUSY-breaking framework, techniques for pinning down the presence of soft SUSY-breaking terms on the TeV-brane are also suggested, based on the analysis of top squark pair production at the International Linear Collider.

DOI: [10.1103/PhysRevD.84.015016](https://doi.org/10.1103/PhysRevD.84.015016)

PACS numbers: 14.80.Rt, 12.60.Jv, 14.80.Da

I. INTRODUCTION

Among the possible theories underlying the standard model (SM) of particle physics, the supersymmetric scenarios and the higher-dimensional models have several deep motivations. In particular, supersymmetry stabilizes the electroweak symmetry-breaking (EWSB) scale with respect to radiative corrections, and, when it is promoted to a local symmetry, it provides a framework for the appearance of the graviton Lagrangian. On the other side, a warp extradimensional model has been proposed by Randall and Sundrum (RS) [1,2] to explain the huge hierarchy between the EWSB energy scale and the gravity scale, while some RS extensions [7] give rise to purely geometrical interpretations of the fermion structure in flavor space. Both supersymmetric and higher-dimensional scenarios can provide viable dark matter candidates (the lightest supersymmetric particle and the lightest Kaluza-Klein particle) and allow for gauge unification.

Since the physics beyond the SM is still unknown, one should consider the possibility of an effective low-energy hybrid theory with both supersymmetry (SUSY) and extra dimension(s). More specifically, SUSY and extra

dimensions could be crucial ingredients in a quantum description of gravity, as both indeed are in string theory. Moreover, D -branes of superstring theory provide a natural mechanism for the confinement of the SM fields in brane models and constitute thus another motivation for introducing SUSY in higher-dimensional scenarios. SUSY and extra dimensions could also be simultaneously involved in the origin of the electroweak symmetry breaking [8,9]. The higher-dimensional framework even provides new and attractive ways of breaking supersymmetry [10], due to a more structured geometry of space-time; SUSY may be broken either in the bulk (i.e., whole space) or on a brane, playing the role of the necessary hidden sector, and then the breaking mediated to the brane where the SM particles are living [11]. A different approach towards the SUSY breaking [12] is to use specific boundary conditions (BC) for different fields (in the same supermultiplet) propagating along compactified extra dimensions [14]. A famous example is the Scherk-Schwarz mechanism [15], which can be applied to the minimal supersymmetric SM (see, e.g., [16]) as well as to the Horava-Witten theory (see, e.g., [17]) [18]. Finally, the supersymmetrization of extradimensional theories allows one to have a realistic tension model

[19], to provide a new source for a tiny cosmological constant [20], to alternatively achieve gauge unification [21], and to address the so-called μ problem in SUSY (see the discussion below).

Hence, there exist several serious motivations for hybrid scenarios with both SUSY and (warped) extra dimensions. It was shown in Ref. [22] that an anti-de Sitter (AdS) space is compatible with SUSY. Later [23], the supermultiplet mass spectrum was derived in AdS_5 , and then the analysis extended to the case of a fifth dimension compactified on an orbifold [7]. In the context of 5D RS SUSY models, efforts have focused on the radius stabilization [24]. The RS SUSY scenario was initially studied with only gravity in the bulk [25] and finally with matter propagating in the bulk [7]. There exist various propositions of SUSY-breaking mechanisms in a warped geometry [26], several analyses of grand unified theory (GUT) theories within RS SUSY frameworks [27], and different studies about supergravity in a warped background [28]. Other works in the RS SUSY context can be found in Ref. [29], and there exist review chapters on 5D warped SUSY models [30]. Papers more oriented on the formalism of SUSY in AdS spaces are given in Ref. [31], and there are also complete lectures on this formalism [32]. One must also mention the attempts to elaborate superstring realizations of the RS model [33]. A related important result was the construction of warped throats from string compactifications with fluxes [34], which are equivalent to $\text{AdS}_5 \times X_5$ in an intermediate regime. Considerable progress was made towards stabilization of string compactifications based on flux compactifications with warped hierarchies [35,36].

In this paper, we will study these supersymmetrized RS scenarios with matter and gauge fields in the bulk. Our first contributions are theoretical; we will write explicitly the complete 5D Lagrangian for a Higgs scalar field confined on the TeV-brane—as required to explain the discrepancy between EWSB and gravity scales and as motivated by the $\text{SU}(2)_R$ breaking from bulk Yukawa interactions (forbidden trilinear chiral superfield couplings in $N = 2$ 4D SUSY [37])—and, when deriving the 4D effective action, we will take into account for the first time the mixing among the several Higgs bosons occurring in the minimal SUSY extensions.

In particular, the 4D effective Higgs couplings to two scalar fields (squarks, sleptons, and their Kaluza-Klein excitations), originating from the so-called D terms, are not trivial to derive due to the localized aspect of the Higgs boson and due to contributions to these effective couplings from the tree level exchange of Kaluza-Klein (KK) scalar modes of $(--)$ chiral superfields [38] (i.e., additional superfields with Dirichlet-Dirichlet boundary conditions which are characteristic of 5D theories). We derive these 4D couplings, which do not appear in the literature, and explain why this specific KK $(--)$ tower must be taken

into account without any cutoff (a non-natural task within a nonrenormalizable 5D theory).

The derivation of Yukawa couplings between Higgs bosons and two scalars in the 4D effective Lagrangian is also subtle: Singularities [Dirac peak functions taken at the origin, $\delta(0)$'s, due to the Higgs local aspect] appear in these couplings—after integrating out the auxiliary fields—but those are not the sign of an incomplete theory. Indeed, those singularities are cancelled out by the infinite sum of KK $(--)$ scalar contributions. A related kind of cancellation was pointed out for some loop calculations in the string theory framework [40] using either the expression of $\delta(0)$ in terms of a sum over the fifth component of the momentum [11] (see Ref. [41] for the warped background case) or a Gaussian brane distribution [42]; in contrast, here we demonstrate the cancellation generally for the tree level couplings, by using a simple method based on the completeness relation, by computing the Higgs couplings (including the Higgs-sfermion couplings and quartic Higgs interactions) in the flavor-motivated case of a warped extra dimension where only Higgs bosons are brane-localized [7]. In addition, in the present work we will derive the 4D effective scalar mass matrices induced, after EWSB, by the localized Higgs vacuum expectation values (VEV). In contrast with the above 4D couplings, these 4D masses computed at tree level do not depend on the energy scale and must be derived consistently either through the integration out of heavy KK $(--)$ scalar modes or through the scalar mixing with KK $(--)$ states, as we will show here. We will finally combine at first order these KK $(--)$ scalar effects on the 4D zero-mode scalar masses with the scalar mixing effects of KK $(++)$ states (having Neumann-Neumann boundary conditions). Such a combination should have been done in Ref. [43] (where effects of KK scalar modes with even \mathbb{Z}_2 parity [i.e., $(++)$ BC] are studied in a 5D SUSY context with brane-localized Yukawa interactions, but the above effects of KK scalars with an odd parity [$(--)$ BC] are considered neither in squark or slepton masses nor in Higgs couplings).

We will then use the new 4D effective Lagrangian, that we will have derived in the RS SUSY framework, for several phenomenological applications.

The first application is an explicit and complete diagrammatic computation of quantum corrections to the Higgs boson mass (δm_{Higgs}) at the one-loop level, including all kinds of KK contributions and each sector (Yukawa plus gauge couplings); we will show how the quadratically divergent parts can cancel each other due to 5D SUSY. This complete cancellation has not been shown before in warped SUSY models, and it constitutes here an additional check of the obtained 4D effective Higgs couplings. More generically, we will clarify the connections between the cancellations of these 5D quadratic divergences and of the 5D triangular anomalies. Our way of finding the quadratic divergence cancellation brings

some new light on the old debate about the validity of this cancellation in δm_{Higgs} within higher-dimensional SUSY models. In particular, the preliminary and complete calculation of 4D effective Higgs couplings allows a more clear overview of the subtle points and in turn allows one to address the “KK regularization” question and cutoff problems.

Our general results on the absence of quadratic divergences in δm_{Higgs} for 5D SUSY models [with a soft breaking] is important in the following sense: It seems to mean that hybrid scenarios—both higher-dimensional and supersymmetric—must not necessarily rely on a geometrical background reducing the gravity scale down to the TeV scale in order to protect the Higgs mass against its quantum corrections (i.e., to not reintroduce the gauge hierarchy problem). One can thus imagine a 5D SUSY scenario where the Higgs mass is protected only by SUSY (which allows one to avoid the remaining little hierarchy problem of pure 5D models solving the gauge hierarchy) or a 5D SUSY scenario where, in addition to SUSY protection, the discrepancy between the fundamental gravity and EWSB energy scales is explained by some geometrical feature like the warp factor: Those two possible classes of higher-dimensional SUSY theories avoid having two redundant solutions to the same Higgs mass instability problem (the fine-tuning problem).

The second application concerns the direct search at present and future high-energy colliders for the (necessary) physics standing beyond the SM; indeed, in the expected case where some signal for new physics would be discovered at the Large Hadron Collider (LHC) and then analyzed more precisely at the International Linear Collider (ILC), the primary phenomenological work would be to identify exactly the nature of the new physics detected. Based on the fact that today the two main types of new physics accessible at colliders are thought to be SUSY and the more recent paradigm of (warped) extra dimensions, three interesting possibilities might arise. The more optimistic is that both superpartners (squarks, gauginos, etc.) and KK excitations would be produced on-shell and observed, proving then the existence of a higher-dimensional SUSY scenario. Another possibility is that only real KK excitations would be produced; however, such a situation would represent a good indication for the existence of a higher-dimensional non-SUSY theory, as (in)direct constraints and gauge hierarchy considerations favor the mass regions around 10^2 GeV for superpartners and higher mass regions above $\mathcal{O}(1)$ TeV for first KK states (of the warped models). The last possibility—among the cases of signals for new physics as it is predicted today—is that only superpartners would be produced on-shell (and maybe some additional Higgs bosons characteristic of SUSY). Then an important and nontrivial question (see, e.g., the related Ref. [44]) would be as follows: Do the observed superpartners [either scalar

or spinorial] belong to a pure SUSY theory or a (warped) higher-dimensional SUSY model?

Generally speaking, it would be difficult to distinguish experimentally between superpartners belonging to 4D or 5D SUSY models. One can think, e.g., of the simple test to look at the precise measurement of cross sections for squark pair production at the ILC: The mixing of the squarks with KK excitations could lead to modifications of the production amplitude—predicted in pure SUSY. However, we will show that, for instance, in a given RS SUSY context (optimistic case with light “scustodians”), such modifications of the top squark production amplitude are typically too small to be observable. In contrast, in this RS context, we will show how the ILC could allow one to discriminate between two different geometrical configurations of SUSY breaking.

We will also demonstrate that in a specific case, with SUSY-breaking sfermion masses in the bulk, there exist distinctive signatures that could allow one to experimentally discriminate between superpartners originating from the 4D minimal supersymmetric SM (MSSM) and from the RS version of the MSSM (with bulk matter and gauge fields and brane-Higgs bosons) [45]. Note that these distinctive signatures could also reveal the existence of other classes of 4D SUSY models, different from the 4D MSSM, and would thus not constitute absolute proofs of the considered RS MSSM model. We briefly present those signatures in the following.

Within a minimal [46] supergravity (mSUGRA) framework, and in the case of SUSY-breaking sfermion masses in the RS bulk, the smuon mass splitting (measured at the ILC or even at the LHC) $m_{\tilde{\mu}_2} - m_{\tilde{\mu}_1}$ ($\tilde{\mu}_{1,2}$ are the two smuon eigenstates [47]) can be larger than in the 4D mSUGRA scenarios [48], allowing then a discrimination between those two types of scenarios. The reason is that in mSUGRA the off-diagonal elements of the 2×2 smuon mass matrix—partially responsible for the mixing and splitting—are proportional to the muon Yukawa coupling constant which is suppressed compared to the top quark one, while in some RS frameworks [7] the muon 5D Yukawa coupling is not suppressed relatively to the top one (the lightness of the muon originates from its wave function overlap with the Higgs boson). We will also show that the RS MSSM can lead to differences in the top squark mass correlations ($m_{\tilde{t}_2}$ versus $m_{\tilde{t}_1}$) with respect to the 4D MSSM case—differences which are here not restricted to the mSUGRA framework.

In addition, in the case of SUSY-breaking sfermion masses in the RS bulk, the Higgs boson couplings to sleptons can be significantly increased with respect to the 4D MSSM. Hence, in such warped scenarios, the decay channels of the heaviest neutral Higgs scalar (characteristic of SUSY and usually denoted as H) [49] into sleptons can have comparable or even larger branching ratios than the channels into (s)quarks and gauginos, leading to final states

at the LHC radically different from the 4D MSSM case. The produced H bosons could initiate slepton cascade decays more often than in the 4D MSSM and in turn give rise to an increase number of events with leptonic final states. We will illustrate this study by giving numerically all the H boson branching ratios as a function of the mass, for characteristic parameter sets, and the cases of the pseudoscalar and charged Higgs fields will be briefly discussed.

At this level, one should mention related works. In fact, within the hybrid higher-dimensional SUSY context, while the literature, e.g., on various SUSY-breaking mechanisms is rich, there exist many fewer papers on phenomenological aspects. We mention Ref. [43], where radiative corrections to scalar masses (excluding quadratically divergent parts) and to gauge and Yukawa couplings are calculated in order to (i) estimate the 5D MSSM upper limit on the lightest Higgs mass and (ii) constrain experimentally the universal scalar (m_0) and gaugino ($m_{1/2}$) masses. See Ref. [51] for another type of constraint on the Higgs mass in higher-dimensional SUSY models. In Ref. [52], based on 4D superfield actions, the evolution of neutrino masses and mixings and confrontation with oscillation data were studied within a flat 5D MSSM. See also Ref. [53] for considerations on the proton decay suppression in SUSY GUT with extra compact dimensions (Yukawa couplings localized or not) as well as Ref. [54] for phenomenology in SUSY gauge-Higgs unification scenarios, Ref. [55] for SUSY composite Higgs models, Ref. [56] for SUSY warped Higgsless models, and Ref. [57] for partly supersymmetric models.

The organization of the paper is as follows. In Sec. II, after a description of the higher-dimensional SUSY framework is considered, we derive the 4D effective couplings and mass matrices of sfermions and Higgs bosons, focusing on illustrative examples. In the first part of Sec. III (Sec. III A), the quadratic divergent contributions to the quantum corrections of the Higgs mass are calculated and the methods of calculation discussed. Up to this point, the results obtained are valid for any RS SUSY model—and can be easily generalized to any higher-dimensional SUSY scenario—with brane-Higgs bosons. In the three following subsections on collider phenomenology, a certain SUSY-breaking setup is chosen for the computations; in Sec. III B, characteristic effects of the RS version of the MSSM are quantified. Effects in the Higgs sector are studied in Sec. III C. Finally, in Sec. III D, we propose some tests, based on the top squark pair production at the ILC, for distinguishing two different geometrical SUSY-breaking configurations. We conclude in Sec. IV.

II. THEORY

A. The model

Field content.—In Appendix A, we give the full 5D field Lagrangian for a toy model with a U(1) gauge symmetry

applying on two chiral superfields Φ_L and Φ_L^c [together with the associated $(--)$ superfields] and two 4D Higgs superfields H_u^0 and H_d^0 localized on the TeV-brane within a warp background. With Appendix A as a starting point, we will give throughout the paper the 4D version of this Lagrangian related to the Higgs boson or, more precisely, the parts which are not trivial or direct to derive from the 4D point of view. For these studied parts, we will extend the 4D Lagrangian to the phenomenological minimal supersymmetric standard model (pMSSM) [58] field content and gauge symmetry.

Energy scales.—The RS framework is constituted by a 5D theory where the extra dimension is warped and compactified over a S^1/\mathbb{Z}_2 orbifold. The nonfactorizable metric is of type AdS, and the space-time, which is thus a slice of AdS₅, has two 4D boundaries: the ultraviolet (UV) boundary at the Planck scale and the infrared (IR) brane with an exponentially suppressed scale in the vicinity of the TeV scale. The Higgs boson has to be localized at this so-called TeV-brane if the EW scale is to be stabilized by such a geometrical structure. We consider the attractive RS version with all other fields propagating in the bulk [7]: This allows us to suppress higher-dimensional operators, potentially troublesome with respect to flavor-changing neutral current effects, by energy scales larger than the TeV scale. This feature has also the advantage to possibly generate the fermion mass hierarchy and flavor structure by a simple geometrical mechanism [7,59,60]. More precisely, the gravity scale on the Planck-brane is $M_{\text{Planck}} = 2.44 \times 10^{18}$ GeV, whereas the effective scale on the TeV-brane $M_\star = e^{-\sigma(\pi R_c)} M_{\text{Planck}}$ [with $\sigma(y) = k|y|$] is suppressed by the warp factor, which depends on the curvature radius $1/k$ of AdS₅ and the compactification radius R_c . For a product $kR_c \approx 11$, $M_\star = \mathcal{O}(1)$ TeV, allowing us to address the gauge hierarchy problem. We will take $kR_c \approx 10.11$ so that the maximum value of $M_{\text{KK}} \approx 2.45ke^{-\pi kR_c}$ [M_{KK} is the first KK photon mass], fixed by the theoretical consistency bound $k < 0.105M_{\text{Planck}}$, is ~ 10 TeV in agreement with the typical indirect limits from EW precision tests (see below). The beauty of the RS model is to possess a unique fundamental energy scale $k \sim R_c^{-1} \sim M_{\text{Planck}}$. Besides, the parameters denoted as c^ψ fix the 5D masses $m_\psi = c^\psi \partial_y \sigma$, affected to each fermion ψ , and thus control the field localizations in the bulk (and in turn the effective 4D masses). Those satisfy $|c^\psi| = \mathcal{O}(1)$ to avoid the introduction of new fundamental scales. The 5D masses for the scalar fields will be discussed throughout the paper.

μ problem.—A usual problem of the supersymmetric theories is to explain why the μ parameter is of the order of the EWSB scale (around the TeV), as imposed by the orders of magnitude of the masses involved in the minimization conditions for the Higgs potential. In RS SUSY, there is a simple way for generating a μ term at the EWSB scale as we discuss now [61]. If the Higgs superfields are confined on the TeV-brane (as motivated by the

gauge hierarchy problem), the gauge invariant μ term in the 5D superpotential W reads in terms of the 4D Higgs superfields as

$$[\mu H_u \cdot H_d] \delta(y - \pi R_c) \in W, \quad \text{with } H_u = \begin{pmatrix} H_u^+ \\ H_u^0 \end{pmatrix}, \quad (1)$$

$$H_d = \begin{pmatrix} H_d^0 \\ H_d^- \end{pmatrix}, \quad \text{and } H_u \cdot H_d = \epsilon_{ab} H_u^a H_d^b,$$

$H_{u,d}$ being $SU(2)_L$ doublets, a and b $SU(2)_L$ indices, and ϵ_{ab} the antisymmetric tensor defined by $\epsilon_{12} = 1$. In analogy with Eq. (A12) for the $U(1)$ model [equivalent to restricting the $SU(2)_L$ model to the neutral Higgs couplings], which leads to the expression of the μ terms written with the fields in Eq. (A28), the term (1) gives rise to the 4D mass terms for the neutral Higgs scalar fields in the potential (after field redefinition and inclusion of the warp metric factor):

$$|\mu_{\text{eff}}|^2 |\phi_{H_u^0}|^2 + |\mu_{\text{eff}}|^2 |\phi_{H_d^0}|^2 \in V_{4D},$$

$$\text{with } |\mu_{\text{eff}}|^2 = \int_{-\pi R_c}^{\pi R_c} dy |\mu|^2 e^{-2\sigma(y)} \delta(y - \pi R_c)$$

$$= |\mu e^{-\sigma(\pi R_c)}|^2,$$

so that the effective μ parameter reads as $\mu_{\text{eff}} = \mu e^{-k\pi R_c} \sim k e^{-k\pi R_c} \sim \text{TeV}$. Note the absence of $\delta(0)$ factors in V_{4D} (or, equivalently, of $[\delta(y - \pi R_c)]^2$ terms in the 5D Lagrangian) after integration over y . In this paper, we will consider this setup with brane-Higgs fields.

Custodial symmetry.—In pure SUSY with $\tan\beta = 1$ [64], if the custodial symmetry $O(3) \approx SU(2)_V$ —resulting after EWSB from the global symmetry $O(4) \approx SU(2)_L \times SU(2)_R$ —was exactly respected, it would protect the well-known relation on gauge boson masses $\rho = m_{W'}^2 / (m_Z^2 \cos^2 \theta_w) = 1$ against quantum corrections, as in the SM. Indeed, the two Higgs $SU(2)_L$ doublets of the pMSSM can form a $(\mathbf{2}, \mathbf{2})$ representation under the $SU(2)_L \times SU(2)_R$ symmetry [65]:

$$\mathcal{H} \equiv (H_d H_u) = \begin{pmatrix} H_d^0 & H_u^+ \\ H_d^- & H_u^0 \end{pmatrix}. \quad (2)$$

However, the custodial symmetry is broken in the gauge and Yukawa coupling sectors. Moreover, the deviations from $\tan\beta = 1$ and the presence of soft SUSY-breaking terms for squarks and sleptons represent new sources of custodial symmetry (spontaneous) breaking if those differ for the up-type and down-type [with respect to $SU(2)_L$] scalars. Nevertheless, the loop-level SUSY corrections to the precision EW observables (contributing to $\delta\rho$) can pass the constraints from precision measurements, even easily in the case of equal soft terms for up and down scalars [50,66].

Concerning the tree-level corrections to precision EW observables in warped models, the global fits of the experimental data are satisfactory for large KK

masses (reducing the KK mixing effects): $M_{\text{KK}} \gtrsim 10 \text{ TeV}$ [67].

In the present paper, where we study hybrid scenarios with both superpartners and KK excitations, we will take identical soft parameters for up and down scalars and KK masses just above $\sim 10 \text{ TeV}$. We will not explore the whole parameter space and work out the precise global EW fits, but this realistic choice guarantees that the theoretical respective, and in turn total, corrections to SM observables have acceptable orders of magnitude given the experimental accuracy on these observables. There are (*a priori*) higher-order corrections involving both superpartners and KK modes that we do not treat here.

Now one may wish to decrease the possible M_{KK} values in order to improve the situation with respect to considerations on the “little hierarchy” problem related to the Higgs mass. In order to reduce the acceptable minimal M_{KK} value from $\sim 10 \text{ TeV}$ down to $\sim 3 \text{ TeV}$, an attractive [68] possibility is to gauge the $SU(2)_L \times SU(2)_R \times U(1)_X$ symmetry in the bulk [69]. The SM gauge group is recovered after the breaking of the $SU(2)_R$ group into another $U(1)_R$, by boundary conditions.

The question arising here is whether it is possible to gauge the $SU(2)_L \times SU(2)_R$ symmetry within a SUSY context. First about the μ term: Can it be written in the case of a bulk gauge custodial symmetry? The question arises as $SU(2)_L \times SU(2)_R$ must remain unbroken on the Higgs brane in order to protect precision EW observables. A simple possibility is to write down the following $SU(2)_R$ invariant term of the superpotential giving rise to the usual μ term:

$$-\frac{1}{2} \mu \mathcal{H} \cdot \mathcal{H} \delta(y - \pi R_c)$$

$$= -\frac{1}{2} \mu (H_d \cdot H_u - H_u \cdot H_d) \delta(y - \pi R_c)$$

$$= \mu H_u \cdot H_d \delta(y - \pi R_c),$$

according to Eq. (1). Higgs couplings to matter invariant under $SU(2)_L \times SU(2)_R$ can also be written with the \mathcal{H} bidoublet giving rise, in particular, to the usual Yukawa couplings in the superpotential, as usual in warped models by promoting matter (superfield) multiplets to $SU(2)_R$ representations (see, e.g., [68,69]). Finally, the gauge interaction sector of a SUSY theory as well as the soft breaking terms can also respect an additional $SU(2)_R$ gauge symmetry. Hence, in this paper we will also consider the case of a bulk gauge $SU(2)_L \times SU(2)_R$ symmetry with $M_{\text{KK}} \sim 3 \text{ TeV}$ and equal soft terms for up and down scalars, another setup which leads to realistic EW fits to the data.

SUSY breaking.—We adopt the classification of the three types of SUSY-breaking framework where (i) the squark and slepton SUSY-breaking masses are induced at loop level by SUSY-breaking gaugino masses as in Ref. [7], (ii) there exist tree-level squark and slepton

masses [in the bulk and/or brane-localized] resulting directly from a 5D SUSY-breaking mechanism, and (iii) the squark and slepton masses are of the KK type like in the scenario à la Scherk-Schwarz with SUSY-breaking BC [15]. This classification is motivated, in particular, by the fact that the framework with scalar SUSY-breaking masses in the bulk leads to modifications of the wave functions and thus of the 4D effective couplings. Moreover, this framework gives rise to a hard breaking of SUSY (reintroducing quadratic divergences in the Higgs mass corrections), which is acceptable in the present warped background where the Higgs mass is still protected by the reduced gravity scale. Finally, this framework with bulk scalar SUSY-breaking masses has the attractive feature to generate scalar superpartner masses mainly through the Yukawa couplings like for SM fermions—as will be described in detail.

We will consider the second class of SUSY-breaking framework mentioned above, including the mSUGRA case where the SUSY-breaking terms are universal and the soft trilinear scalar couplings (the A couplings) are proportional to the Yukawa couplings. The first class is typically restricted to the kind of model described in Ref. [7] (with SUSY breaking on the TeV-brane), while the third class has a SUSY-breaking mechanism deeply related to BC. We will show that the second type of SUSY breaking allows one to develop tests for distinguishing between some pure SUSY and warped SUSY models at colliders.

B. 4D scalar couplings

In this section, we derive the 4D effective couplings of the brane-Higgs boson to two scalar superpartners (of type squark and slepton) in the RS SUSY framework, as well as the 4D Higgs self-couplings.

1. Scalar Yukawa couplings to two Higgs bosons

In this first subsection, we calculate the 4D Yukawa-type coupling of a scalar field (e.g., ϕ_R) to a Higgs boson (of $\phi_{H_u^0}$ type, as an illustrative example) within our simple U(1) model defined in Appendix A 1 corresponding the superfield action given in Appendix A 2.

The obtained scalar Yukawa couplings are included in the following term of Eq. (A26) in terms of the 5D fields:

$$\mathcal{L}_{5D} = -\sqrt{G}|\mathcal{Y}\delta(y - \pi R_c)\phi_{H_u^0}\phi_R - [\partial_y - (c_L + \frac{3}{2})(\partial_y\sigma)]\phi_L^c|^2. \quad (3)$$

By expanding over the KK decomposition (B11) and integrating over the fifth dimension, the first squared term gives rise to the 4D scalar Yukawa coupling (after field redefinition)

$$\begin{aligned} & \frac{\delta^4 \mathcal{L}_{4D}}{\delta\phi_{H_u^0}\bar{\phi}_{H_u^0}\phi_R^{(n)}\bar{\phi}_R^{(m)}} \\ &= -i|\mathcal{Y}|^2 \int_{-\pi R_c}^{\pi R_c} dy \delta^2(y - \pi R_c) \bar{f}_m^{++}(c_R; y) f_n^{++}(c_R; y) \\ &= -i|\mathcal{Y}|^2 \delta(0) \bar{f}_m^{++}(c_R; \pi R_c) f_n^{++}(c_R; \pi R_c), \end{aligned} \quad (4)$$

whose corresponding diagram is drawn in Fig. 1.

It turns out that the crossed products in Eq. (3) also bring a contribution to the 4D effective scalar Yukawa coupling, as we explain now; the crossed terms read as

$$\begin{aligned} & \sqrt{G}\delta(y - \pi R_c)[\mathcal{Y}\phi_{H_u^0}\phi_R[\partial_y - (c_L + \frac{3}{2})(\partial_y\sigma)]\bar{\phi}_L^c \\ &+ \bar{\mathcal{Y}}\bar{\phi}_{H_u^0}\bar{\phi}_R[\partial_y - (c_L + \frac{3}{2})(\partial_y\sigma)]\phi_L^c] \in \mathcal{L}_{5D}. \end{aligned} \quad (5)$$

Combining the KK decomposition (B12) of the 5D field ϕ_L^c together with the relation (B16), which originates from the equation of motion, leads to

$$\begin{aligned} & \left[\partial_y - \left(c_L + \frac{3}{2} \right) (\partial_y \sigma) \right] \phi_L^c(x^\mu, y) \\ &= \sum_{n=1}^{\infty} \phi_L^{c(n)}(x^\mu) \left[\partial_y - \left(c_L + \frac{3}{2} \right) (\partial_y \sigma) \right] f_n^{--}(c_L; y) \\ &= -e^\sigma \sum_{n=1}^{\infty} m_L^{(n)} \phi_L^{c(n)}(x^\mu) f_n^{++}(c_L; y), \end{aligned} \quad (6)$$

$m_L^{(n)}$ being the n th KK scalar mass. Using this relation in Eq. (5) and expanding ϕ_R over its KK tower gives the 4D couplings (taking into account field redefinitions):

$$\begin{aligned} & - \left[\mathcal{Y}\phi_{H_u^0} \sum_{m=0, n=1}^{\infty} m_L^{(n)} f_m^{++}(c_R; \pi R_c) \bar{f}_n^{++}(c_L; \pi R_c) \right. \\ & \times \phi_R^{(m)} \bar{\phi}_L^{c(n)} + \bar{\mathcal{Y}}\bar{\phi}_{H_u^0} \sum_{m=0, n=1}^{\infty} m_L^{(n)} \bar{f}_m^{++}(c_R; \pi R_c) \\ & \left. \times f_n^{++}(c_L; \pi R_c) \bar{\phi}_R^{(m)} \phi_L^{c(n)} \right] \in \mathcal{L}_{4D}. \end{aligned} \quad (7)$$

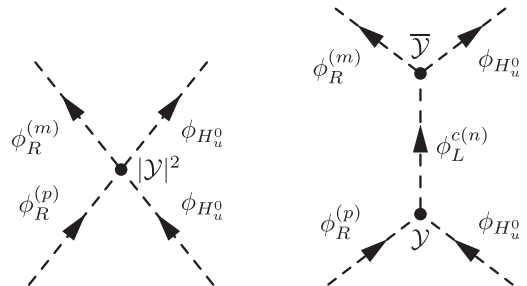


FIG. 1. Feynman diagrams of the contributions to the 4D effective scalar Yukawa coupling $\frac{\delta^4 \mathcal{L}_{4D}}{\delta\phi_{H_u^0}\bar{\phi}_{H_u^0}\phi_R^{(p)}\bar{\phi}_R^{(m)}}$. The second indirect contribution is induced by the exchange of the KK tower of (—) scalar superpartners $\phi_L^{c(n)}$. The relevant coupling constants are described in detail in the text.

These two types of 4D coupling to KK modes give rise to new contributions to scalar Yukawa couplings through the exchange of the KK tower states $\phi_L^{c(n)}$, as exhibits the second Feynman diagram of Fig. 1 [70]. The resulting new contributions to 4D scalar Yukawa couplings are given in the following, taking real wave functions:

$$\frac{\delta^4 i \mathcal{L}_{4D}}{\delta \phi_{H_u^0} \bar{\phi}_{H_u^0} \phi_R^{(p)} \bar{\phi}_R^{(m)}} \Big|_{\text{indirect}} = -|\mathcal{Y}|^2 \sum_{n \geq 1} \frac{i m_L^{(n)2}}{k^2 - m_L^{(n)2}} f_p^{++}(c_R; \pi R_c) f_m^{++}(c_R; \pi R_c) (f_n^{++}(c_L; \pi R_c))^2, \quad (8)$$

k^μ being the $\phi_L^{c(n)}$ four-momentum. These couplings can be rewritten as follows, according to the completeness relation of Eq. (B2) together with the 5D propagator definition [$G_5^f(k^2; y, y')$] from Appendix C:

$$\begin{aligned} \frac{\delta^4 i \mathcal{L}_{4D}}{\delta \phi_{H_u^0} \bar{\phi}_{H_u^0} \phi_R^{(p)} \bar{\phi}_R^{(m)}} \Big|_{\text{indirect}} &= -i |\mathcal{Y}|^2 \sum_{n \geq 0} \left\{ \frac{k^2}{k^2 - m_L^{(n)2}} - 1 \right\} f_p^{++}(c_R; \pi R_c) f_m^{++}(c_R; \pi R_c) (f_n^{++}(c_L; \pi R_c))^2 \\ &= -i |\mathcal{Y}|^2 f_p^{++}(c_R; \pi R_c) f_m^{++}(c_R; \pi R_c) k^2 G_5^{f^{++}(c_L)}(k^2; \pi R_c, \pi R_c) \\ &\quad + i |\mathcal{Y}|^2 \delta(0) f_p^{++}(c_R; \pi R_c) f_m^{++}(c_R; \pi R_c) \\ &= i |\mathcal{Y}|^2 f_p^{++}(c_R; \pi R_c) f_m^{++}(c_R; \pi R_c) [\delta(0) - k^2 G_5^{f^{++}(c_L)}(k^2; \pi R_c, \pi R_c)]. \end{aligned} \quad (9)$$

By summing the two contributions, from Eqs. (4) and (9), the divergent $\delta(0)$ terms cancel each other, and we obtain the 4D effective scalar Yukawa couplings:

$$\frac{\delta^4 i \mathcal{L}_{4D}}{\delta \phi_{H_u^0} \bar{\phi}_{H_u^0} \phi_R^{(p)} \bar{\phi}_R^{(m)}} \Big|_{\text{total}} = -i |\mathcal{Y}|^2 f_p^{++}(c_R; \pi R_c) f_m^{++}(c_R; \pi R_c) k^2 G_5^{f^{++}(c_L)}(k^2; \pi R_c, \pi R_c). \quad (10)$$

Hence, starting from couplings in a 5D SUSY theory, we have derived consistent 4D effective couplings. More precisely, at this level the Lagrangian of Eq. (10) given for any energy k^2 still describes a real 5D SUSY theory [the KK sum in $G_5^{f^{++}(c_L)}(k^2; \pi R_c, \pi R_c)$ is infinite], but its form is given from a 4D point of view (4D fields are used).

An interesting check of Eq. (10) is the following one. In the low-energy limit $k^2 \ll m_L^{(n)2}$ ($n \geq 1$), only the zero mode in the 5D propagator survives at *zeroth* order, so that the superpartner coupling above simplifies to [71]

$$\begin{aligned} \frac{\delta^4 i \mathcal{L}_{4D}}{\delta \phi_{H_u^0} \bar{\phi}_{H_u^0} \phi_R^{(0)} \bar{\phi}_R^{(0)}} \Big|_{\text{total}} &\rightarrow -i |\mathcal{Y}|^2 (f_0^{++}(c_R; \pi R_c) f_0^{++}(c_L; \pi R_c))^2 \\ &= -i |\mathcal{Y}_{4D}|^2, \end{aligned} \quad (11)$$

i.e., exactly the squared \mathcal{Y}_{4D} Yukawa coupling of associated fermion zero modes (with a brane Higgs) [68], as one expects in a pure 4D SUSY theory (where all KK states decouple).

2. D-term couplings to two Higgs bosons

Now, we derive the 4D couplings, issued from D terms, of scalar fields (continuing on the ϕ_R example) to the two $\phi_{H_u^0}$ bosons in the U(1) model of Appendixes A 1 and A 2.

The obtained D -term couplings of ϕ_R , in terms of 5D fields, are included in Eq. (A26):

$$\begin{aligned} \mathcal{L}_{5D} &= -\frac{\sqrt{G}}{2} [|\partial_y - 2(\partial_y \sigma)| \Sigma \\ &\quad - g(q_R \Delta_{\phi_R} + q_{H_u^0} \phi_{H_u^0} \bar{\phi}_{H_u^0} \delta(y - \pi R_c))]^2. \end{aligned} \quad (12)$$

The 4D effective D -term couplings are deduced from the above 5D Lagrangian (taking real gauge coupling constants):

$$\begin{aligned} \frac{\delta^4 i \mathcal{L}_{4D}}{\delta \phi_{H_u^0} \bar{\phi}_{H_u^0} \phi_R^{(n)} \bar{\phi}_R^{(m)}} &= -i q_{H_u^0} q_R |g|^2 \int_{-\pi R_c}^{\pi R_c} dy \delta(y - \pi R_c) \bar{f}_m^{++}(c_R; y) f_n^{++}(c_R; y) \\ &= -i q_{H_u^0} q_R |g|^2 \bar{f}_m^{++}(c_R; \pi R_c) f_n^{++}(c_R; \pi R_c). \end{aligned} \quad (13)$$

As for the Yukawa couplings, there are additional contributions to the 4D effective D -term couplings. Indeed, other couplings arising from Eq. (12) are

$$\begin{aligned} \sqrt{G} g (q_R \bar{\phi}_R \phi_R + q_{H_u^0} \bar{\phi}_{H_u^0} \phi_{H_u^0} \delta(y - \pi R_c)) \\ \times [|\partial_y - 2(\partial_y \sigma)| \Sigma + \text{H.c.}] \in \mathcal{L}_{5D}. \end{aligned} \quad (14)$$

The KK decomposition of the 5D field Σ in Eq. (B4) together with the relation (B7) allows us to write

$$\begin{aligned}
& [\partial_y - 2(\partial_y \sigma)] \Sigma(x^\mu, y) \\
&= \sum_{n=1}^{\infty} \Sigma^{(n)}(x^\mu) [\partial_y - 2(\partial_y \sigma)] g_n^{--}(y) \\
&= -e^{2\sigma} \sum_{n=1}^{\infty} M^{(n)} \Sigma^{(n)}(x^\mu) g_n^{++}(y), \quad (15)
\end{aligned}$$

$M^{(n)}$ being the n th KK gauge boson mass. Inserting this relation in Eq. (14) and expanding ϕ_R over its KK tower gives the 4D couplings for the redefined fields:

$$\begin{aligned}
& -q_R g \sum_{m,p=0;n=1}^{\infty} M^{(n)} \bar{\phi}_R^{(m)} \phi_R^{(p)} \Sigma^{(n)} \mathcal{F}_R^{mnp} \\
& -q_{H_u^0} g \bar{\phi}_{H_u^0} \phi_{H_u^0} \sum_{n=1}^{\infty} M^{(n)} \Sigma^{(n)} g_n^{++}(\pi R_c) + \text{H.c.} \in \mathcal{L}_{4D}, \quad (16)
\end{aligned}$$

with $\mathcal{F}_R^{mnp} = \int_{-\pi R_c}^{\pi R_c} dy \bar{f}_m^{++}(c_R; y) g_n^{++}(y) f_p^{++}(c_R; y)$. These 4D couplings induce new contributions to the D -term couplings via the exchange of the KK modes $\Sigma^{(n)}$, as shown in Fig. 2. These contributions read as

$$\begin{aligned}
& \left. \frac{\delta^4 i \mathcal{L}_{4D}}{\delta \phi_{H_u^0} \bar{\phi}_{H_u^0} \phi_R^{(p)} \bar{\phi}_R^{(m)}} \right|_{\text{indirect}} \\
&= -q_R q_{H_u^0} |g|^2 \sum_{n \geq 1} \frac{i}{k^2 - M^{(n)2}} M^{(n)2} \mathcal{F}_R^{mnp} g_n^{++}(\pi R_c), \quad (17)
\end{aligned}$$

k^μ being the $\Sigma^{(n)}$ four-momentum. Let us rewrite these couplings with the help of the completeness relation (B2) and 5D propagator:

$$\begin{aligned}
& \left. \frac{\delta^4 i \mathcal{L}_{4D}}{\delta \phi_{H_u^0} \bar{\phi}_{H_u^0} \phi_R^{(p)} \bar{\phi}_R^{(m)}} \right|_{\text{indirect}} = -i q_R q_{H_u^0} |g|^2 \sum_{n \geq 0} \left\{ \frac{k^2}{k^2 - M^{(n)2}} - 1 \right\} \mathcal{F}_R^{mnp} g_n^{++}(\pi R_c) \\
&= -i q_R q_{H_u^0} |g|^2 \int_{-\pi R_c}^{\pi R_c} dy \bar{f}_m^{++}(c_R; y) f_p^{++}(c_R; y) k^2 G_5^{g^{++}}(k^2; y, \pi R_c) \\
&\quad + i q_R q_{H_u^0} |g|^2 f_m^{++}(c_R; \pi R_c) f_p^{++}(c_R; \pi R_c). \quad (18)
\end{aligned}$$

Then, the complete 4D couplings are of course obtained by summing the two contributions (13) and (18):

$$\left. \frac{\delta^4 i \mathcal{L}_{4D}}{\delta \phi_{H_u^0} \bar{\phi}_{H_u^0} \phi_R^{(p)} \bar{\phi}_R^{(m)}} \right|_{\text{total}} = -i q_R q_{H_u^0} |g|^2 \int_{-\pi R_c}^{\pi R_c} dy \bar{f}_m^{++}(c_R; y) f_p^{++}(c_R; y) k^2 G_5^{g^{++}}(k^2; y, \pi R_c), \quad (19)$$

having taken into account the canceling terms. Once more, starting from couplings in a 5D SUSY theory, we have derived consistent 4D effective couplings; the Lagrangian (19) corresponds to a real 5D SUSY theory but written from the 4D point of view.

We finish this part by making the same check as in the previous subsection. In the low-energy limit $k^2 \ll M^{(n)2}$ ($n \geq 1$), only the zero mode in the 5D propagator survives

at zeroth order, so that the superpartner couplings (19) simplify to

$$\begin{aligned}
& \left. \frac{\delta^4 i \mathcal{L}_{4D}}{\delta \phi_{H_u^0} \bar{\phi}_{H_u^0} \phi_R^{(0)} \bar{\phi}_R^{(0)}} \right|_{\text{total}} \rightarrow -i q_R q_{H_u^0} \frac{|g|^2}{2\pi R_c} \\
&= -i q_R q_{H_u^0} |g_{4D}|^2, \quad (20)
\end{aligned}$$

since the gauge boson zero-mode profile encoded in $g_0^{++}(y) = 1/\sqrt{2\pi R_c}$ is flat along the fifth dimension. Thus the couplings in this limiting case correspond rigorously to the dimensionless $-i q_R q_{H_u^0} |g_{4D}|^2$ gauge coupling product of associated fermions, as expected in a pure 4D SUSY theory.

3. Comments on the obtained 4D couplings to Higgs bosons

It is interesting to note that, in order to obtain the 4D effective couplings to two Higgs bosons [Yukawa couplings and D terms] which are consistent [i.e., without the $\delta(0)$ divergences and recovering the 4D SUSY couplings in the limit $k^2 \ll m^{(n)2}, M^{(n)2}$], we had to use the completeness relation, which relies on an infinite sum over the KK levels. The reason is that these couplings belong to the 4D effective Lagrangian of a fundamental 5D SUSY theory—the infinite KK tower reflects this 5D aspect.

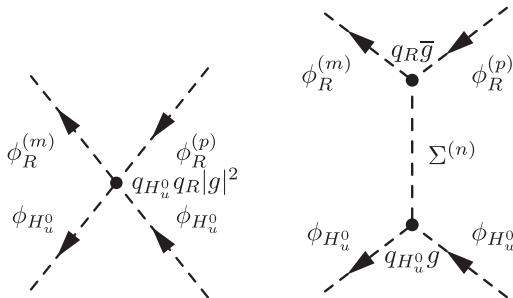


FIG. 2. Feynman diagrams of the contributions to the 4D effective scalar gauge coupling $\frac{\delta^4 \mathcal{L}_{4D}}{\delta \phi_{H_u^0} \bar{\phi}_{H_u^0} \phi_R^{(p)} \bar{\phi}_R^{(m)}}$. The second indirect contribution is induced by the exchange of the KK tower of (—) scalar modes $\Sigma^{(n)}$. The relevant coupling constants are described in detail in the text.

Besides, no truncating cutoff must be applied when implementing the completeness relation [for the sum not involving KK masses in Eqs. (9) and (18)]; otherwise, the consistent 4D effective couplings cannot be obtained, while there is no reason why a nonrenormalizable theory—as we are considering here—could not possess a 4D description. The reason for not applying a cutoff (due to the nonrenormalizable aspect of the 5D SUSY theory) is that in Eqs. (4)–(9) and (13)–(18) one is integrating the fifth dimension and summing *all* the exchanged heavy KK states to get an effective 4D vision of the 5D theory. Only once the 4D effective couplings are obtained so that the 4D description is completed, must the cutoff be put, e.g., in Eq. (10) [on $G_5^{f^{++}(c_L)}(k^2; \pi R_c, \pi R_c)$], to take into account the nonrenormalizable aspect of the 5D SUSY theory.

4. Final single couplings to the Higgs boson H

In this part, we deduce from the last three subsections the total 4D effective scalar couplings to the single Higgs boson H in the more realistic framework where the gauge symmetry group is as in the SM (EWSB has occurred) and the superfield content is extended to the pMSSM one. In particular, this framework is based on the coexistence of two complex Higgs $SU(2)_L$ doublets H_u and H_d of superfields with opposite hypercharges ($Y_{H_u} = -Y_{H_d} = +1$)

which guarantees the absence of chiral anomalies originating from triangular fermionic loops. The five scalar degrees of freedom, not absorbed in the longitudinal polarizations of the massive gauge bosons, constitute the five physical Higgs bosons: two CP -even neutral Higgs fields h (the lightest one) and H , one pseudoscalar A boson, and one pair of charged scalar particles H^\pm . We will give explicitly the H couplings in the RS SUSY framework, and similar couplings hold for the other Higgs fields. All Higgs bosons are assumed to be stuck on the TeV-brane.

We will focus on the top quark (t) superpartner couplings to H as an illustrative example, since the couplings of other scalar superpartners are analog. The n th KK level modes of the top squark fields are denoted as $\tilde{t}_L^{(n)}$ and $\tilde{t}_R^{(n)}$, respectively, for the superpartners of the left-handed (t_L) and right-handed (t_R) top quarks. $\tilde{t}_L^{(n)}$ and $\tilde{t}_R^{(n)}$ are similar to the 4D ($++$) scalar fields $\phi_L^{(n)}$ and $\phi_R^{(n)}$ defined in Eqs. (A3), (A6), and (B11) for the U(1) model, except of course with respect to the gauge quantum numbers. In the interaction basis $\{\tilde{t}_L^{(0)}, \tilde{t}_R^{(0)}, \tilde{t}_L^{(1)}, \tilde{t}_R^{(1)}\}$ (generalization to higher KK states is straightforward), the top squark-top squark couplings to a single H boson appearing after EWSB are encoded in the matrix [in our notations H denotes the scalar field]

$$\begin{aligned}
i\mathcal{C}_{H\tilde{t}\tilde{t}} \equiv & |\mathcal{Y}|^2 \sin\alpha v_u \times \begin{pmatrix} (f_L^0)^2 k^2 G_5^{f^{++}(c_{\tilde{t}_R})}(k^2; \pi R_c, \pi R_c) & 0 & f_L^0 f_L^1 (f_R^0)^2 & 0 \\ 0 & (f_R^0)^2 k^2 G_5^{f^{++}(c_{\tilde{t}_L})}(k^2; \pi R_c, \pi R_c) & 0 & f_R^0 f_R^1 (f_L^0)^2 \\ f_L^0 f_L^1 (f_R^0)^2 & 0 & (f_L^1 f_R^0)^2 & 0 \\ 0 & f_R^0 f_R^1 (f_L^0)^2 & 0 & (f_L^0 f_R^1)^2 \end{pmatrix} \\
& - \frac{\mathcal{Y} \cos\alpha \mu_{\text{eff}}}{\sqrt{2}} \begin{pmatrix} 0 & f_L^0 f_R^0 & 0 & f_L^0 f_R^1 \\ f_L^0 f_R^0 & 0 & f_L^1 f_R^0 & 0 \\ 0 & f_L^1 f_R^0 & 0 & f_L^1 f_R^1 \\ f_L^0 f_R^1 & 0 & f_L^1 f_R^1 & 0 \end{pmatrix} + g_Z^2 \pi R_c \cos(\alpha + \beta) v \\
& \times \begin{pmatrix} Q_Z^{t_L} \int dy f_L^0(y)^2 k^2 G_5^{g^{++}}(k^2; y, \pi R_c) & 0 & 0 & 0 \\ 0 & -Q_Z^{t_R} \int dy f_R^0(y)^2 k^2 G_5^{g^{++}}(k^2; y, \pi R_c) & 0 & 0 \\ 0 & 0 & Q_Z^{t_L}/2\pi R_c & 0 \\ 0 & 0 & 0 & -Q_Z^{t_R}/2\pi R_c \end{pmatrix} \\
& + \frac{A e^{-k\pi R_c} \sin\alpha}{\sqrt{2}} \begin{pmatrix} 0 & f_L^0 f_R^0 & 0 & f_L^0 f_R^1 \\ f_L^0 f_R^0 & 0 & f_L^1 f_R^0 & 0 \\ 0 & f_L^1 f_R^0 & 0 & f_L^1 f_R^1 \\ f_L^0 f_R^1 & 0 & f_L^1 f_R^1 & 0 \end{pmatrix}, \tag{21}
\end{aligned}$$

where we have used the compact notation, e.g., $f_{L/R}^n = f_n^{++}(c_{\tilde{t}_{L/R}}; \pi R_c)$. Besides, based on the 5D superpotential of Eq. (A12) and on the deduced field Lagrangian in Eq. (A28), the 4D effective μ parameter appearing above reads as (after field redefinition and inclusion of the metric warp factor)

$$\mu_{\text{eff}} = \mu e^{-k\pi R_c} \sim k e^{-k\pi R_c} \sim \text{TeV}. \tag{22}$$

No $\delta(0)$ factors appear after integration over y . The soft trilinear scalar coupling constant in Eq. (21) is taken at $A \sim 1$ to avoid the introduction of a new scale in the bulk. This 4D effective coupling matrix is deduced from Eq. (10) for the Yukawa couplings and from Eq. (19) for the D -term couplings [where the effects of the $(--)$ KK towers of $\phi_{L/R}^c$ and Σ type fields, as defined in Eqs. (A5)–(A7) and (A9), have been taken into account]. This coupling matrix, that will be taken at the energy $k^2 = m_H^2$ (for the Z coupling constant $g_Z = g_{4D}/\cos\theta_W$ and top charges to the Z gauge boson: $Q_Z^{L/R} = I_{3L/R}^L - Q_{e.m.}^L \sin^2\theta_W$), can be easily generalized, e.g., to sbottoms.

Let us comment more precisely on the 5D effects. The Higgs mixing between $\phi_{H_d^0}$ and $\phi_{H_u^0}$ into the mass eigenstates h and H is parametrized by the mixing angle denoted here, as usual, as α [66]. $\sin\alpha$, which enters the above coupling matrix, receives some corrections in the present 5D framework, as the $|\phi_{H_u^0}|^2|\phi_{H_d^0}|^2$ and $|\phi_{H_{u,d}^0}|^4$ couplings do so (see the next subsection). Moreover, the top squark-top squark-Higgs couplings are affected by the mixing between the top squarks and their KK $(++)$ excitations. The $H\tilde{t}_i\tilde{t}_j$ couplings, where \tilde{t}_i [$i = 1, \dots, 4$] are the top squark mass eigenstates, are obtained after transformation from the basis $\{\tilde{t}_L^{(0)}, \tilde{t}_R^{(0)}, \tilde{t}_L^{(1)}, \tilde{t}_R^{(1)}\}$ to the top squark mass basis (rotation matrices being obtained from diagonalizing the top squark mass matrix given later).

The third effect is the exchange of KK $(--)$ modes, encoded in the 5D propagators G_5 appearing in the matrix (21). Such KK $(--)$ contributions to couplings between H and KK top squarks would represent higher-order corrections to the $H\tilde{t}_{L/R}^{(0)}\tilde{t}_{L/R}^{(0)}$ couplings and are thus not written in matrix (21).

All these heavy KK mixing and KK exchange effects will not be computed numerically as they are subleading compared to other direct 5D effects in the structure of zero-mode $H\tilde{f}_{L/R}^{(0)}\tilde{f}_{L/R}^{(0)}$ couplings ($\tilde{f} \equiv$ sfermion), that will be studied in detail in Sec. III C.

5. Self-couplings of the Higgs boson

Finally, we derive the nontrivial 4D quartic couplings, e.g., of the Higgs boson $\phi_{H_u^0}$, still within the context of the toy model defined in Appendix A. A totally similar study could be made for the $\phi_{H_u^0}\bar{\phi}_{H_u^0}\phi_{H_d^0}\bar{\phi}_{H_d^0}$ couplings (without a combinatorial factor nor the additional $\Sigma^{(n)}$ exchange in the t channel discussed below).

As above, we start from the 5D couplings included in Eq. (A26):

$$\mathcal{L}_{5D} = -\frac{\sqrt{G}}{2} [|\partial_y - 2(\partial_y\sigma)]\Sigma - g(q_{H_u^0}\phi_{H_u^0}\bar{\phi}_{H_u^0}\delta(y - \pi R_c))^2. \quad (23)$$

The 4D quartic couplings directly deduced from this Lagrangian are

$$\frac{\delta^4 i \mathcal{L}_{4D}}{\delta\phi_{H_u^0}^2\bar{\phi}_{H_u^0}^2} = -\frac{i}{2} q_{H_u^0}^2 |g|^2 \delta(0) \times 4. \quad (24)$$

We have included the combinatorial factor 4 as we consider a process rather than a coupling here since Eq. (24) will be combined with other contributions.

Indeed, here again, there exist additional contributions to the 4D couplings as Eq. (23) also induces the $\phi_{H_u^0}$ couplings of Eq. (14) and in turn of Eq. (16). These later 4D couplings induce the two following new contributions to the quartic terms, via two possible exchanges of the KK $\Sigma^{(n)}$ [see Fig. 3]:

$$\begin{aligned} & \frac{\delta^4 i \mathcal{L}_{4D}}{\delta\phi_{H_u^0}^2\bar{\phi}_{H_u^0}^2} \Big|_{\text{indirect}} \\ &= -q_{H_u^0}^2 |g|^2 \sum_{n \geq 1} \frac{i}{k^2 - M^{(n)2}} M^{(n)2} (g_n^{++}(\pi R_c))^2 \\ & - q_{H_u^0}^2 |g|^2 \sum_{m \geq 1} \frac{i}{q^2 - M^{(m)2}} M^{(m)2} (g_m^{++}(\pi R_c))^2, \quad (25) \end{aligned}$$

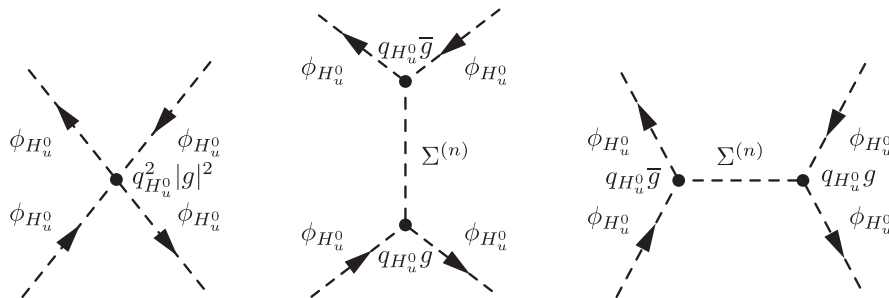


FIG. 3. Feynman diagrams of the contributions to the 4D effective self-scalar gauge coupling $\frac{\delta^4 \mathcal{L}_{4D}}{\delta\phi_{H_u^0}^2\bar{\phi}_{H_u^0}^2}$. The second and third indirect contributions are induced by the exchanges of the KK tower of $(--)$ scalar modes $\Sigma^{(n)}$ in the s channel and t channel, respectively (the choice of calling “ s -channel” or “ t -channel” a given diagram depends on which final state is considered). The relevant coupling constants are described in detail in the text.

k^μ being the $\Sigma^{(n)}$ four-momentum in the s channel, while q^μ represents the $\Sigma^{(n)}$ momentum in the t channel. Rewriting these couplings with the completeness relation in mind gives

$$\begin{aligned} \left. \frac{\delta^4 i \mathcal{L}_{4D}}{\delta \phi_{H_u^0}^2 \bar{\phi}_{H_u^0}^2} \right|_{\text{indirect}} &= -i q_{H_u^0}^2 |g|^2 \sum_{n \geq 0} \left\{ \frac{k^2}{k^2 - M^{(n)2}} - 1 \right\} (g_n^{++}(\pi R_c))^2 - i q_{H_u^0}^2 |g|^2 \sum_{m \geq 0} \left\{ \frac{q^2}{q^2 - M^{(m)2}} - 1 \right\} (g_m^{++}(\pi R_c))^2 \\ &= i q_{H_u^0}^2 |g|^2 [2\delta(0) - k^2 G_5^{g^{++}}(k^2; \pi R_c, \pi R_c) - q^2 G_5^{g^{++}}(q^2; \pi R_c, \pi R_c)]. \end{aligned} \quad (26)$$

Adding the contributions (24) and (26) gives the complete 4D quartic terms:

$$\begin{aligned} \left. \frac{\delta^4 i \mathcal{L}_{4D}}{\delta \phi_{H_u^0}^2 \bar{\phi}_{H_u^0}^2} \right|_{\text{total}} &= -i q_{H_u^0}^2 |g|^2 k^2 G_5^{g^{++}}(k^2; \pi R_c, \pi R_c) \\ &\quad - i q_{H_u^0}^2 |g|^2 q^2 G_5^{g^{++}}(q^2; \pi R_c, \pi R_c). \end{aligned} \quad (27)$$

Note the cancellation of $\delta(0)$ terms which leads to consistent 4D effective couplings.

In the check of the low-energy limit $k^2, q^2 \ll M^{(n)2}$ [$n \neq 0$], the Higgs coupling (27) is reduced to the following form (the combinatorial factor 4 is taken off to get the pure quartic Lagrangian coupling):

$$\left. \frac{\delta^4 i \mathcal{L}_{4D}}{\delta \phi_{H_u^0}^2 \bar{\phi}_{H_u^0}^2} \right|_{\text{total}} \rightarrow -\frac{i}{2} q_{H_u^0}^2 \frac{|g|^2}{2\pi R_c} = -\frac{i}{2} q_{H_u^0}^2 |g_{4D}|^2, \quad (28)$$

recalling that $g_0^{++}(y) = 1/\sqrt{2\pi R_c}$. The quartic Higgs coupling in this limit corresponds thus well to the exact squared gauge coupling expected in a pure 4D SUSY theory.

For completeness (and it will prove to be useful for the following), we give the result for the $\phi_{H_u^0} \bar{\phi}_{H_u^0} \phi_{H_d^0} \bar{\phi}_{H_d^0}$ coupling, obtained through the same method:

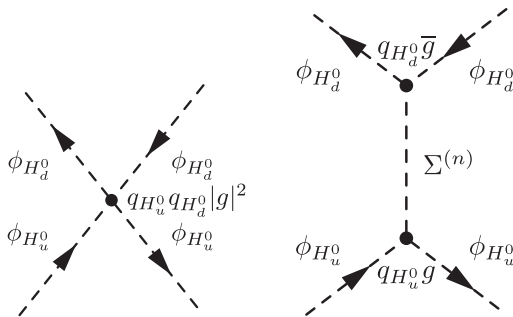


FIG. 4. Feynman diagrams of the contributions to the 4D effective scalar gauge coupling $\frac{\delta^4 i \mathcal{L}_{4D}}{\delta \phi_{H_u^0}^2 \bar{\phi}_{H_u^0}^2 \phi_{H_d^0}^2 \bar{\phi}_{H_d^0}^2}$. The second indirect contribution is induced by the exchange of the KK tower of $(-)$ scalar modes $\Sigma^{(n)}$.

$$\begin{aligned} \left. \frac{\delta^4 i \mathcal{L}_{4D}}{\delta \phi_{H_u^0} \bar{\phi}_{H_u^0} \phi_{H_d^0} \bar{\phi}_{H_d^0}} \right|_{\text{total}} &= -i q_{H_u^0} q_{H_d^0} |g|^2 k^2 G_5^{g^{++}}(k^2; \pi R_c, \pi R_c). \end{aligned} \quad (29)$$

This coupling is obtained from the two contributions drawn in Fig. 4.

C. Scalar mass matrix

We now calculate the 4D effective mass matrix for sfermions induced by brane-Higgs bosons within RS SUSY. One must develop different methods than in the above approach of 4D Higgs couplings.

1. Effect of the ϕ^c KK tower on $\phi^{(0)}$ masses through mixing

In this subsection, we derive the 4D masses coming from Yukawa interactions for the ϕ_R scalar field [the same analysis can be done for ϕ_L] in the toy model of Appendixes A 1 and A 2, assuming that the $\phi_{H_u^0}$ boson acquires a VEV $v_u = \sqrt{2} \langle \phi_{H_u^0} \rangle \sim 10^2$ GeV.

In addition to the $\bar{\phi}_R^{(0)} \phi_R^{(0)}$ mass, proportional to $(\mathcal{Y} v_u)^2$, which is obtained directly from the Lagrangian (A26), the exchanges of the KK modes $\phi_L^{c(n)}$ also contribute to this mass, as Fig. 1 illustrates in the case where $\phi_{H_u^0}$ acquires a VEV. In order to compute the whole zero-mode mass, one needs to estimate the mixing between $\phi_R^{(0)}$ and $\phi_L^{c(n)}$, a mixing induced by the VEV at the origin of the additional contributions as Fig. 1 shows— analogously to the mixing with the heavy Majorana neutrino in the type I seesaw model [72]. For that purpose, we write down the complete 4D mass matrix in the infinite basis $\vec{\phi} = (\phi_R^{(0)}, \phi_L^{c(1)}, \phi_L^{c(2)}, \dots)$ and search for the smallest eigenvalue. Indeed, the lightest eigenstate is typically mainly composed by the $\phi_R^{(0)}$ state, given usually the realistic KK $\phi_L^{c(n)}$ masses which are around a few TeV at least and hence much larger than the VEV-induced $\phi_R^{(0)}$ mass. From Lagrangian (A26), this 4D mass matrix reads as $-\vec{\phi} \mathcal{M}_{RR}^2 \vec{\phi}^t \in \mathcal{L}_{4D}$ with [73]

$$\mathcal{M}_{RR}^2 = \begin{pmatrix} \mathcal{Y}^2 \hat{v}_u^2 \int dy \delta^2 f_R^0(y)^2 & \mathcal{Y} \hat{v}_u m_L^{(1)} \int dy' \delta f_R^0(y') f_L^1(y') & \mathcal{Y} \hat{v}_u m_L^{(2)} \int dy' \delta f_R^0(y') f_L^2(y') & \dots \\ \mathcal{Y} \hat{v}_u m_L^{(1)} \int dy' \delta f_R^0(y') f_L^1(y') & m_L^{(1)2} & 0 & \dots \\ \mathcal{Y} \hat{v}_u m_L^{(2)} \int dy' \delta f_R^0(y') f_L^2(y') & 0 & m_L^{(2)2} & \dots \\ \vdots & \vdots & \vdots & \ddots \end{pmatrix}, \quad (30)$$

where we have used again the compact notation $f_{L/R}^n(y) = f_n^{++}(c_{L/R}; y)$, $f_{L/R}^n(y) = f_n^{--}(c_{L/R}; y)$, and $\hat{v}_u = v_u/\sqrt{2}$, $\delta = \delta(y - \pi R_c)$. For writing the off-diagonal elements, we have made use of relation (B16), which can be written in a compact form as $D_5^L f_L^n(y) = -m_L^{(n)} e^\sigma f_L^n(y)$, and then have redefined the scalar wave functions with e^σ factors as usual in RS. The generalized characteristic equation, of which the (squared mass) eigenvalues m^2 are solutions, reads as

$$\left(\mathcal{Y}^2 \hat{v}_u^2 \int dy \delta^2 f_R^0(y)^2 - m^2 - \sum_{n=1}^{\infty} \frac{[\mathcal{Y} \hat{v}_u m_L^{(n)} \int dy' \delta f_R^0(y') f_L^n(y')]^2}{m_L^{(n)2} - m^2} \right) \prod_{n=1}^{\infty} (m_L^{(n)2} - m^2) = 0. \quad (31)$$

As $m^2 = m_L^{(n)2}$ leads to divergences in the above equality, those are not solutions. Hence, Eq. (31) simplifies to

$$\mathcal{Y}^2 \hat{v}_u^2 \int dy \delta^2 f_R^0(y)^2 - m^2 + \sum_{n=1}^{\infty} \frac{[\mathcal{Y} \hat{v}_u m_L^{(n)} \int dy' \delta f_R^0(y') f_L^n(y')]^2}{m^2 - m_L^{(n)2}} = 0. \quad (32)$$

Using here also the equality $m_L^{(n)2}/(m^2 - m_L^{(n)2}) = -1 + m^2/(m^2 - m_L^{(n)2})$ together with the completeness relation applied as $\sum_{n=0}^{\infty} f_L^n(y) f_L^n(y') = \delta(y - y')$, one can rewrite

$$\begin{aligned} & \mathcal{Y}^2 \hat{v}_u^2 \delta(0) f_R^0(\pi R_c)^2 - m^2 - \mathcal{Y}^2 \hat{v}_u^2 f_R^0(\pi R_c)^2 \delta(0) + \mathcal{Y}^2 \hat{v}_u^2 m^2 f_R^0(\pi R_c)^2 G_5^{f^{++}(c_L)}(m^2; \pi R_c, \pi R_c) \\ & = 0 m^2 (1 - \mathcal{Y}^2 \hat{v}_u^2 f_R^0(\pi R_c)^2 G_5^{f^{++}(c_L)}(m^2; \pi R_c, \pi R_c)) = 0. \end{aligned} \quad (33)$$

Since $m^2 = 0$ is not a physically acceptable solution,

$$m^2 = \frac{f_L^0(\pi R_c)^2}{\frac{1}{\mathcal{Y}^2 \hat{v}_u^2 f_R^0(\pi R_c)^2} - \sum_{n=1}^{\infty} \frac{f_L^n(\pi R_c)^2}{m^2 - m_L^{(n)2}}}. \quad (34)$$

The check at this level is that, in the decoupling limit $m_L^{(n)} \rightarrow \infty$ for any $n \geq 1$, we recover the equality between the Yukawa mass for (zero-mode) fermions and their scalar superpartner, as expected in a 4D SUSY theory:

$$m^2 \rightarrow \mathcal{Y}^2 \hat{v}_u^2 f_R^0(\pi R_c)^2 f_L^0(\pi R_c)^2 = \mathcal{Y}_{4D}^2 \hat{v}_u^2 = m_{\text{fermion}}^2. \quad (35)$$

The divergence cancellation in Eq. (33) and this 4D SUSY limiting case confirm that our solution for the smallest eigenvalue will be consistent. This consistency is due to the infinite aspect of the $\phi_L^{c(n)}$ basis considered here, in analogy to the calculation of Yukawa couplings in Sec. II B. Now in the case (of realistic scenarios) where the eigenvalue of the lightest eigenstate m_{lightest}^2 is much smaller than $m_L^{(1)2}$, one obtains at leading order from Eq. (34)

$$m_{\text{lightest}}^2 \simeq \frac{f_L^0(\pi R_c)^2}{\frac{1}{\mathcal{Y}^2 \hat{v}_u^2 f_R^0(\pi R_c)^2} + \sum_{n=1}^{\infty} \frac{f_L^n(\pi R_c)^2}{m_L^{(n)2}}}. \quad (36)$$

An eigenvalue m^2 much smaller than $m_L^{(1)2}$ can only be the smallest one since all the others are larger than $m_L^{(1)2}$. As a matter of fact, at leading order in $f_L^0(\pi R_c)^2/f_L^n(\pi R_c)^2$ for $n \geq 1$, Eq. (34) can be rewritten as

$$m^2 \left(-\frac{1}{\mathcal{Y}^2 \hat{v}_u^2 f_R^0(\pi R_c)^2} + \sum_{n=1}^{\infty} \frac{f_L^n(\pi R_c)^2}{m^2 - m_L^{(n)2}} \right) \simeq 0. \quad (37)$$

Here the solution $m^2 \simeq 0$, at leading order in $f_L^0(\pi R_c)^2/f_L^n(\pi R_c)^2$, corresponds to the lightest solution (36). Concentrating on the other solutions, those satisfy

$$1 = \mathcal{Y}^2 \hat{v}_u^2 f_R^0(\pi R_c)^2 \sum_{n=1}^{\infty} \frac{f_L^n(\pi R_c)^2}{m^2 - m_L^{(n)2}}. \quad (38)$$

For this sum to be equal to unity, at least one of the terms must be positive, that is to say that $m^2 - m_L^{(n)2} > 0$ for at least one value of $n \geq 1$. Even if it occurs for $n = 1$, one would obtain that $m^2 > m_L^{(1)2}$, which means that all the solutions m^2 of Eq. (38) have to be larger than $m_L^{(1)2}$ at least. The above method was inspired from a higher-dimensional analysis performed in Ref. [74].

2. Effect of the Σ KK tower on $\phi^{(0)}$ masses through integration out

Let us calculate the 4D zero-mode masses due to SUSY D terms for ϕ_L (to vary our examples), still in the context of Appendix A. There exist contributions from the exchange of the KK modes $\Sigma^{(n)}$ if $\phi_{H_u^0}$ acquires a VEV, as is illustrated in Fig. 2 by replacing ϕ_R by ϕ_L . Such contributions to the $\bar{\phi}_L^{(0)} \phi_L^{(0)}$ mass are not arising from a mixing between $\phi_L^{(0)}$ and some KK excitations (as happens in the previous subsection for Yukawa terms). These low-energy contributions must instead be calculated by

integrating out the $\Sigma^{(n)}$ fields, exactly like the heavy triplet scalar is integrated out within the type II seesaw scenario [72]. Hence we derive here the complete $|\phi_{H_u^0}|^2 \bar{\phi}_L^{(i)} \phi_L^{(j)}$ couplings induced by integrating out all the $\Sigma^{(n)}$ modes, which contribute to the $\bar{\phi}_L^{(0)} \phi_L^{(0)}$ mass after $\phi_{H_u^0}$ gets its VEV.

As we are going to concentrate on the explicit derivation of the various contributions to the $|\phi_{H_u^0}|^2 \bar{\phi}_L^{(i)} \phi_L^{(j)}$ couplings, we will consider a Lagrangian part depending only on the fields $\phi_{H_u^0}$, ϕ_L , and Σ . This Lagrangian is obtained from Eqs. (A28) and (A30) in terms of the 5D fields:

$$\begin{aligned} \mathcal{L}_{4D}^{D\text{terms}} = & \frac{1}{2} \sum_{n=1}^{\infty} |\partial_\mu \Sigma^{(n)}|^2 - \frac{1}{2} \sum_{n=1}^{\infty} M^{(n)2} \Sigma^{(n)2} - q_L g \sum_{i,j=0}^{\infty} \sum_{n=1}^{\infty} \mathcal{T}_L^{ijn} M^{(n)} \Sigma^{(n)} \bar{\phi}_L^{(i)} \phi_L^{(j)} - q_{H_u^0} g \sum_{n=1}^{\infty} g_n^{++} (\pi R_c) M^{(n)} \Sigma^{(n)} \bar{\phi}_{H_u^0} \phi_{H_u^0} \\ & - q_L q_{H_u^0} g^2 \sum_{i,j=0}^{\infty} \bar{\phi}_L^{(i)} \phi_L^{(j)} f_i^{++}(c_L; \pi R_c) f_j^{++}(c_L; \pi R_c) \bar{\phi}_{H_u^0} \phi_{H_u^0}, \end{aligned} \quad (39)$$

with $\mathcal{T}_L^{ijn} = \int_{-\pi R_c}^{\pi R_c} dy f_i^{++}(c_L; y) f_j^{++}(c_L; y) g_n^{++}(y)$.

The equation of motion for each field $\Sigma^{(n)}$ ($n \geq 1$) is then given by

$$\begin{aligned} & -(\partial_\mu \partial^\mu + M^{(n)2}) \Sigma^{(n)} \\ & = q_L g \sum_{i,j=0}^{\infty} \mathcal{T}_L^{ijn} M^{(n)} \bar{\phi}_L^{(i)} \phi_L^{(j)} + q_{H_u^0} g g_n^{++} (\pi R_c) M^{(n)} \bar{\phi}_{H_u^0} \phi_{H_u^0}, \end{aligned} \quad (40)$$

which can be rewritten at second order in $\partial_\mu \partial^\mu / M^{(n)2}$:

$$\begin{aligned} & q_{H_u^0} q_L g^2 \sum_{n=1}^{\infty} g_n^{++} (\pi R_c) \bar{\phi}_{H_u^0} \phi_{H_u^0} \sum_{i,j=0}^{\infty} \mathcal{T}_L^{ijn} \bar{\phi}_L^{(i)} \phi_L^{(j)} - q_L q_{H_u^0} g^2 \sum_{i,j=0}^{\infty} \bar{\phi}_L^{(i)} \phi_L^{(j)} f_i^{++}(c_L; \pi R_c) f_j^{++}(c_L; \pi R_c) \bar{\phi}_{H_u^0} \phi_{H_u^0} \\ & + q_{H_u^0} q_L g^2 \sum_{i,j=0;n=1}^{\infty} g_n^{++} (\pi R_c) \mathcal{T}_L^{ijn} \frac{\partial_\mu (\bar{\phi}_{H_u^0} \phi_{H_u^0}) \partial^\mu (\bar{\phi}_L^{(i)} \phi_L^{(j)})}{M^{(n)2}} \in \mathcal{L}_{4D}^{D\text{terms}}. \end{aligned} \quad (42)$$

The first term in this Lagrangian part can be rewritten, according to the orthonormalization condition (B1) and completeness relation (B2), as

$$\begin{aligned} & q_{H_u^0} q_L g^2 \sum_{n=1}^{\infty} g_n^{++} (\pi R_c) \bar{\phi}_{H_u^0} \phi_{H_u^0} \sum_{i,j=0}^{\infty} \mathcal{T}_L^{ijn} \bar{\phi}_L^{(i)} \phi_L^{(j)} \\ & = q_{H_u^0} q_L g^2 \int_{-\pi R_c}^{\pi R_c} dy [\delta(y - \pi R_c) - g_0^{++} (\pi R_c) g_0^{++}(y)] \bar{\phi}_{H_u^0} \phi_{H_u^0} \sum_{i,j=0}^{\infty} f_i^{++}(c_L; y) f_j^{++}(c_L; y) \bar{\phi}_L^{(i)} \phi_L^{(j)} \\ & = q_{H_u^0} q_L g^2 \sum_{i,j=0}^{\infty} f_i^{++}(c_L; \pi R_c) f_j^{++}(c_L; \pi R_c) \bar{\phi}_{H_u^0} \phi_{H_u^0} \bar{\phi}_L^{(i)} \phi_L^{(j)} - q_{H_u^0} q_L \frac{g^2}{2\pi R_c} \bar{\phi}_{H_u^0} \phi_{H_u^0} \sum_{i=0}^{\infty} \bar{\phi}_L^{(i)} \phi_L^{(i)}. \end{aligned} \quad (43)$$

Then plugging this expression into Eq. (42) brings

$$\begin{aligned} -e^{4\sigma} \mathcal{L}_{5D}^{D\text{terms}} = & -\frac{e^{2\sigma}}{2} \partial_\mu \Sigma \partial^\mu \Sigma + \frac{1}{2} |D_5^k \Sigma|^2 \\ & - g(q_L \bar{\phi}_L \phi_L + q_{H_u^0} \delta \bar{\phi}_{H_u^0} \phi_{H_u^0}) D_5^k \Sigma \\ & + g^2 q_L q_{H_u^0} |\phi_L \phi_{H_u^0}|^2 \delta. \end{aligned}$$

Using once more Eq. (15), replacing the 5D fields by their KK decomposition, redefining them with warp factors (to recover the canonical 4D kinetic terms), and applying the orthonormalization condition (B1), one gets the 4D Lagrangian

$$\begin{aligned} \Sigma^{(n)} \simeq & -\frac{g}{M^{(n)}} \left[1 - \frac{\partial_\mu \partial^\mu}{M^{(n)2}} + \left\{ \frac{\partial_\mu \partial^\mu}{M^{(n)2}} \right\}^2 \right] \\ & \times \left(q_L \sum_{i,j=0}^{\infty} \mathcal{T}_L^{ijn} \bar{\phi}_L^{(i)} \phi_L^{(j)} + q_{H_u^0} g_n^{++} (\pi R_c) \bar{\phi}_{H_u^0} \phi_{H_u^0} \right). \end{aligned} \quad (41)$$

Now we integrate out all the $\Sigma^{(n)}$ fields by inserting Eq. (41) into Eq. (39) which gives rise to the following terms in the Lagrangian, restricting ourselves to the first order in $\partial_\mu \partial^\mu / M^{(n)2}$:

$$-q_{H_u^0} q_L \frac{g^2}{2\pi R_c} \bar{\phi}_{H_u^0} \phi_{H_u^0} \sum_{i=0}^{\infty} \bar{\phi}_L^{(i)} \phi_L^{(i)} + q_{H_u^0} q_L g^2 \sum_{i,j=0;n=1}^{\infty} g_n^{++} (\pi R_c) \mathcal{T}_L^{ijn} \frac{\partial_\mu (\bar{\phi}_{H_u^0} \phi_{H_u^0}) \partial^\mu (\bar{\phi}_L^{(i)} \phi_L^{(j)})}{M^{(n)2}} \in \mathcal{L}_{4D}^D \text{ terms}. \quad (44)$$

At this stage, a useful check is to recover the 4D SUSY Lagrangian—in our simple toy model with a U(1) gauge symmetry and a minimal matter content—by taking the limiting case $M^{(n)}, m_{L/R}^{(n)} \rightarrow \infty$ ($n \geq 1$). Indeed, in this case Eq. (44) simplifies to the 4D SUSY Lagrangian

$$\begin{aligned} \mathcal{L}_{4D}^D \text{ terms} &\rightarrow -q_{H_u^0} q_L \frac{g^2}{2\pi R_c} \bar{\phi}_{H_u^0} \phi_{H_u^0} \bar{\phi}_L^{(0)} \phi_L^{(0)} \\ &= -q_{H_u^0} q_L g_{4D}^2 \bar{\phi}_{H_u^0} \phi_{H_u^0} \bar{\phi}_L^{(0)} \phi_L^{(0)}, \end{aligned} \quad (45)$$

where g_{4D} represents the 4D effective gauge coupling constant. This test confirms the consistency of the obtained 4D couplings in Eq. (44). This consistency relies on the full summation over the infinite Σ KK tower in Eq. (43), similarly to the derivation of D -term couplings in Sec. II B.

In conclusion, the KK corrections with respect to the 4D SUSY $|\phi_{H_u^0}|^2 |\phi_L^{(0)}|^2$ coupling arise at the order $1/M^{(n)2}$.

At this order $1/M^{(n)2}$ (and above) the corrections in Eq. (44) affect the $|\phi_{H_u^0}|^2 |\phi_L^{(0)}|^2$ coupling but not the consequent masses as the “ ∂_μ ” acting on the constant $\phi_{H_u^0}$ VEV vanishes. This means that there are no KK tower-induced corrections to any D -term mass at order $1/M^{(n)2}$ with respect to 4D SUSY.

3. Complete scalar mass matrices

We have done all the necessary preliminary calculations to obtain different 4D mass contributions, so that we can now write the whole 4D effective scalar mass matrix within the pMSSM. We will give the top squark mass matrix as an example, the other scalar superpartner masses being easily deducible from it. This \tilde{t} mass matrix in the interaction basis $\vec{\tilde{t}} = \{\tilde{t}_L^{(0)}, \tilde{t}_R^{(0)}, \tilde{t}_L^{(1)}, \tilde{t}_R^{(1)}\}$ reads as $-\vec{\tilde{t}} \mathcal{M}_{\tilde{t}\tilde{t}}^2 \vec{\tilde{t}} \in \mathcal{L}_{4D}$, with

$$\begin{aligned} \mathcal{M}_{\tilde{t}\tilde{t}}^2 &\equiv \begin{pmatrix} 0 & 0 & 0 & 0 \\ 0 & 0 & 0 & 0 \\ 0 & 0 & m_L^{(1)2} & 0 \\ 0 & 0 & 0 & m_R^{(1)2} \end{pmatrix} \\ &+ \mathcal{Y}^2 \hat{v}_u^2 \begin{pmatrix} (f_L^0 f_R^0)^2 \left[1 - \mathcal{Y}^2 \hat{v}_u^2 (f_L^0)^2 \sum_{n=1}^{\infty} \frac{(f_n^0)^2}{m_R^{(n)2}} \right] & 0 & f_L^0 f_L^1 (f_R^0)^2 & 0 \\ 0 & (f_L^0 f_R^0)^2 \left[1 - \mathcal{Y}^2 \hat{v}_u^2 (f_R^0)^2 \sum_{n=1}^{\infty} \frac{(f_n^0)^2}{m_L^{(n)2}} \right] & 0 & f_R^0 f_R^1 (f_L^0)^2 \\ f_L^0 f_L^1 (f_R^0)^2 & 0 & (f_L^1 f_R^0)^2 & 0 \\ 0 & f_R^0 f_R^1 (f_L^0)^2 & 0 & (f_L^0 f_R^1)^2 \end{pmatrix} \\ &- \frac{\mu_{\text{eff}} \mathcal{Y} \hat{v}_u}{\tan \beta} \begin{pmatrix} 0 & f_L^0 f_R^0 & 0 & f_L^0 f_R^1 \\ f_L^0 f_R^0 & 0 & f_L^1 f_R^0 & 0 \\ 0 & f_L^1 f_R^0 & 0 & f_L^1 f_R^1 \\ f_L^0 f_R^1 & 0 & f_L^1 f_R^1 & 0 \end{pmatrix} + \cos 2\beta m_Z^2 \begin{pmatrix} Q_Z^{tL} & 0 & 0 & 0 \\ 0 & -Q_Z^{tR} & 0 & 0 \\ 0 & 0 & Q_Z^{tL} & 0 \\ 0 & 0 & 0 & -Q_Z^{tR} \end{pmatrix} \\ &+ \tilde{m} e^{-2k\pi R_c} \begin{pmatrix} f_L^0 f_L^0 & 0 & f_L^0 f_L^1 & 0 \\ 0 & f_R^0 f_R^0 & 0 & f_R^0 f_R^1 \\ f_L^0 f_L^1 & 0 & f_L^1 f_L^1 & 0 \\ 0 & f_R^0 f_R^1 & 0 & f_R^1 f_R^1 \end{pmatrix} + A e^{-k\pi R_c} \hat{v}_u \begin{pmatrix} 0 & f_L^0 f_R^0 & 0 & f_L^0 f_R^1 \\ f_L^0 f_R^0 & 0 & f_L^1 f_R^0 & 0 \\ 0 & f_L^1 f_R^0 & 0 & f_L^1 f_R^1 \\ f_L^0 f_R^1 & 0 & f_L^1 f_R^1 & 0 \end{pmatrix}, \end{aligned} \quad (46)$$

with the notation $f_{L/R}^n = f_n^{++}(c_{\tilde{t}_{L/R}}; \pi R_c)$. m_Z is the Z^0 gauge boson mass, $\mu_{\text{eff}} = \mu e^{-k\pi R_c} \sim \text{TeV}$ [cf. Eq. (22)], $A \sim 1$ as above, and, to not introduce a new bulk scale, the soft mass localized on the TeV-brane for bulk top squarks (see later discussion for the alternative possibilities of SUSY-breaking masses either on the Planck-brane or in the bulk) is taken at $\tilde{m} \sim k$. We have taken a unique soft

mass \tilde{m} for having a more simple matrix here, but the above mass matrix is easily extended to the case $\tilde{m}_L \neq \tilde{m}_R$ (respective soft masses for $\tilde{t}_L^{(0)}$ and $\tilde{t}_R^{(0)}$).

The fourth mass matrix of Eq. (46) originates from the D terms, while the Yukawa masses (second matrix) have been generalized from Eq. (36). We have denoted as $\tilde{t}_L^{(0)}$ and $\tilde{t}_R^{(0)}$ the first two states of the basis, but one should clarify the

point that $\tilde{t}_{L/R}^{(0)}$ possess in fact small admixtures of the $\tilde{t}_{L/R}^{c(n)}$ KK states [identical to the fields denoted as $\phi_{L/R}^{c(n)}$ defined in the KK decomposition (B12)], a kind of mixing described in the study of mass matrix (30) and at the origin of the two corrections to the first elements in the second matrix of Eq. (46). The KK sum in these corrections for the top squark, typically localized near the TeV-brane, must be cut at $\sim 2M_{\text{KK}}^{(1)}$ as is usual in this 5D framework (see the perturbativity considerations on the top Yukawa coupling, e.g., in Ref. [68]).

In conclusion, the effect of $(--)$ KK towers on the $\tilde{t}^{(0)}$ mass is taken into account at first order in $1/M^{(n)2}$ (or $1/m_{L/R}^{(n)2}$) via the corrective terms in the second matrix of Eq. (46), whereas the $(--)$ KK effects in D -term masses have been shown above to vanish at this first order [see Eq. (44)]. The mixing effect of $(++)$ KK towers on the $\tilde{t}^{(0)}$ mass is taken into account at first order by diagonalizing the mass matrix (46), which includes the first KK modes.

III. PHENOMENOLOGY

A. Quantum corrections to the Higgs mass

In this section, we compute explicitly the quantum corrections—at the one-loop level—to the $\phi_{H_u^0}$ Higgs mass (similar corrections hold for the complex $\phi_{H_d^0}$ boson) in the model defined in Appendix A without the μ term for simplification reasons and without introducing any (soft) SUSY-breaking mechanism. Indeed, our goal in this part is to study generically the possible reintroduction, due to the existence of warped extra dimensions, of the gauge hierarchy problem in a SUSY framework. For that purpose, we focus on the quadratic divergent contributions exclusively, by using the 4D effective couplings derived in previous sections.

Before starting, let us discuss the general aspect of this loop analysis, through an overview of the assumptions made. First, our results on the cancellation of quadratic divergences, although obtained within a minimal SUSY model, also apply to the pMSSM gauge group, Lagrangian, and field content. Indeed, those results rely (partially) on the gauge symmetry structure whatever gauge group it is [in particular, Abelian or not].

Second, there are no masses for the Higgs bosons in our framework (as neither μ terms nor soft scalar masses), and in turn the Higgs fields do not acquire VEV. Nevertheless, all our conclusions on quadratic cancellations still hold, for example, in the pMSSM after spontaneous EWSB. The vanishing mass hypothesis also allows us to work in the Higgs rest frame where the external four-momenta are exactly equal to zero, a Lorentz transformation choice which does not affect our conclusions due to the invariant nature of the (Higgs) mass.

Finally, we work generically without choosing a specific gauge; the gauge choice will be parametrized by the

nonfixed λ quantity entering the n th KK gauge boson propagator:

$$\frac{-i}{k^2 - M^{(n)2}} \left[\eta_{\mu\nu} + \frac{1 - \lambda}{\lambda} \frac{k_\mu k_\nu}{k^2 - \frac{1}{\lambda} M^{(n)2}} \right].$$

Recall that, for instance, $\lambda = 0$ ($\lambda = 1$) corresponds to the Landau (Feynman) gauge, which is characterized by $\partial^\mu A_\mu = 0$ as considered in the other parts of this paper together with $A_5 = 0$ —for a gauge boson field A_M . We thus find that the λ -dependent terms vanish which means that the physical result on Higgs mass corrections is not gauge-dependent, as expected. This approach confers to the analysis, and *a fortiori* to the result, a general character. Although we do not fix λ , or equivalently $\text{Im}(z)$ [which determines the A_μ field in Eq. (A8)], we choose to work in the Wess-Zumino gauge, where the extra fields that generically appear in the V expression have been transformed to zero [see Eq. (A8)] due to the specific choices of $\text{Re}(z)$, η , and f —if a gauge transformation on generic vectorial (chiral) superfields V (Ω) is defined by $V \rightarrow V + Z + \bar{Z}$ ($\Omega \rightarrow \Omega + \sqrt{2}\partial_y Z$), the chiral superfield Z involves the scalar field z , spinor η , and auxiliary f . We choose the Wess-Zumino gauge for simplicity in the loop calculation, but the physical result that we obtain would clearly be the same in another gauge.

1. Yukawa coupling sector

Starting with the fermion contributions, the first step is to get the 4D effective Yukawa couplings of the fermions to the Higgs boson $\phi_{H_u^0}$; from the Lagrangian obtained in Eq. (A29), we know that those couplings after field redefinition (absorbing the \sqrt{G} factor) are $\lambda_{nm} \equiv -\int dy \mathcal{Y} f_L^n(y) f_R^m(y) \delta(y - \pi R_c)$, assuming a real Yukawa coupling for simplicity.

The loop diagrams involving Yukawa couplings and resulting in quadratic divergences are those drawn in Figs. 5 and 6. From the formal point of view, for a loop having fermions of different masses as in Fig. 5, say, m_{f^1} and m_{f^2} , running in, one can write the loop integral as (calling λ the Yukawa coupling constants)

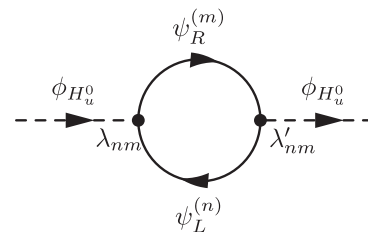


FIG. 5. Quadratically divergent quantum corrections at one loop to the $\phi_{H_u^0}$ mass due to the exchange of KK Dirac fermions $\psi_{L/R}^{(n)}$. Couplings are described in the text.

$$- \int \frac{d^4 k}{(2\pi)^4} \text{Tr} \left[(-i\lambda) \left(\frac{1 - \gamma_5}{2} \right) \left(\frac{i}{-m_{f_1}} \right) (-i\lambda) \left(\frac{1 + \gamma_5}{2} \right) \left(\frac{i}{-m_{f_2}} \right) \right] = -2\lambda^2 \int \frac{d^4 k}{(2\pi)^4} \left[\frac{k^2}{(k^2 - m_{f_1}^2)(k^2 - m_{f_2}^2)} \right]. \quad (47)$$

The four-momentum of the fields exchanged in the loop is generically denoted as k^μ . Note the presence of the $\frac{1 \pm \gamma_5}{2}$ chirality projectors, since such scalar couplings flip the fermion chirality, as well as the overall minus sign due to the Fermi-Dirac statistics, which is crucial for the SUSY

cancellation of divergences. Now expanding over different KK fermion towers results in the following contribution to the $\phi_{H_u^0}$ Higgs mass, respecting the correct order between the discrete KK sum and the four-momentum loop integral

$$I_F = -2 \sum_{\{n,m\}=0,0}^{N,M} \int \frac{d^4 k}{(2\pi)^4} \left[\frac{k^2}{(k^2 - m_L^{(n)2})(k^2 - m_R^{(m)2})} \right] \lambda_{nm} \lambda'_{nm}, \quad (48)$$

where $\lambda'_{nm} \equiv - \int dy' \mathcal{Y} f_L^n(y') f_R^m(y') \delta(y' - \pi R_c)$ and $m_{L/R}^{(n)}$ [with $m_{L/R}^{(0)} = 0$] are the KK fermion masses. We have truncated the KK summation at the indices N and M such that $m_L^{(N)}, m_R^{(M)} \sim \Lambda$ and consistently the momentum integration at the cutoff of the 5D theory Λ (one has typically $\Lambda \sim M_{\text{KK}}^{(2)}$, the second KK gauge mass), the reason being that the nonrenormalizable 5D SUSY theory is valid only below this cutoff. The integral gives us

$$\begin{aligned} I_F &= -2\mathcal{Y}^2 \sum_{\{n,m\}=0,0}^{N,M} \int \frac{d^4 k}{(2\pi)^4} k^2 \int dy \int dy' \left[\frac{f_L^n(y) f_L^n(y')}{k^2 - m_L^{(n)2}} \frac{f_R^m(y) f_R^m(y')}{k^2 - m_R^{(m)2}} \right] \delta(y - \pi R_c) \delta(y' - \pi R_c) \\ &= -2\mathcal{Y}^2 \sum_{\{n,m\}=0,0}^{N,M} \int \frac{d^4 k}{(2\pi)^4} k^2 \frac{f_L^n(\pi R_c) f_L^n(\pi R_c)}{k^2 - m_L^{(n)2}} \frac{f_R^m(\pi R_c) f_R^m(\pi R_c)}{k^2 - m_R^{(m)2}}. \end{aligned} \quad (49)$$

We now calculate the scalar superpartner contributions. First, one has to derive the 4D effective Yukawa coupling of the matter scalars to the Higgs boson $\phi_{H_u^0}$; we have obtained it in Eq. (10), renaming it now for commodity as $\tilde{\lambda}_n|_{L/R} = -i\mathcal{Y}^2 [f_{L/R}^n(\pi R_c)]^2 k^2 G_5^{f_{cR/L}^{++}}(k^2; \pi R_c, \pi R_c)$; the KK scalar contributions to the $\phi_{H_u^0}$ mass come only from these ‘‘diagonal’’ nn Yukawa couplings as Fig. 6 shows. As explained at the end of the part commenting on the scalar 4D couplings to two Higgs bosons in Sec. II B, the KK summation in $G_5^{f_{cR/L}^{++}}(k^2; \pi R_c, \pi R_c)$ has to be truncated, and we truncate it consistently at the index N such that $m_L^{(N)} \sim \Lambda$. From Fig. 6, we see that expanding over different KK scalar towers results in the contribution

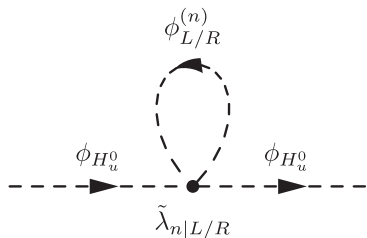


FIG. 6. Quadratically divergent quantum corrections at one loop to the $\phi_{H_u^0}$ mass due to the exchange of KK scalar superpartners $\phi_{L/R}^{(n)}$. Couplings are described in the text.

$$I_S = \sum_{n=0}^N \int \frac{d^4 k}{(2\pi)^4} \left\{ \frac{i\tilde{\lambda}_n|_L}{k^2 - m_L^{(n)2}} + \frac{i\tilde{\lambda}_n|_R}{k^2 - m_R^{(n)2}} \right\}, \quad (50)$$

where $m_{L/R}^{(n)}$ are the KK scalar masses. As there is no SUSY breaking here, the fermions and their scalar superpartners have identical KK masses and wave functions. We have cut the KK tower and momentum integration at Λ ($\sim M_{\text{KK}}^{(2)}$) as for the fermion contribution. We get

$$\begin{aligned} I_S &= \mathcal{Y}^2 \sum_{n=0}^N \int \frac{d^4 k}{(2\pi)^4} \left[\frac{[f_L^n(\pi R_c)]^2}{k^2 - m_L^{(n)2}} k^2 G_5^{f_{cR}^{++}}(k^2; \pi R_c, \pi R_c) \right. \\ &\quad \left. + \frac{[f_R^n(\pi R_c)]^2}{k^2 - m_R^{(n)2}} k^2 G_5^{f_{cL}^{++}}(k^2; \pi R_c, \pi R_c) \right] \\ &= 2\mathcal{Y}^2 \sum_{\{n,m\}=0,0}^{N,M} \int \frac{d^4 k}{(2\pi)^4} k^2 \frac{[f_R^n(\pi R_c)]^2}{k^2 - m_R^{(n)2}} \frac{[f_L^m(\pi R_c)]^2}{k^2 - m_L^{(m)2}} \end{aligned} \quad (51)$$

after inverting a *finite* summation (in 5D propagators) with the *cut* integration over k .

One thus finds $I_F + I_S = 0$ due to SUSY. Strictly speaking, we have in fact obtained this quadratic divergence cancellation analytically in the generic case of any cutoff (i.e., for any Λ value). Was this result predictable? In the limiting case $\Lambda < M_{\text{KK}}$ —the first KK gauge mass M_{KK} is the smallest KK mass among bosons and

fermions—where $n = m = 0$, one recovers the 4D SUSY model (with a cutoff) so that the above result of quadratic cancellation constitutes only a good check. On the opposite side, for $\Lambda \rightarrow \infty$ assuming a known UV completion for the 5D theory (or more realistically $\Lambda \simeq M_*$ in our RS context) so that the theory is totally 5D (or only up to the effective gravity scale), it is not surprising to find that the pure 5D SUSY guarantees the quadratic cancellation. Finally, for any intermediate cutoff truncating KK sums and loop integrations, our generic result is that the cancellation systematically occurs [the same cutoff Λ must be applied on Eqs. (49) and (51) so that these expressions remain exactly opposite] in what could be called a “truncated 5D theory”; this constitutes the proof of a supersymmetric cancellation KK level by KK level (i.e., the n th KK scalar contribution compensates the n th KK fermion contribution), a nonobvious result. A similar result holds for the quadratic divergence cancellation in the gauge coupling sector treated below.

2. Comments about the cancellation of quadratic divergences

Based on the above example of cancellation of quadratic divergences in the Yukawa coupling sector (compensation between fermions and their scalar superpartner), we discuss here why our approach brings some new light on the old debate about this cancellation in Higgs mass quantum corrections in higher-dimensional SUSY theories (the SUSY-breaking aspect is not considered here) with localized Higgs interactions.

First, there were questions [75,76] on the sense of the “KK regularization” [77] in higher-dimensional SUSY theories. The KK regularization is the divergence cancellation which relies on performing first the infinite summation of loop-exchanged KK states and second the infinite four-momentum loop-integral; this order corresponds to a nonjustified inversion in the analytical computation of an *infinite* number of KK contributions at the one-loop level to the Higgs mass.

We have shown, in the part commenting on the scalar 4D couplings to two Higgs bosons in Sec. II B, that writing the scalar effective 4D couplings requires one to perform an infinite summation on KK tower without applying any cutoff. Only once one has derived these scalar effective 4D couplings can the analytical loop computation—in a 4D framework—of KK scalar contributions to the Higgs mass be started: That is the correct order. Hence, the loop four-momentum integration must be performed *after* the aforementioned infinite KK summation, as exhibits Eq. (50) (where an infinite summation has already been calculated to obtain $\tilde{\lambda}_n|_{L/R}$), even if this is in contrast with naive thinking. In Eq. (51), the summations in G_5 —which originate from the remaining summation in $\tilde{\lambda}_n|_{L/R}$ —are finite, so it makes sense to invert those with the cut

integration, in order to obtain the quadratic divergence cancellation with Eq. (49) [78].

Related doubts pointed out in Ref. [75] concerned the effect of the necessary cutoff, due to the nonrenormalizable aspect of 5D SUSY models, which prevents one from making any infinite KK summation and in turn to find the quadratic cancellation: Indeed, the authors of Ref. [75] have demonstrated that the cancellation results partially from SUSY and partially from a compensation between the quadratic terms of a finite number of KK modes with masses below the cutoff and the logarithmic terms of an infinite number of KK states above it. It was believed that the procedure in Ref. [75] based on a sharp cut of the KK tower, spoiling the supersymmetry of the underlying theory, could prevent quadratic cancellations. However, the proper time cutoff (made separately from the KK level truncation) not spoiling four-dimensional symmetries can be applied [79] and similar problems arise: Quantum corrections to the Higgs mass become insensitive to details of physics at the UV scale only under certain conditions. Another alternative to the sharp KK tower truncation is the suppression by a Gaussian brane distribution [42] (the couplings of high KK modes are suppressed by a finite width of the brane) which indeed allows one to recover a finite Higgs mass—including the cutoff effect but keeping an infinite sum and so evading the drawbacks outlined in Ref. [75]. Nevertheless, it appears also in Ref. [42] that other distributions leading to a linear sensitivity on the momentum cutoff exist, a remark forbidding a general conclusion [80]. These two works [42,79] have thus not really solved the problems raised in Ref. [75] on a general justification of the finiteness of the Higgs mass. The way to describe the cutoff problem of Ref. [75] within our framework is as follows. An infinite KK summation has to be computed for applying the completeness relation and hence for finding the $\tilde{\lambda}_n|_{L/R}$ form obtained in Eq. (10) and used in Eq. (50) to give rise to the quadratic cancellation (between I_S and I_F); however, the infinite character seems meaningless, as the KK states with masses above Λ make no sense in a theory valid only up to the cutoff scale. In fact, it turns out, as we have discussed in the part commenting on the scalar 4D couplings (Sec. II B), that an infinite KK summation must really be calculated in order to write down a consistent 4D Lagrangian for the fundamental 5D SUSY theory; the cutoff is indeed applied but only after the 4D couplings have been derived (which requires an infinite summation computation), and it is applied on the remaining not-computed sums in the coherent 4D framework [82].

We have not brought arguments against the claims of Ref. [75], but we have proposed a different approach avoiding their problems (for the KK regularization), and we have justified the required infinite KK summation (including the cutoff aspect). Therefore, the quadratic cancellation appears to be well treated in our context and thus to

be meaningful. Similar arguments hold for the independent quadratic cancellation in the gauge coupling sector (involving also the Higgs boson, Higgsino, gauge boson, and gaugino contributions to the Higgs mass) that will be treated in the following subsection.

There exist other approaches like the Pauli-Villars regularization [83] or the elegant 5D (mixed position-momentum space) framework [84], based on formally correct treatments of the divergences avoiding subtleties

on KK excitations and 4D Lagrangians, which also conclude positively on the validity of quadratic cancellations.

3. Gauge coupling sector

First, the exchange of U(1) gauge boson KK modes contributes (cf. Fig. 7), via the gauge couplings derived in Eq. (A30), to the quadratic divergences appearing in the $\phi_{H_u^0}$ mass corrections. This contribution reads as

$$\begin{aligned} I_A &= \sum_{n=0}^N \int \frac{d^4 k}{(2\pi)^4} \int dy i q_{H_u^0}^2 g^2 [g_n^{++}(y)]^2 \eta^{\mu\nu} \delta(y - \pi R_c) \frac{-i}{k^2 - M^{(n)2}} \left[\eta_{\mu\nu} + \frac{1-\lambda}{\lambda} \frac{k_\mu k_\nu}{k^2 - \frac{1}{\lambda} M^{(n)2}} \right] \\ &= q_{H_u^0}^2 g^2 \sum_{n=0}^N \int \frac{d^4 k}{(2\pi)^4} \frac{[g_n^{++}(\pi R_c)]^2}{k^2 - M^{(n)2}} \left[4 + \frac{1-\lambda}{\lambda - M^{(n)2}/k^2} \right], \end{aligned} \quad (52)$$

where we have used the 4D effective gauge coupling obtained from Eq. (A30). As for the Yukawa sector, the KK summation and momentum integration are truncated at the 5D cutoff Λ .

The exchanges of $A_\mu^{(n)}$ states together with the Higgs boson also contribute as drawn in Fig. 8. Still truncating the sum and integration at Λ , we obtain [see again Eq. (A30)]

$$\begin{aligned} I'_A &= \sum_{n=0}^N \int \frac{d^4 k}{(2\pi)^4} \int dy \int dy' (-i q_{H_u^0} g k^\mu g_n^{++}(y) \delta(y - \pi R_c)) (-i q_{H_u^0} g k^\nu g_n^{++}(y') \delta(y' - \pi R_c)) \\ &\quad \times \frac{i}{k^2} \frac{-i}{k^2 - M^{(n)2}} \left[\eta_{\mu\nu} + \frac{1-\lambda}{\lambda} \frac{k_\mu k_\nu}{k^2 - \frac{1}{\lambda} M^{(n)2}} \right] \\ &= -q_{H_u^0}^2 g^2 \sum_{n=0}^N \int \frac{d^4 k}{(2\pi)^4} \frac{[g_n^{++}(\pi R_c)]^2}{k^2 - M^{(n)2}} \left[1 + \frac{1-\lambda}{\lambda - M^{(n)2}/k^2} \right]. \end{aligned} \quad (53)$$

Similarly, the exchanges of $\psi_{\lambda_1}^{(n)}$ gaugino states (four-component spinorial notation) and Higgsinos ($\psi_{H_u^0}$) contribute as in Fig. 9. Deducing the 4D effective gaugino couplings from the superfield action (A12) [as done exactly in Eq. (A29)], one finds the mass contribution

$$\begin{aligned} I_G &= - \sum_{n=0}^N \int \frac{d^4 k}{(2\pi)^4} \int dy \int dy' (-\sqrt{2} q_{H_u^0} g g_n^{++}(y) \delta(y - \pi R_c)) (\sqrt{2} q_{H_u^0} g g_n^{++}(y') \delta(y' - \pi R_c)) \text{Tr} \left[\frac{i(+M^{(n)})}{k^2 - M^{(n)2}} \frac{1-\gamma_5}{2} \frac{i}{k^2} \frac{1+\gamma_5}{2} \right] \\ &= -4 q_{H_u^0}^2 g^2 \sum_{n=0}^N \int \frac{d^4 k}{(2\pi)^4} \frac{[g_n^{++}(\pi R_c)]^2}{k^2 - M^{(n)2}}. \end{aligned} \quad (54)$$

This loop contribution carries a minus sign in front of the sum due to the Fermi-Dirac statistics. Since there is no SUSY breaking, the gauge boson modes have the same KK masses and wave functions as their fermionic superpartners.

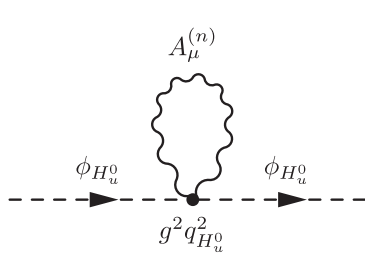


FIG. 7. Quadratically divergent quantum corrections at one loop to the $\phi_{H_u^0}$ mass due to the exchange of KK gauge bosons $A_\mu^{(n)}$. Couplings are described in the text.

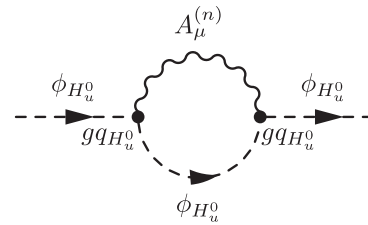


FIG. 8. Quadratically divergent quantum corrections at one loop to the $\phi_{H_u^0}$ mass due to the exchange of KK gauge bosons $A_\mu^{(n)}$ together with the Higgs boson itself. Couplings are described in the text.

Other divergences arise from the Higgs exchange itself; see Fig. 10. The preliminary 4D result of Eqs. (29) and (27) allow us to write down these two mass corrections, respectively, as

$$I_{H_d^0} = \int \frac{d^4 k}{(2\pi)^4} (-iq_{H_u^0} q_{H_d^0} g^2 p^2 G_5^{g^{++}}(p^2; \pi R_c, \pi R_c)) \frac{i}{k^2} \rightarrow q_{H_u^0} q_{H_d^0} g^2 \int \frac{d^4 k}{(2\pi)^4} \frac{[g_0^{++}(\pi R_c)]^2}{k^2} = \frac{q_{H_u^0} q_{H_d^0} g^2}{2\pi R_c} \int \frac{d^4 k}{(2\pi)^4} \frac{1}{k^2}, \quad (55)$$

$$\begin{aligned} I_{H_u^0} &= \int \frac{d^4 k}{(2\pi)^4} (-iq_{H_u^0}^2 g^2 p^2 G_5^{g^{++}}(p^2; \pi R_c, \pi R_c)) \frac{i}{k^2} + \int \frac{d^4 k}{(2\pi)^4} (-iq_{H_u^0}^2 g^2 k^2 G_5^{g^{++}}(k^2; \pi R_c, \pi R_c)) \frac{i}{k^2} \\ &\rightarrow \frac{q_{H_u^0}^2 g^2}{2\pi R_c} \int \frac{d^4 k}{(2\pi)^4} \frac{1}{k^2} + q_{H_u^0}^2 g^2 \int \frac{d^4 k}{(2\pi)^4} G_5^{g^{++}}(k^2; \pi R_c, \pi R_c) \\ &= \frac{q_{H_u^0}^2 g^2}{2\pi R_c} \int \frac{d^4 k}{(2\pi)^4} \frac{1}{k^2} + q_{H_u^0}^2 g^2 \sum_{n=0}^N \int \frac{d^4 k}{(2\pi)^4} \frac{[g_n^{++}(\pi R_c)]^2}{k^2 - M^{(n)2}}. \end{aligned} \quad (56)$$

In Eq. (55), the limit $p^2 \rightarrow 0$ has been performed [by using Eq. (C6)] since the effective coupling involved in Fig. 10 confers to this loop diagram a tadpole-form contribution; indeed, the effective diagram in Fig. 10 may be obtained by summing the two diagrams of Fig. 4 after joining the two $\phi_{H_d^0}$ legs and affecting, respectively, to the $\phi_{H_d^0}$, $\Sigma^{(n)}$, and $\phi_{H_u^0}$ fields the momentum k^2 (integrated loop momentum), $p^2 = 0$, and 0 (chosen external momentum), respectively. In Eq. (56), the limit $p^2 \rightarrow 0$ has also been performed, since the effective coupling involved in Fig. 10 for an internal $\phi_{H_u^0}$ field also confers to this loop diagram a tadpole-form contribution. Here there is even an additional

contribution from the exchange of $\Sigma^{(n)}$ with the same momentum k^2 as in the loop. All this can be seen from generating Fig. 10 by summing the three diagrams of Fig. 3 after joining the two upper $\phi_{H_u^0}$ legs in each diagram. We have also truncated the KK summation by the 5D cutoff Λ (like the integration), in the 5D propagator $G_5^{g^{++}}(k^2; \pi R_c, \pi R_c)$, and then inverted it with the integral.

The last contributions to quadratic divergences generated by gauge couplings are the scalar exchanges in Figs. 11 and 12. In the same way as just above, the 4D D -term coupling previously obtained in Eq. (19) leads to the corresponding mass corrections:

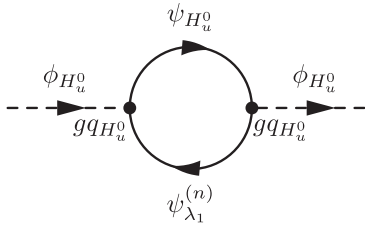


FIG. 9. Quadratically divergent quantum corrections at one loop to the $\phi_{H_u^0}$ mass due to the exchange of KK gaugino modes $\psi_{\lambda_1}^{(n)}$ with the Higgsino state $\psi_{H_u^0}$. Couplings are described in the text.

$$\begin{aligned} I_{L/R} &= \sum_{n=0}^N \int \frac{d^4 k}{(2\pi)^4} \left(-iq_{L/R} q_{H_u^0} g^2 \right. \\ &\quad \times \left. \int dy [f_{L/R}^n(y)]^2 p^2 G_5^{g^{++}}(p^2; y, \pi R_c) \right) \frac{i}{k^2 - m_{L/R}^{(n)2}} \\ &\rightarrow \frac{q_{L/R} q_{H_u^0} g^2}{2\pi R_c} \sum_{n=0}^N \int \frac{d^4 k}{(2\pi)^4} \int dy [f_{L/R}^n(y)]^2 \frac{1}{k^2 - m_{L/R}^{(n)2}} \\ &= \frac{q_{L/R} q_{H_u^0} g^2}{2\pi R_c} \sum_{n=0}^N \int \frac{d^4 k}{(2\pi)^4} \frac{1}{k^2 - m_{L/R}^{(n)2}} \end{aligned} \quad (57)$$

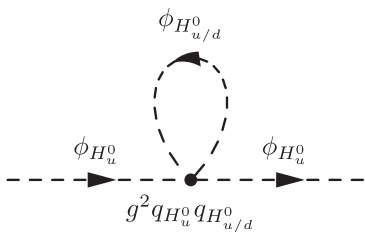


FIG. 10. Quadratically divergent quantum corrections at one loop to the $\phi_{H_u^0}$ mass due to self-couplings and couplings with the scalar field $\phi_{H_u^0/d}$ (described in the text).

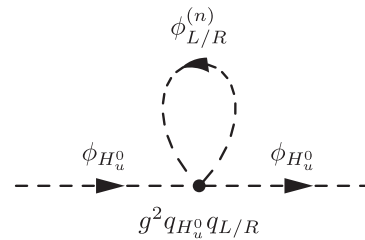


FIG. 11. Quadratically divergent quantum corrections at one loop to the $\phi_{H_u^0}$ mass due to gauge couplings with KK scalar superpartners $\phi_{L/R}^{(n)}$ (described in the text).

in the limit $p^2 \rightarrow 0$ and using the orthonormalization condition for wave functions.

Similarly, the 4D effective couplings of two $\phi_{L/R}^{c(m)}$ [defined in Eq. (B12)] to two Higgs bosons—induced

by $\Sigma^{(n)}$ exchanges—can be directly derived from the scalar field Lagrangian (A26), by using relation (B7), and lead to the respective tadpole contributions of Fig. 12:

$$I_{L/R}^c = \sum_{m=1}^M \int \frac{d^4 k}{(2\pi)^4} \left(q_{L/R} q_{H_u^0} g^2 \int dy [f_{L/R}^{cm}(y)]^2 \sum_{n=1}^N M^{(n)2} \frac{g_n^{++}(y) i g_n^{++}(\pi R_c)}{p^2 - M^{(n)2}} \right) \frac{i}{k^2 - m_{L/R}^{(m)2}},$$

reminding one that $f_{L/R}^{cm}(y) = f_m^{--}(c_{L/R}; y)$. Applying now the completeness relation and the equality $M^{(n)2}/(p^2 - M^{(n)2}) = \{p^2/(p^2 - M^{(n)2})\} - 1$, one can recast this contribution into the expression

$$\begin{aligned} I_{L/R}^c &= - \sum_{m=1}^M \int \frac{d^4 k}{(2\pi)^4} \left(q_{L/R} q_{H_u^0} g^2 \int dy [f_{L/R}^{cm}(y)]^2 p^2 G_5^{g^{++}}(p^2; y, \pi R_c) \right) \frac{1}{k^2 - m_{L/R}^{(m)2}} \\ &\rightarrow - \sum_{m=1}^M \int \frac{d^4 k}{(2\pi)^4} \frac{q_{L/R} q_{H_u^0} g^2}{2\pi R_c} \int dy [f_{L/R}^{cm}(y)]^2 \frac{1}{k^2 - m_{L/R}^{(m)2}} \\ &= - \frac{q_{L/R} q_{H_u^0} g^2}{2\pi R_c} \sum_{m=1}^M \int \frac{d^4 k}{(2\pi)^4} \frac{1}{k^2 - m_{L/R}^{(m)2}} \end{aligned} \quad (58)$$

in the limit $p^2 \rightarrow 0$.

At this stage, where all quadratically divergent contributions have been estimated, a useful check is to take the 4D SUSY limit: $k^2/m_{L/R}^{(n)2} \ll 1$ and $k^2/M^{(n)2} \ll 1$ [$n \geq 1$] at the zeroth order. Doing so, one recovers indeed the whole quadratically divergent mass correction for the gauge coupling sector of the 4D SUSY theory:

$$\begin{aligned} I_A + I'_A + I_G + I_{H_u^0} + I_{H_d^0} + I_L + I_R + I_L^c + I_R^c \\ \rightarrow q_{H_u^0} (q_{H_u^0} + q_{H_d^0} + q_L + q_R) g_{4D}^2 \int \frac{d^4 k}{(2\pi)^4} \frac{1}{k^2}, \end{aligned}$$

with $g_{4D} = g/\sqrt{2\pi R_c}$ as already defined. Indeed, in 4D SUSY the quadratically divergent Higgs mass corrections cancel each other only if the anomaly cancellation condition $q_{H_u^0} + q_{H_d^0} + q_L + q_R = 0$ is verified, recalling that the quadratic divergence cancellation is induced by the simultaneous presence of SUSY and a gauge symmetry

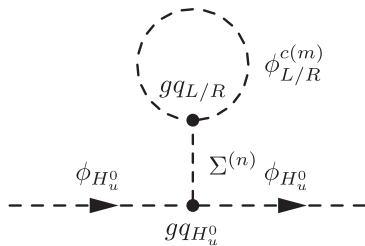


FIG. 12. Quadratically divergent quantum corrections at one loop to the $\phi_{H_u^0}$ mass due to the exchange of KK (---) scalar superpartners $\phi_{L/R}^{c(m)}$ and KK (---) scalar modes $\Sigma^{(n)}$ (couplings discussed in the text).

(which relies on the absence of Adler-Bardeen-Jackiw anomalies [85] originating from triangular loops of fermions).

In the present RS SUSY context with localized Higgs fields, we thus have first to wonder what the global 5D anomaly cancellation condition is. The contributions to triangular loops, of the fermions belonging to the chiral matter superfields Φ_L and Φ_L^{--} , should vanish due to the vectorial nature of the 5D theory [i.e., the presence of Φ_L^{--}]. The same comment holds for the Φ_L^c and Φ_L^{c--} superfields. The orbifolding apparently spoils this 5D vectorial nature [i.e., no zero mode for Φ_L^{--}], but the anomaly cancellation is recovered in the matter sector through certain tree-level contributions (see, e.g., Ref. [86]) induced by the Chern-Simons term (see Ref. [87] for the case of warped orbifolds) together with mixings generated by the Stückelberg term (for instance, see Ref. [88]). For intervals in AdS_5 , anomalies might lead to some constraints on the consistent effective field theory description [89]. Finally, one must recall here that the whole 5D anomaly cancellation condition includes the anomaly cancellation condition of the low-energy 4D chiral theory whose role is to ensure the anomaly cancellation for the contributions of the zero modes and possibly fields of the considered model confined on 3-branes (in other words, for all states except the KK excitations).

Coming back to our 5D SUSY model, we see that one gets (whatever are the KK masses)

$$\begin{aligned} I_A + I'_A + I_G + I_{H_u^0} + I_{H_d^0} + I_L + I_R + I_L^c + I_R^c \\ = q_{H_u^0} (q_{H_u^0} + q_{H_d^0} + q_L + q_R) \frac{g^2}{2\pi R_c} \int \frac{d^4 k}{(2\pi)^4} \frac{1}{k^2}, \end{aligned}$$

so that the quadratic divergence cancellation for the Higgs mass in the gauge sector (and hence in all sectors) is guaranteed by the 4D condition $q_{H_u^0} + q_{H_d^0} + q_L + q_R = 0$ for the chiral zero modes and 4D Higgsinos (localized on the TeV-brane) which is part of the 5D anomaly cancellation condition. On the other side, the vectorial nature of the 5D SUSY theory, which induces the cancellation of 5D anomalies, is also responsible for the cancellation of the KK $\phi_{L/R}^{(n)}$ contributions to the Higgs mass quadratic divergences [entering Eq. (57)] with the KK $\phi_{L/R}^{c(m)}$ contributions [see Eq. (58)]. This cancellation results from a compensation KK level by KK level and remains thus true for any 5D cutoff value.

As a general conclusion (the present analysis being not based on arguments restricted to warped geometries), in higher-dimensional SUSY models, the quadratic divergence cancellation in the Higgs mass is ensured by the higher-dimensional anomaly cancellation condition (as occurs in 4D with the difference that the higher-dimensional anomaly condition can be more complex than the 4D one, since it may include the adjustment of the Chern-Simons term to restore the vectorial behavior [90]).

We finish this part by a comment, for completeness. While the condition $q_{H_u^0} + q_{H_d^0} + q_L + q_R = 0$ is issued from anomalies of type U(1)-gravity-gravity, there is a second condition, namely, $q_{H_u^0}^3 + q_{H_d^0}^3 + q_L^3 + q_R^3 = 0$, coming from the cubic U(1)-U(1)-U(1) anomalies. Let us mention here the third condition on U(1) charges in our toy model: $q_{H_u^0} + q_L + q_R = 0$ related to the existence of a Yukawa interaction for $\Phi_{L/R}$ [see Eq. (A12)]. Our motivation for writing an interaction of this type was clearly to consider all the quadratically divergent contributions to the Higgs mass and, in particular, those involving Yukawa couplings (discussed above).

B. Sfermion mass splitting

1. Phenomenological framework

We first describe in more detail the phenomenological framework of this section. We consider the class of SUSY-breaking scenario where (soft) squark or slepton masses appear in the bulk and on the boundaries [see the SUSY-breaking classification of Sec. II A]. The model studied is the warped 5D pMSSM. We do not compute numerically the heavy KK state mixing effects, since we focus on dominant low-energy structural effects on scalar couplings induced by the SUSY-breaking scenario discussed below.

Let us thus discuss what are the favored geometrical setups concerning the SUSY-breaking scalar mass locations. First, to have a generic approach, we assume that all bulk sfermions have additional (i.e., SUSY-breaking) 5D mass terms of course invariant under the \mathbb{Z}_2 parity: Those are also taken of the type shown in Eq. (A27) but with other c parameters. We have shown in Appendix B 3 that adding

such masses is equivalent to introducing new 5D scalar parameters, say, $c_{\tilde{f}_{L/R}}$, completely independent from the fermion (or superfield) parameters $c_{f_{L/R}}$ and thus affects the scalar localizations. In analogy with RS flavor models for fermions, we will generally make the hypothesis that the first generations of sfermions are typically localized towards the UV boundary (large $c_{\tilde{f}_{L/R}}$), whereas the last families are rather located near the IR boundary (small $c_{\tilde{f}_{L/R}}$). Remaining general, the first scalar generations have also SUSY-breaking masses localized on the two boundaries, and the large soft masses on the Planck-brane are thus not reduced by wave function overlaps. These Planckian masses mimic $(-+)$ BC so that the first-generation sfermion zero modes decouple from the low-energy theory as occurs in the model of Ref. [63]. This class of scenario represents thus a realization of partially split SUSY models which allow one to improve the situation [91] with respect to flavor-changing neutral currents (FCNC). In contrast, the last sfermion generations have soft masses on the TeV-brane which are not suppressed by wave function overlaps. These soft masses enlarge the parameter space that we will explore. Having typically small $c_{\tilde{f}_{L/R}}$ for the last sfermion families is also an attractive possibility, as it leads to sfermion masses which are mainly generated by the Yukawa interactions after EWSB, as for SM fermions, and to specific collider signatures as discussed in the following subsections.

For the considered case $c_{\tilde{f}_{L/R}} < c_{f_{L/R}}$, the Yukawa-like couplings of these last-generation sfermions to Higgs bosons [first coupling matrix in Eq. (21)] are increased—modulo a square and a Higgs rotation angle or VEV—relatively to the effective 4D fermion Yukawa couplings [see Eq. (11)], which are themselves equal to the 4D SUSY scalar Yukawa couplings (forgetting small KK corrections). The same comparison holds for the interactions proportional to μ_{eff} [second coupling matrix of Eq. (21)]. Since the RS SUSY scenario considered increases globally sfermion couplings to Higgs bosons compared to the usual 4D SUSY case, which brings new significant contributions to the (s)quark triangular loop of the gluon-gluon-fusion mechanism for Higgs production at hadron colliders [main production channel] [92,93], one might wonder whether such a model is not excluded by present experimental searches [95] at Tevatron run II for 4D SUSY Higgs fields (or estimated results from SM Higgs searches [96], e.g., in the decoupling limit). First, it must be remarked that the Tevatron production cross sections and decay branching ratios as well as various theoretical uncertainties have been recently reevaluated for SUSY Higgs bosons [97], that 4D SUSY Higgs searches were not exhaustive in the parameter space exploration [95], and that other effects could appear in 5D SUSY Higgs productions. Second, the obtained lower limit of the lightest neutral Higgs (denoted as h) mass is not so close to the 4D SUSY theoretical upper

bound, which furthermore can be enhanced in the 5D SUSY context [43] enlarging the allowed mass range. In fact, the main 4D SUSY contribution to the gluon-fusion mechanism is the top squark exchange in the loop, due to its large Yukawa coupling. In the above RS SUSY setup, the only additional new contribution is the sbottom exchange, as we assume the decoupling of the first two generations of squarks to avoid constraints from the $K^0 - \bar{K}^0$ mixing (one could even assume the decoupling of the squark doublet \tilde{Q}_L and sbottom singlet \tilde{b}_R). Since we take masses $m_{\tilde{b}} \sim 10^2$ GeV (from little hierarchy arguments), the sbottom Yukawa couplings are of the same order as the top (quark) Yukawa interactions, and hence comparable Higgs production rates are expected in 4D versus RS SUSY, which is realistic. Concerning sleptons, we assume that only the first generation decouples since these noncolored scalar fields affect only 4D SUSY Higgs searches through the radiative Higgs decay into two photons, a decay representing only one of the various channels investigated. Going into the details of the calculation of the Higgs production and decays, different sfermion exchanges might suppress each other by destructive interferences of the triangular loops [92] depending on the signs of various 4D effective couplings over parameter ranges, and some more freedom might even arise from 5D SUSY model building.

Concerning bulk gauginos, their 4D soft masses are taken effectively, i.e., without specifying the higher-dimensional geometry (as we do not study possible 4D or 5D SUSY differences in that sector). For example, these masses could be localized on the TeV-brane—without suffering from large overlap suppression like light generations.

2. Charge- and color-breaking minima

Before presenting numerical results, we need to discuss another SUSY aspect which is significantly modified in this RS context: the charge- and color-breaking (CCB) minima. We will show that no drastic constraints arise on the parameter space and even that no SUGRA-like scenario—in the sense where trilinear soft scalar terms are proportional to the Yukawa coupling constants (reducing effectively the trilinear scale A)—needs to be assumed [as usually required in 4D SUSY] in order to satisfy those constraints.

In 4D mSUGRA, the constraints coming from imposing the absence of CCB global minima for the potential of squark or slepton VEVs read typically as [98] (see [99] for the next-to-minimal supersymmetric standard model case), taking the example of the usually dangerous selectron direction,

$$(\mathcal{Y}_{4D}^e A^e)^2 < 3((\tilde{m}_R^e)^2 + (\tilde{m}_L^e)^2 + \hat{m}_d^2)(\mathcal{Y}_{4D}^e)^2, \quad (59)$$

where \tilde{m}_L^e and \tilde{m}_R^e denote the selectron soft masses and $\hat{m}_d^2 = m_{H_d}^2 + \mu^2$ with m_{H_d} being the down Higgs soft mass. $\mathcal{Y}_{4D}^e \sim 10^{-5}$ is the Yukawa coupling constant for the electron, and $A^e \sim 10^2$ GeV. Since the Yukawa couplings simplify each other in the above inequality, they are often not written in the literature, but here we keep them for the 5D discussion below. The general conclusion on the 4D case is that the CCB constraints, as illustrates the one above, remain respected if the soft parameters A , \tilde{m} , m_{H_d} , and also μ are all of the order of the EWSB scale (which is compatible with both the Higgs fine-tuning considerations and electroweak potential minimization relations).

For mSUGRA models in a warped background, the CCB constraint (59) is replaced by (neglecting the KK mixing corrections)

$$(\mathcal{Y}^e A^e e^{-\sigma(\pi R_c)} f_L^0 f_R^0)^2 < 3(\tilde{m}_R^e (f_R^0 e^{-\sigma(\pi R_c)})^2 + \tilde{m}_L^e (f_L^0 e^{-\sigma(\pi R_c)})^2 + \hat{m}_d|_{\text{eff}}^2)(\mathcal{Y}^e f_L^0 f_R^0)^2 \quad (60)$$

as deduced from the form of 4D Higgs couplings (21)—of type \mathcal{Y}^2 and A —and the form of 4D soft scalar masses on TeV-brane in Eq. (46). Here $f_{L/R}^0 = f_0^{+}(c_{\tilde{e}_{L/R}}; \pi R_c)$; $A^e \mathcal{Y}^e = \mathcal{O}(1)$ (as discussed in the next subsection on slepton masses in mSUGRA) and $\hat{m}_d|_{\text{eff}}^2 = m_{H_d}^2 + \mu_{\text{eff}}^2$ [see the discussion on μ_{eff} in Sec. II A]. Now, the RS CCB criteria of type Eq. (60) simplifies to

$$(A^e e^{-\sigma(\pi R_c)})^2 < 3(\tilde{m}_R^e (f_R^0 e^{-\sigma(\pi R_c)})^2 + \tilde{m}_L^e (f_L^0 e^{-\sigma(\pi R_c)})^2 + \hat{m}_d|_{\text{eff}}^2), \quad (61)$$

where $A^e e^{-\sigma(\pi R_c)} \sim 10^2$ GeV so that this condition is as natural as in 4D mSUGRA for effective soft masses at the EWSB scale, which is the case since $\hat{m}_d|_{\text{eff}} \sim 10^2$ GeV and, e.g., $\tilde{m}_R^e (f_R^0 e^{-\sigma(\pi R_c)})^2 \sim k^2 e^{-2\sigma(\pi R_c)} \sim (10^2 \text{ GeV})^2$ [$\tilde{m}_R \sim k$ from the discussion below Eq. (46) and see Eq. (B13) for the wave function order of magnitude] as confirmed by all the values obtained in the next subsections.

In an RS framework with a SUSY breaking not specifically of the type SUGRA, the CCB constraint of Eq. (60) simply becomes

$$(A^e e^{-\sigma(\pi R_c)} f_L^0 f_R^0)^2 < 3(\tilde{m}_R^e (f_R^0 e^{-\sigma(\pi R_c)})^2 + \tilde{m}_L^e (f_L^0 e^{-\sigma(\pi R_c)})^2 + \hat{m}_d|_{\text{eff}}^2)(\mathcal{Y}^e f_L^0 f_R^0)^2 \quad (62)$$

with now $A^e = \mathcal{O}(1)$ being dimensionless [cf. Eq. (46)]. After simplification, it reads as

$$(A^e e^{-\sigma(\pi R_c)})^2 < 3(\tilde{m}_R^e (f_R^0 e^{-\sigma(\pi R_c)})^2 + \tilde{m}_L^e (f_L^0 e^{-\sigma(\pi R_c)})^2 + \hat{m}_d |_{\text{eff}}^2) (\mathcal{Y}^e)^2, \quad (63)$$

a condition which is also systematically fulfilled in orders of magnitude since $(\mathcal{Y}^e)^{-1} e^{-\sigma(\pi R_c)} \sim k e^{-\sigma(\pi R_c)} \sim 10^2 \text{ GeV}$. Hence, we conclude that within RS SUSY the CCB constraint is generically satisfied, with respect to the orders of magnitude, even without assuming a SUGRA-like breaking.

Strictly speaking, the CCB-induced conditions must be imposed at the energy scale $Q \sim \langle \tilde{f} \rangle$, but the running of soft parameters in the RS SUSY framework is beyond our scope.

There exists a related kind of bound which originates from forbidding true minima along scalar potential directions unbounded from below (UFB) [100] (cf. [99] for the next-to-minimal supersymmetric standard model). The condition for such minima not to be deeper than the standard EWSB minimum implies the following bound: $m_0/m_{1/2} > \mathcal{O}(1)$ (in case one assumes universal soft terms). This typical UFB bound should also be quite easily satisfied in an RS SUSY context, applying it for simplicity on the 4D effective soft masses.

Finally, one must recall that the actual relevance of these CCB and UFB bounds is not entirely evident in general, because, even if, e.g., an existing CCB minimum is deeper than the standard EWSB one, it can be acceptable if the tunneling rate out of the standard minimum is small relatively to the age of the Universe. The various analyses in the literature lead to the conclusion that these tunneling rates are often quite small (the original paper is the third one of Ref. [98]). The relevance of the CCB and UFB bounds is thus model-dependent as it depends on cosmology and, in particular, on which minimum we drop after inflation [101].

3. Numerical results for top squark masses: A first discrimination test

First, we investigate the heavy quark superpartner (namely, the top squark denoted as \tilde{t}) sector. The flavor context of the pMSSM, considered in this paper, will be recalled in Sec. III C, where all flavors are potentially involved. In the present analysis, we propose a test to discriminate the 4D pMSSM with respect to 5D warped pMSSM by looking at the different ways to generate top squark masses in these two setups. To be general, we consider here within 4D and 5D SUSY the case where the soft breaking parameters are chosen effectively, only constrained from the experimental data.

In Fig. 13, we have represented the domains possibly explored in 4D or warped SUSY in the plan of the two top squark mass eigenstates. The blue lines represent the lower limit on $m_{\tilde{t}_2}$ obtained in 4D SUSY (see the discussion below). The two plots shown correspond to scans of the fundamental parameters in the case where SUSY breaking occurs in the bulk (see Appendix B 3), and, for the right plot, soft SUSY-breaking terms (top squark masses and trilinear couplings) have been added on the TeV-brane. For the left plot the only parameters entering the scan are the SUSY parameters $\tan\beta$ and μ (or μ_{eff} [see Eq. (22)]), the 5D top squark parameters $c_{\tilde{t}_{L/R}}$, and the soft masses $\tilde{m}_{L/R}$ (for 4D SUSY), whereas for the right scan we have further considered the 4D trilinear coupling A_t as well as the TeV-brane SUSY-breaking parameters $\tilde{m}_{L/R}|_{\text{eff}} = \tilde{m}_{L/R} k e^{-2k\pi R_c}$ and $A_t|_{\text{eff}} = A_t k e^{-k\pi R_c}$ appearing in the top squark mass matrix of warped SUSY models [as seen from Eqs. (46) and (B13)]. The $A_t|_{\text{eff}}$ term is localized on the TeV-brane due to the Higgs localization. In the case of

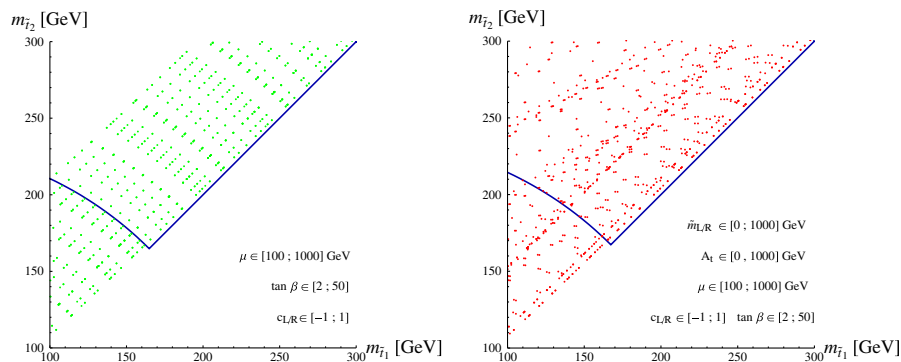


FIG. 13 (color online). Allowed regions in the plan $m_{\tilde{t}_2}$ versus $m_{\tilde{t}_1}$ (in GeV) within 4D SUSY [demarcated by the blue lines] and RS SUSY [green and red points]. The plot on the left side corresponds to the situation where there are no more SUSY-breaking terms on the TeV-brane (for the 5D case). The thick blue lines represent a lower limit on $m_{\tilde{t}_2}$ obtained analytically. The parameters are scanned in the intervals indicated on the plot. $c_{L/R} = c_{\tilde{t}_{L/R}}$ are the 5D top squark parameters. In the RS case, the so-called effective parameter μ_{eff} is the equivalent of the μ parameter in 4D SUSY [cf. Eq. (22)]. The interval indicated on \tilde{m} (A_t) corresponds to the scan interval for the soft top squark masses $\tilde{m}_{L/R}$ (trilinear coupling A_t) in 4D SUSY and $\tilde{m}_{L/R}|_{\text{eff}} = \sqrt{\tilde{m}_{L/R} k e^{-2k\pi R_c}}$ ($A_t|_{\text{eff}} = A_t k e^{-k\pi R_c}$) in the RS SUSY case.

the absence of soft top squark mass terms on the TeV-brane (left plot), the top squark mass is generated, in particular, by its coupling with the Higgs boson—which can itself be increased through the top squark-Higgs wave function overlap controlled by the SUSY-breaking top squark mass term in the bulk.

The parameters are scanned over the following ranges: $\tan\beta \in [2; 50]$, $\mu, \mu_{\text{eff}} \in [100; 1000]$ GeV, $c_{\tilde{t}_{L/R}} \in [-1, 1]$, $\tilde{m}_{L/R}, \tilde{m}_{L/R}|_{\text{eff}} \in [0; 1000]$ GeV, and $A_t, A_t|_{\text{eff}} \in [0; 1000]$ GeV. The interval on $\tan\beta$ is conservative given present constraints [66,102]. The μ or μ_{eff} ($|c_{\tilde{t}_{L/R}}|$) interval is justified by its required order of magnitude at the EWSB scale (around ~ 1) as discussed in Sec. II A. The $\tilde{m}_{L/R}$ range is motivated by the usual effective scale of 4D SUSY-breaking scenarios limiting the Higgs mass fine-tuning, and the $\tilde{m}_{L/R}|_{\text{eff}}$ range is motivated by the energy scale orders in RS: $\tilde{m}_{L/R}|_{\text{eff}} = (\tilde{m}_{L/R} k e^{-2k\pi R_c})^{1/2} \sim (k^2 e^{-2k\pi R_c})^{1/2} \sim 10^2$ GeV [see the discussion below Eq. (22)]. Finally, the chosen A_t interval is based on usual 4D SUSY-breaking scenarios, and the considered $A_t|_{\text{eff}}$

range comes from the scales characteristic of RS: $A_t|_{\text{eff}} = A_t k e^{-k\pi R_c} \sim 1 \times k e^{-k\pi R_c} \sim 10^2$ GeV [see again below Eq. (22)]. In order to have a consistent comparison between 4D and 5D models, we have chosen the same ranges in both setups. The scans in the plots are not performed on negative values of the A_t (or $A_t|_{\text{eff}}$) nor of the μ (or μ_{eff}) terms, but taking the opposite signs does not change the conclusions. The last remark on the scans is that having chosen slightly larger parameter ranges—but remaining with the same orders of magnitude as above since those are physically motivated—would have not affected significantly the obtained numerical results presented here.

Let us now explain the differences arising between the 4D and 5D models in the plots of Fig. 13. For that purpose, we need to start from the top squark mass matrix structure. The top squark mass matrix within the RS scenario has been derived in Eq. (46). Moving to 4D SUSY, we recall the general form of the top squark mass matrix in the $\{\tilde{t}_L, \tilde{t}_R\}$ basis:

$$\mathcal{M}_{\tilde{t}}^2|_{4\text{D SUSY}} = \begin{pmatrix} m_t^2 + Q_Z^L \cos 2\beta m_Z^2 + \tilde{m}_L^2 & A_t - \frac{\mu m_t}{\tan\beta} \\ A_t - \frac{\mu m_t}{\tan\beta} & m_t^2 - Q_Z^R \cos 2\beta m_Z^2 + \tilde{m}_R^2 \end{pmatrix}, \quad (64)$$

where $Q_Z^L \equiv \frac{1}{2} - \frac{2}{3} \sin^2 \theta_W$, $Q_Z^R \equiv -\frac{2}{3} \sin^2 \theta_W$, and m_t is the top quark mass. One can note at this level that the SM top mass entering this mass matrix (and taken in agreement with recent Tevatron measurements [103]) is larger than the experimental lower bound on the top squark mass, $m_{\tilde{t}_1} > 95.7$ GeV [50,102]. The mass matrix (64) can be diagonalized by 2×2 orthogonal matrices, resulting in the following mass eigenvalues for the top squark eigenstates $\tilde{t}_{1,2}$:

$$m_{\tilde{t}_{1,2}}^2 = \frac{1}{2} \left(2m_t^2 + \frac{1}{2} \cos 2\beta m_Z^2 + \tilde{m}_L^2 + \tilde{m}_R^2 \mp \sqrt{\left((Q_Z^L + Q_Z^R) \cos 2\beta m_Z^2 + \tilde{m}_L^2 - \tilde{m}_R^2 \right)^2 + 4 \left(A_t - \frac{\mu m_t}{\tan\beta} \right)^2} \right). \quad (65)$$

For 4D SUSY, in Fig. 13, we observe that $m_{\tilde{t}_2}$ has a lower limit (blue line) depending on $m_{\tilde{t}_1}$: This limit is due to the structure of matrix (64), and it has thus been possible to obtain it analytically. Indeed, from Eq. (65), summing the two squared masses, we get

$$m_{\tilde{t}_2}^2 + m_{\tilde{t}_1}^2 = 2m_t^2 + \frac{1}{2} \cos 2\beta m_Z^2 + \tilde{m}_L^2 + \tilde{m}_R^2. \quad (66)$$

For arbitrary large soft masses \tilde{m}_L^2 and \tilde{m}_R^2 , there is no constraint on how high can $m_{\tilde{t}_2}$ be compared to $m_{\tilde{t}_1}$ as illustrated in Fig. 13. We are thus interested in how low can $m_{\tilde{t}_2}$ be with respect to $m_{\tilde{t}_1}$ in the low soft mass region (where it appears on the plot to exist a nontrivial lower limit on $m_{\tilde{t}_2}$). Obviously, one must have $m_{\tilde{t}_2} \geq m_{\tilde{t}_1} \geq 100$ GeV from the definition together with the experimental constraint on top squark searches mentioned above. The $m_{\tilde{t}_2}$ lowest value thus corresponds to $\tilde{m}_{L/R} = 0$ together with a vanishing $\tilde{t}_L - \tilde{t}_R$ mixing, resulting in $m_{\tilde{t}_2}^{\text{lowest}} = m_{\tilde{t}_1} = \sqrt{m_t^2 + (1/4) \cos 2\beta m_Z^2} \sim m_t$. When there is a non-vanishing mixing, for $m_{\tilde{t}_1} \leq m_{\tilde{t}_2}^{\text{lowest}}$, we have from Eq. (66)

$$m_{\tilde{t}_2} \geq \sqrt{2m_t^2 + \frac{1}{2} \cos 2\beta m_Z^2 - m_{\tilde{t}_1}^2} \quad (67)$$

$$\text{for } m_{\tilde{t}_1} \leq \sqrt{m_t^2 + \frac{1}{4} \cos 2\beta m_Z^2},$$

which corresponds to the first branch of the blue line in both plots of Fig. 13—fitting perfectly the lower limit of the 4D SUSY scan point domain that we have also generated for checking [it is shown in Fig. 14]. The second branch, as mentioned above, simply reveals the constraint

$$m_{\tilde{t}_2} \geq m_{\tilde{t}_1} \quad \text{for } m_{\tilde{t}_1} \geq \sqrt{m_t^2 + \frac{1}{4} \cos 2\beta m_Z^2}. \quad (68)$$

The minimum $m_{\tilde{t}_2}$ value is thus

$$m_{\tilde{t}_2}^{\text{lowest}} = m_{\tilde{t}_1} \quad \text{for } m_{\tilde{t}_1} = \sqrt{m_t^2 + \frac{1}{4} \cos 2\beta m_Z^2} \sim m_t. \quad (69)$$

Note that this result is a quite general result for 4D SUSY models.

Having determined explicitly the 4D SUSY structural limit on $m_{\tilde{t}_2}$ as a function of $m_{\tilde{t}_1}$, we now turn our attention to the results in the context of RS SUSY shown in Fig. 13.

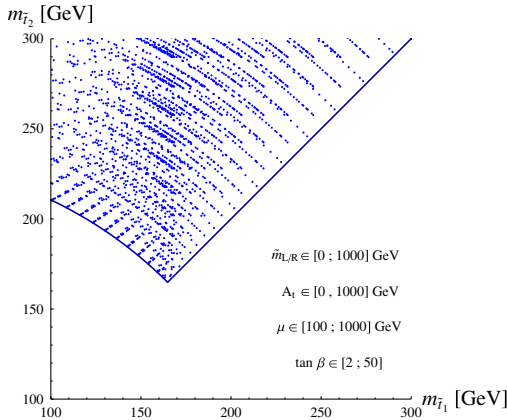


FIG. 14 (color online). Allowed regions in the plan $m_{\tilde{t}_2}$ versus $m_{\tilde{t}_1}$ (in GeV) within 4D SUSY. These regions have been obtained for parameters scanned in the intervals indicated on the plot itself.

Looking at those two plots, we observe an important difference between the 4D and 5D SUSY models; $m_{\tilde{t}_2}$ can now reach smaller values (for a given $m_{\tilde{t}_1}$ value) than those in 4D SUSY [limited by the blue line] and is now constrained only by

$$m_{\tilde{t}_2} \geq m_{\tilde{t}_1} \geq 100 \text{ GeV.} \quad (70)$$

This difference with the 4D case can be understood as follows. The 4D SUSY conservative constraint of Eq. (69) is changed in RS to the global constraint $m_{\tilde{t}_2} \geq \mathcal{Y} \hat{v}_u f_0^{++}(c_{\tilde{t}_L}; \pi R_c) f_0^{++}(c_{\tilde{t}_R}; \pi R_c)$ as deduced from Eq. (46). If there were no SUSY breaking in the bulk, one would have $c_{\tilde{t}_{L/R}} = c_{t_{L/R}}$ and by consequence $\mathcal{Y} \hat{v}_u f_0^{++}(c_{\tilde{t}_L}; \pi R_c) f_0^{++}(c_{\tilde{t}_R}; \pi R_c) = m_t$ [neglecting the KK top (quark) mixing effect as already mentioned] so that the constraint (69) would be recovered. However, when SUSY is broken in the bulk, $c_{\tilde{t}_{L/R}}$ are now effectively free parameters that can lead to either larger or smaller values of $\mathcal{Y} \hat{v}_u f_0^{++}(c_{\tilde{t}_L}; \pi R_c) f_0^{++}(c_{\tilde{t}_R}; \pi R_c)$ relative to m_t . In particular, the lower limit in Eq. (67) materialized by the first branch in plots is relaxed down to the bound (70) in RS SUSY, thus explaining the RS scanned points going beyond the blue line.

Hence a measurement of $m_{\tilde{t}_2}$ at high-energy colliders in the lower-left region of the RS scans shown here (below the blue line) would greatly disfavor 4D SUSY models in their minimal form while constituting possible signatures of RS SUSY scenarios. Such a discrimination test should be already possible before a future precision ILC physics, at the LHC, given the experimental accuracies expected on squark mass reconstructions. Indeed, an uncertainty of $\sim 5\%$ – 10% on top squark masses should be reachable at the LHC [104] which is clearly sufficient for the potential test suggested here, given the large top squark mass deviations in RS with respect to the pure 4D SUSY scenario shown in Fig. 13. This typically expected accuracy of

$\sim 5\%$ – 10% on top squark masses corresponds to illustrative examples studied in Ref. [104], but, of course, the exact performance would rely on effectively observed events at the LHC as well as on the realized SUSY model and parameters chosen by nature. Note finally that for the values taken throughout this paper, $m_{\tilde{\nu}_1} > 120$ GeV and $m_{\tilde{\chi}_1^0} > 150$ GeV, the conservative experimental lower bound on the top squark mass is exactly $m_{\tilde{t}_1} > 95.7$ GeV [50,102] so that the region only accessible in RS SUSY in Fig. 13 is not yet excluded and could be revealed by an LHC discovery.

The last comment—which is interesting for understanding the formal RS SUSY construction and will prove to be useful for Sec. III D—is about the difference between the two plots of Fig. 13. In the first scenario (left plot) where breaking occurs only in the bulk, while, as discussed, $m_{\tilde{t}_2}$ can reach any values ≥ 100 GeV, on the other side we observe that the scan reaches a maximum value of $m_{\tilde{t}_2}$ depending on $m_{\tilde{t}_1}$. This is due to the chosen usual range for the $c_{\tilde{t}_{L/R}}$ parameters spanning from -1 to $+1$, together with the absence of soft mass terms on the TeV-brane. Indeed, in the absence of such mass terms, high values of $m_{\tilde{t}_2}$ are limited by the diagonal Yukawa-type mass contributions and thus by the largest allowed overlap of the top squark wave functions with the Higgs boson, an overlap being limited from above by the minimal $c_{\tilde{t}_{L/R}}$ values. In contrast, the scan is not limited from above for the second RS scenario (right plot) due to the presence of soft mass terms on the TeV-brane (and even of trilinear scalar couplings).

4. Numerical results for smuon masses in mSUGRA

In this part, we consider within 4D SUSY the subcase of the mSUGRA scenario where the soft breaking parameters have universal values at the GUT scale, m_0 , $m_{1/2}$, and A_0 , the whole trilinear scalar couplings $A_0 \mathcal{Y}$ being proportional to Yukawa coupling constants \mathcal{Y} . The two other input (SUSY) parameters are $\tan \beta$ and $\text{sgn}(\mu)$. The soft masses $\tilde{m}_{L/R}$ will be run here [105] from their GUT value m_0 down to low energy, where we study collider physics, and the obtained values included into the mass matrix form (64). To adopt a general approach, we will take the low-energy $|A|$ parameter to be between zero and the TeV scale. This maximum scale is justified, in 4D mSUGRA, by the order of effective SUSY-breaking scales and by the condition of the absence of CCB minima [see typically Eq. (59)].

In a minimal RS version of the mSUGRA scenario, the set of parameters entering the scalar mass matrices can be taken as follows. First, the parameter μ_{eff} [see Eq. (22)], which enters the mass matrix form (46), is taken at the μ value one gets in 4D mSUGRA since it is the equivalent parameter. The possible kind of differences arising between 4D and 5D models in the running necessary to derive the μ parameter is not studied here; this is a potential source of additional differences that could lead to new

tests for distinguishing between 4D and 5D SUSY. Similarly, for the diagonal scalar mass matrix elements, we take the same values as the ones obtained from the 4D mSUGRA running, motivated by the fact that we will focus on differences between 4D and 5D mSUGRA arising in the off-diagonal mass matrix elements. Last but not least, in a mSUGRA-like scenario, one would have a new [compared to Eq. (46)] trilinear coupling constant $A\mathcal{Y} = \mathcal{O}(1)$ with $A \sim (1/\mathcal{Y}) \sim k$ to not introduce new scales. The quantity $A|_{\text{eff}} = A\mathcal{Y}ke^{-k\pi R_c} \sim \text{TeV}$ ($A = 0$ could also be an acceptable scale) appearing now in the A terms of Eq. (46), namely, in $A\mathcal{Y}e^{-k\pi R_c}\hat{v}_u f_L^0 f_R^0$, is taken to be equal numerically to the 4D SUSY-breaking parameter A introduced just above, neglecting once again possible differences arising in the 5D running.

Let us now emphasize 4D versus 5D differences in the smuon mass matrix (studying the example of the smuon is motivated by the theoretical framework described above and the experimental performances discussed below) within this context.

In 4D mSUGRA, the off-diagonal entry to squared smuon mass $A_\mu \mathcal{Y}_\mu \hat{v}_d$, driven by the muon mass (m_μ), is typically around 10^2 GeV^2 at most, which leads to a $\tilde{\mu}_L \tilde{\mu}_R$ smuon mass term induced by the Higgs VEV much smaller than the diagonal soft mass terms $\tilde{m}_L^2 \tilde{\mu}_L \tilde{\mu}_L$ and $\tilde{m}_R^2 \tilde{\mu}_R \tilde{\mu}_R$ [see the matrix form (64)]. Indeed, one should typically have $\tilde{m}_{L,R}^2 \gtrsim 10^4 \text{ GeV}^2$ so that smuon mass eigenvalues are not excluded by the conservative current experimental lower bound $m_{\tilde{\mu}_1} > 94 \text{ GeV}$ [50,102].

The other off-diagonal $\tilde{\mu}_L \tilde{\mu}_R$ contribution to the smuon mass is at most $m_{\mu,\mu} \tan\beta \sim 510^3 \text{ GeV}^2$, for extremely optimized parameter values, so that this contribution remains also systematically smaller than $\tilde{m}_{L,R}^2 \gtrsim 10^4 \text{ GeV}^2$. Hence the two left-right mass mixing terms are limited in 4D mSUGRA, relative to the complete diagonal elements of the 2×2 smuon squared mass matrix.

In the RS version of mSUGRA, one has a trilinear-induced mass term $A_\mu \mathcal{Y}_\mu e^{-k\pi R_c} \hat{v}_d f_L^0 f_R^0$, where the $f_{L/R}^0$ wave function values at $y = \pi R_c$ are not constrained from above by the muon mass because $f_{L/R}^0 = f_0^{++}(c_{\tilde{\mu}_{L/R}}; \pi R_c)$, whereas the muon mass is controlled by independent fermionic 5D parameters $c_{\mu_{L/R}}$ in the present SUSY-breaking scheme.

Similarly, the off-diagonal left-right smuon squared mass $\mu_{\text{eff}} \mathcal{Y}_\mu \hat{v}_d \tan\beta f_L^0 f_R^0$ of Eq. (46) can take benefit from large factors from the scalar wave function overlaps with the Higgs brane, while $\tan\beta$ takes comparable values as in 4D SUSY and $\mathcal{Y}_\mu \sim 1/k$ is compensated by $f_L^0 f_R^0 \propto k$ [cf. Eq. (B13)]. Therefore, in contrast to the 4D mSUGRA case, the off-diagonal mixing smuon mass terms are not constrained by the muon mass and can thus get higher values.

In consequence, the left-right mass mixing for smuon masses can reach higher amounts within RS mSUGRA

than in 4D mSUGRA. In turn (having a universal mass m_0 tends to have a configuration with identical diagonal squared masses), the splitting between the mass eigenvalues $m_{\tilde{\mu}_1}$ and $m_{\tilde{\mu}_2}$ can be much larger as Fig. 15 illustrates.

In order to obtain this figure, we have scanned the input parameters over these ranges: $\tan\beta \in [1; 60]$, $m_0 \in [300; 2000] \text{ GeV}$, $m_{1/2} \in [150; 600] \text{ GeV}$, $c_{\tilde{L}/R} \in [-1, 1]$, and $A_\mu, A_\mu|_{\text{eff}} \in [0; 1000] \text{ GeV}$ (see the above discussion). The interval on $\tan\beta$ corresponds to the domain allowed by the Higgs potential minimization conditions in mSUGRA [66]. The choice of m_0 and $m_{1/2}$ ranges is based on the constraints coming from SUSY searches at colliders combined with the requirement that the lightest supersymmetric particle (LSP) is not the tau lepton superpartner (the stau) [102,106]; taking higher m_0 and $m_{1/2}$ values does not modify significantly the scan presented in Fig. 15. The output smuon mass ranges (i.e., the shown plot domain in Fig. 15) is motivated by the order of magnitude of the usual effective 4D SUSY-breaking scale—near the EWSB scale—allowing one to protect the Higgs boson against too dramatic mass fine-tuning. The scans here are not done for negative values of the A_μ (or $A_\mu|_{\text{eff}}$) terms, and the μ (or μ_{eff}) terms are not taken negatively, but choosing the opposite signs would not change the present conclusions. Besides, only values in the range $[100; 1000] \text{ GeV}$ have been kept for the $|\mu|$ (or $|\mu_{\text{eff}}|$) quantity; this is imposed by the orders of experimental bounds and the Higgs potential minimization conditions already mentioned. The last remark, as before, is that having chosen slightly larger parameter ranges—staying with the same orders of magnitude physically motivated—would have not affected significantly the obtained numerical results shown in this part.

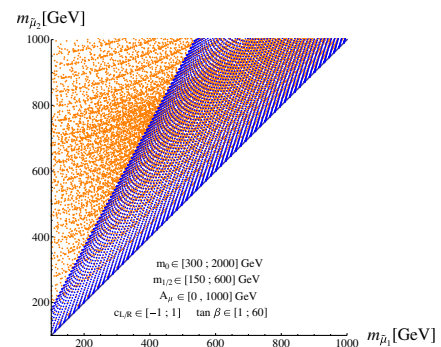


FIG. 15 (color online). Points obtained in the plan $m_{\tilde{\mu}_2}$ versus $m_{\tilde{\mu}_1}$ (in GeV), for an mSUGRA-type scenario within 4D SUSY [blue points] and RS SUSY [orange points], from a scan performed in the intervals indicated on the plot. The interval indicated on A_μ corresponds to the range for the soft trilinear coupling A_μ in 4D SUSY and for the $A_\mu|_{\text{eff}}$ effective dimension-one parameter defined in RS SUSY (see the text). $c_{L/R} = c_{\tilde{\mu}_{L/R}}$ denote now the 5D smuon parameters.

In conclusion, if a $m_{\tilde{\mu}_2}$ measurement is obtained at the ILC or even at the LHC at a value larger—including the experimental uncertainty in this comparison—than the 4D SUSY upper limit appearing in Fig. 15 for a given $m_{\tilde{\mu}_1}$ value (assumed to be measured also), this result would rule out the 4D mSUGRA scenario [at least in its simplest form] and constitute a good indication for an RS mSUGRA model. Indeed, all $m_{\tilde{\mu}_2}$ values above the upper 4D mSUGRA limit can be reached within RS mSUGRA as shown by the scan over parameters. Such a discrimination should be already possible at the LHC given the accuracies expected on slepton mass reconstructions: A $\sim 5\%$ – 10% uncertainty is reasonable to expect [104] and clearly sufficient in a large part of parameter space (at high $m_{\tilde{\mu}_2}$) for the proposed potential test—given the large mass splitting reachable theoretically in RS mSUGRA [illustrated in Fig. 15]. This typical uncertainty of $\sim 5\%$ – 10% on the smuon mass corresponds to illustrative examples studied in Ref. [104], but, of course, this performance will be quite model- and parameter-dependent and can be improved by combining different related mass measurements. Note that the present experimental bound $m_{\tilde{\mu}_1} > 94$ GeV [50,102] is respected on the plot of Fig. 15.

C. H boson decays

The phenomenological framework of this section is the same as the one described in Sec. III B. We have seen that in this RS framework the interactions between Higgs bosons and sfermions can be significantly increased with respect to the 4D SUSY case. This is mainly due to the fact that the 5D $c_{\tilde{f}_{L/R}}$ parameters involved in these Higgs interactions are quite free (more precisely, $c_{\tilde{f}_{L/R}}$ affect only squark and slepton masses) in RS SUSY, whereas the same Higgs interactions are fixed by SM Yukawa coupling constants (related to SM fermion masses) in 4D SUSY. In this section, we will look at the effects of these increases on Higgs decay branching ratios. The analysis emphasis will be put on the example of the heaviest neutral Higgs boson H as, kinematically, the lightest h field (being heavier than ~ 91 GeV from LEP results but smaller than ~ 140 GeV from SUSY Higgs structure [66]) cannot decay into pairs of on-shell sfermions (having lower experimental limits of $\sim 10^2$ GeV [50,102]) and hence does not feel optimal RS effects, except of course if the theoretical upper limit on its mass m_h can really be sufficiently relaxed in warped SUSY [43]. The pseudoscalar field A and charged Higgs boson H^\pm can similarly have increased decay widths into sleptons, as we will show occurs for H in RS SUSY.

Technically, the branching ratio formulas for Higgs bosons can be found in Ref. [66] together with EW and next-to-leading-order radiative corrections. We have included the leading corrections involved: the b quark

running mass and the radiative corrections to the neutral Higgs boson masses m_h and m_H , as well as the corrections to the trilinear Higgs coupling $\Delta\lambda_{Hhh}$ within the ϵ approximation (see Ref. [66], Sec. 1.3.3, for details).

These branching ratios depend on the various Higgs couplings; in RS SUSY, the H boson couplings to SM fermions, Higgs or gauge bosons, and Higgsinos or gauginos are taken as in 4D SUSY (since heavy KK mixing and exchange effects are neglected as mentioned above), while the H sleptons are deduced from top squark couplings incouplings to squarks—Eq. (21)—and rotation to the sfermion mass basis.

The higher-dimensional parameters entering these effective H couplings to squarks or sleptons are $c_{\tilde{q}_{L/R}}$, $c_{\tilde{\ell}_{L/R}}$ (with absolute values around unity), μ_{eff} [see Eq. (22)], and $A|_{\text{eff}} = Ake^{-k\pi R_c} \sim \text{TeV}$, which appears in the scalar coupling matrix of Eq. (21). The TeV scale parameter μ_{eff} ($A|_{\text{eff}}$) will be taken numerically as μ (A) in 4D SUSY. Similarly, the effective quantity $\tilde{m}_{L/R}|_{\text{eff}} = (\tilde{m}_{L/R}ke^{-2k\pi R_c})^{1/2} \sim \text{TeV}$ that shows up in scalar mass matrices of type (46) is taken numerically approximately equal to the 4D soft mass $\tilde{m}_{L/R} \sim \text{TeV}$ [see Eq. (64)]. We denote as usual the effective 4D soft gaugino masses for the bino and wino, respectively, M_1 and M_2 .

In Fig. 16, we show the branching ratios for the main decay channels of the H boson as a function of its mass for a given set of parameters. Both 4D and 5D SUSY scenarios are represented. The tree-level Higgs mass m_H (like m_h and the neutral Higgs mixing angle α) depends on the parameter $\tan\beta$ and on m_A (pseudoscalar mass) which has been varied (above ~ 200 GeV) to span the m_H interval in Fig. 16. The modifications of radiative corrections due to heavy KK modes are expected to raise Higgs masses by an amount of at most $\mathcal{O}(10)$ GeV [43], so that Fig. 16 would not be significantly affected by those. The heavy Higgs mass and $\tan\beta$ ranges considered in Fig. 16 and in the following Higgs branching ratio plots, namely, $m_H \in [200, 1000]$ GeV and $\tan\beta \in [6, 30]$ [107], are clearly in agreement with the several constraints coming from direct charged and neutral Higgs boson searches at LEP [66] or Tevatron run II [102] within a SUSY framework. The modifications of these constraints due to KK mode effects should not be significant here for $M_{\text{KK}} \gtrsim 3$ TeV (cf. Sec. II A).

For the sake of convenience, in this section, we write only the sets of parameter values in the captions of Higgs branching ratio plots. But let us give here some general comments about these sets chosen in the plots. First, the branching ratios are shown for either positive or negative values of the A (or $A|_{\text{eff}}$) and μ (or μ_{eff}) terms as these signs do not affect the main ratio behaviors. Second, all the superpartner mass eigenvalues considered respect their last conservative or combined experimental lower limits derived from direct SUSY searches at colliders [50,102,108], some of which we quote here for

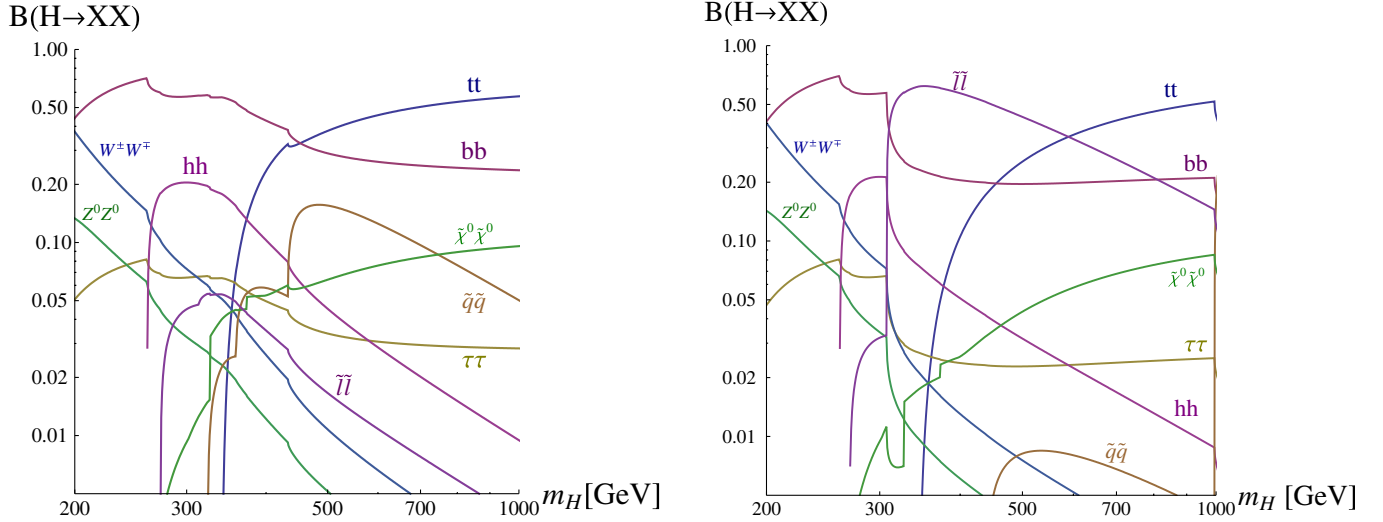


FIG. 16 (color online). Branching ratios of the H boson decays as a function of its mass m_H (in GeV) within pure SUSY [left] and RS SUSY [right]. The types of final states are indicated directly on the plot; all kinematically allowed channels for neutralinos (among $\tilde{\chi}_i^0 \tilde{\chi}_j^0$, with $i, j = \{1, 2, 3, 4\}$) and squarks and sleptons are summed. The τ lepton channel is included but not the ones with branching ratios below $\sim 10^{-2}$ in this m_H range (like the triangular-loop-induced decays into photons and gluons). The values for the gaugino sector parameters in the two plots are $\mu = \mu_{\text{eff}} = 170$ GeV, $\tan\beta = 6$ and $M_1 = 160$ GeV, $M_2 = 1000$ GeV, leading to the neutralino masses $m_{\tilde{\chi}_1^0} \approx 128$ GeV and $m_{\tilde{\chi}_2^0} \approx 174$ GeV and lightest chargino mass $m_{\tilde{\chi}_1^\pm} \approx 167$ GeV. The other common parameters are taken at $A_t|_{\text{eff}} = A_t = A_b = A_\nu = A_{\ell^\pm} = -500$ GeV. The soft masses in 4D SUSY are $\tilde{m}_L^q = 170$ GeV and $\tilde{m}_R^q = 1000$ GeV for the squarks and $\tilde{m}_L^\ell = 180$ GeV and $\tilde{m}_R^\ell = 1000$ GeV for the sleptons. For this set of parameters, the smallest mass eigenvalues obtained are $m_{\tilde{\nu}_{\mu 1}} \approx m_{\tilde{\nu}_{\tau 1}} \approx 169$ GeV for sneutrinos, $m_{\tilde{\mu}_1} \approx m_{\tilde{\tau}_1} \approx 186$ GeV for charged sleptons, $m_{\tilde{t}_1} \approx 216$ GeV for the top squark, and $m_{\tilde{b}_1} \approx 179$ GeV for the sbottom quark. In RS SUSY, the effective soft masses are $\tilde{m}_L^q|_{\text{eff}} = 275$ GeV, $\tilde{m}_R^q|_{\text{eff}} = 1000$ GeV, $\tilde{m}_L^\ell|_{\text{eff}} = 105$ GeV, and $\tilde{m}_R^\ell|_{\text{eff}} = 1000$ GeV leading to $m_{\tilde{\nu}_{\mu 1}} \approx m_{\tilde{\nu}_{\tau 1}} \approx 135$ GeV, $m_{\tilde{\mu}_1} \approx m_{\tilde{\tau}_1} \approx 154$ GeV, and $m_{\tilde{t}_1} \approx m_{\tilde{b}_1} \approx 218$ GeV, while the 5D parameters are $c_{\tilde{q}_L} = c_{\tilde{q}_R} = 0.2$ for squarks and $c_{\tilde{\ell}_L} = c_{\tilde{\ell}_R} = -0.5$ for sleptons (for all flavors).

comparison: $m_{\tilde{\chi}_1^0} > 120$ GeV, $m_{\tilde{\chi}_2^0} > 116$ GeV, $m_{\tilde{\chi}_1^\pm} > 164$ GeV, $m_{\tilde{\nu}_1} > 120$ GeV, $m_{\tilde{\ell}_1} > 107$ GeV, $m_{\tilde{t}_1} > 95$ GeV, and $m_{\tilde{b}_1} > 89$ GeV. In order to compare the Higgs couplings via its branching ratios, we have chosen the parameters so that the superpartner mass eigenvalues are approximately identical in the 4D and 5D pMSSM (KK corrections might be up to a few percent and are irrelevant in this analysis); this is also motivated by the present philosophy of developing tests of discrimination between the two SUSY scenarios (4D versus 5D) for a situation where light SUSY particles would have been discovered [and thus their masses at least approximately estimated]. Note also that the lightest neutralino is systematically the LSP in our choices of parameters so that $\tilde{\chi}_1^0$ represents the potential candidate for dark matter as in usual 4D SUSY theories. In order to minimize the corrections to EW observables, we have further imposed $A_t = A_b, A_\nu = A_\ell$, and $\tilde{m}_{L/R}^d = \tilde{m}_{L/R}^d$ for soft squark masses and $\tilde{m}_L^\nu = \tilde{m}_L^\nu$ for the slepton ones (in the RS case as well). Finally, the sfermion mass matrices as well as soft trilinear scalar couplings are taken universal for all families and diagonal in the flavor basis (which guarantees the absence of FCNC at tree level) as motivated by the SUSY flavor problem. Note that these hypotheses imply the absence of flavor mixing in the scalar

sector which allows a better identification of the smuon and top squark studied in Secs. III B and III D. We also assume that all phases in the soft SUSY-breaking potential are zero to eliminate all new sources of CP violation. Those assumptions are characteristic of the pMSSM [58].

For simplifying the discussion on this first Fig. 16, we have chosen large effective TeV-brane soft masses $\tilde{m}_R^{q,\ell}$ and $\tilde{m}_L^{q,\ell}|_{\text{eff}}$ so that the heaviest sfermion mass eigenvalues become large enough to close the associated channels $H \rightarrow \tilde{f}_1 \tilde{f}_2$ and $\tilde{f}_2 \tilde{f}_2$. We see in Fig. 16 that by starting from a 4D SUSY regime where the W^\pm boson, top quark, and lightest neutral Higgs channels are dominant (the top dominance is due, in particular, to the low $\tan\beta$ regime increasing the top-Higgs coupling) and then moving to the RS case with small $c_{\tilde{\ell}_{L/R}}$ values, the slepton channel is globally increased and even becomes dominant at intermediate m_H values. This slepton channel has a width decreasing with the third power of the H mass which explains its branching behavior on the plot. The first reason for having larger slepton branching ratios in that RS case is that the slepton-Higgs couplings are favored by the large wave function overlaps between sleptons and the localized Higgs boson induced by the small $c_{\tilde{\ell}_{L/R}}$ values taken. The other reason, of the same kind, is the choice of large $c_{\tilde{q}_{L/R}}$

reducing the squark overlaps with Higgs bosons relatively to the 4D SUSY case. Indeed, one can clearly observe, by comparing the two plots of Fig. 16, the decrease of the branching ratio $B(H \rightarrow \tilde{q} \tilde{q})$ in RS which leads to an increase of $B(H \rightarrow \tilde{\ell} \tilde{\ell})$.

We now present in Fig. 17 the branching ratios for the main decay channels of the H boson as a function of m_H for another set of parameters [specified in the caption]. The soft masses \tilde{m}_R^q , in particular, are smaller than in the previous figure so that the top squark masses are smaller and channels into the heaviest state \tilde{q}_2 open up, leading to a dominant squark channel at intermediate m_H in the 4D SUSY case. The $M_{1,2}$ parameters are also typically lower than in Fig. 16, so that channels into charginos open up and neutralino channels have larger phase space factors, which modifies the branching profiles rendering, in particular, the various gaugino channels dominant above $m_H \approx 800$ GeV in 4D SUSY. We see as well in Fig. 17 that, compared to this new 4D SUSY regime with alternatively dominant squark and bottom channels, in RS the slepton channel rates can again be greatly enhanced (and still become dominant at intermediate m_H) for small enough $c_{\tilde{\ell}_{L/R}}$ values increasing the slepton-Higgs couplings. This enhancement of $B(H \rightarrow \tilde{\ell} \tilde{\ell})$ is also correlated with the large $c_{\tilde{q}_{L/R}}$ values allowing one to have small squark-Higgs couplings relatively to 4D SUSY and, in turn, to have small amounts of $B(H \rightarrow \tilde{q} \tilde{q})$. We note from the RS plot that $B(H \rightarrow \tilde{\ell} \tilde{\ell})$

reaches values a bit smaller than $\sim 50\%$, whereas it was above $\sim 60\%$ in Fig. 16, which is due to the $\tilde{m}_L^\ell|_{\text{eff}}$ value taken larger here.

We present in Fig. 18 the branching ratios for the main H decay channels as a function of m_H in the high $\tan\beta$ regime. We see in this figure that, by starting from such a 4D SUSY regime where the bottom channel is extremely dominant and going to the RS case, the Higgs-to-slepton branching ratio is largely enhanced—once again due to the small $c_{\tilde{\ell}_{L/R}}$ values—reaching significant levels around 20% and even dominantly at $\sim 40\%$ for a large m_H (thanks to the $H \rightarrow \tilde{\ell}_1 \tilde{\ell}_2$ opening). This $B(H \rightarrow \tilde{\ell} \tilde{\ell})$ enhancement is also due to the large $c_{\tilde{q}_{L/R}}$ values, which tend to suppress $B(H \rightarrow \tilde{q} \tilde{q})$ relatively to the 4D SUSY configuration. The reasons why the H decay width into sleptons cannot be comparable in size to the one for bottom quark final states, at $m_H \lesssim 800$ GeV in RS, are the large $\tan\beta$, phase space, and color factor.

Of course, in the different configuration of relatively high $c_{\tilde{\ell}_{L/R}}$ values, the slepton-Higgs couplings, and in turn the associated Higgs channels, are not significantly increased with respect to the 4D pMSSM, as illustrated in Fig. 19 in a low $\tan\beta$ example; note that in the RS case the sneutrino channel opens up at a larger m_H due to sneutrinos being a bit heavier than in the 4D case. The main difference between the two plots of Fig. 19 is the decrease of the squark channel in RS due to still quite large $c_{\tilde{q}_{L/R}}$

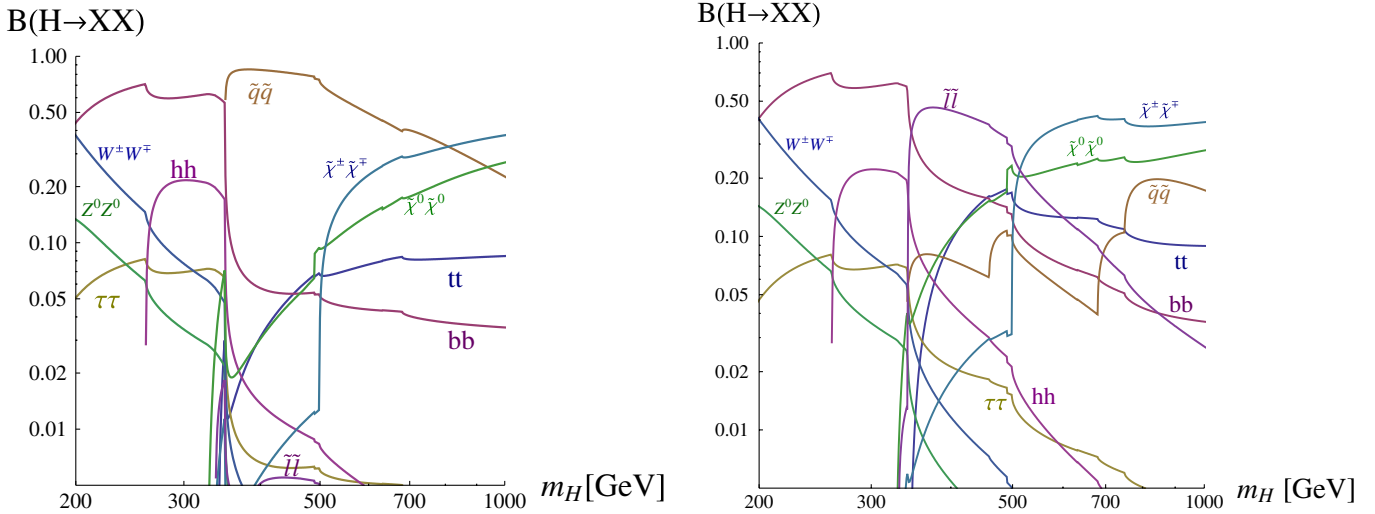


FIG. 17 (color online). Branching ratios of the H boson decays as a function of its mass m_H (in GeV) within pure SUSY [left] and RS SUSY [right]. The types of final states are indicated directly on the plot; all kinematically allowed channels for neutralinos (among $\tilde{\chi}_i^0 \tilde{\chi}_j^0$, with $i, j = \{1, 2, 3, 4\}$), charginos (among $\tilde{\chi}_k^\pm \tilde{\chi}_l^\mp$, with $k, l = \{1, 2\}$), and squarks and sleptons are summed, as in Fig. 16. The values for the gaugino sector parameters are $\mu = \mu_{\text{eff}} = 300$ GeV, $\tan\beta = 6$, $M_1 = 600$ GeV, and $M_2 = 190$ GeV leading to $m_{\tilde{\chi}_1^0} \approx 163$ GeV, $m_{\tilde{\chi}_2^0} \approx 305$ GeV, and $m_{\tilde{\chi}_1^\pm} \approx 164$ GeV. The other common parameters are $A_t|_{\text{eff}} = A_t = A_b = -200$ GeV and $A_\nu|_{\text{eff}} = A_\nu = A_{e^\pm} = -300$ GeV. The soft masses in 4D SUSY are $\tilde{m}_L^q = 210$ GeV, $\tilde{m}_R^q = 220$ GeV, and $\tilde{m}_{L/R}^\ell = 180$ GeV, which give rise to $m_{\tilde{\nu}_{\mu 1}} \approx m_{\tilde{\nu}_{\tau 1}} \approx 169$ GeV, $m_{\tilde{\mu}_1} \approx m_{\tilde{\tau}_1} \approx 175$ GeV, $m_{\tilde{t}_1} \approx 175$ GeV, and $m_{\tilde{b}_1} \approx 206$ GeV. In RS SUSY, the effective soft masses are $\tilde{m}_L^q|_{\text{eff}} = 500$ GeV, $\tilde{m}_R^q|_{\text{eff}} = 260$ GeV, $\tilde{m}_L^\ell|_{\text{eff}} = 125$ GeV, and $\tilde{m}_R^\ell|_{\text{eff}} = 1000$ GeV, giving $m_{\tilde{\nu}_{\mu 1}} \approx m_{\tilde{\nu}_{\tau 1}} \approx 165$ GeV, $m_{\tilde{\mu}_1} \approx m_{\tilde{\tau}_1} \approx 171$ GeV, $m_{\tilde{t}_1} \approx 171$ GeV, and $m_{\tilde{b}_1} \approx 229$ GeV, while the 5D parameters are $c_{\tilde{q}_L} = c_{\tilde{b}_R} = 0$, $c_{\tilde{t}_R} = 0.3$, and $c_{\tilde{\ell}_{L/R}} = -0.5$.

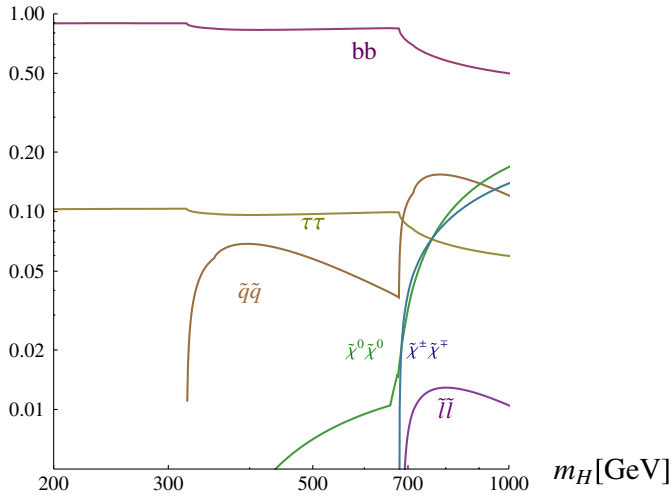
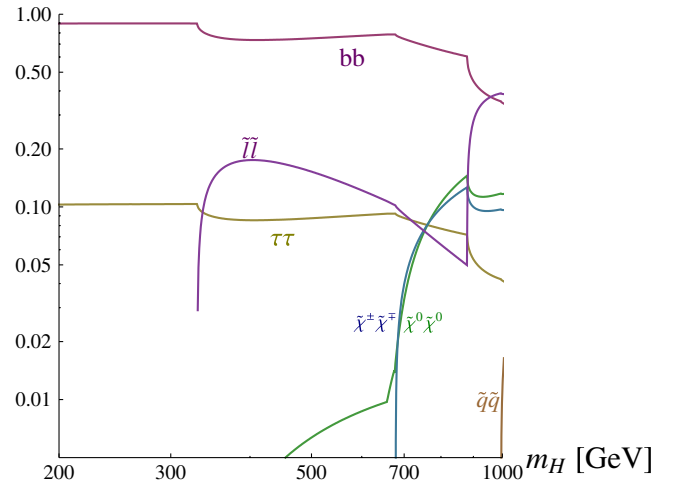
$B(H \rightarrow XX)$  $B(H \rightarrow XX)$ 

FIG. 18 (color online). Branching ratios for the H boson decays as a function of m_H (in GeV) within pure SUSY [left] and RS SUSY [right]. The types of final states are indicated directly on the plot; all kinematically allowed channels for neutralinos, charginos, and squarks or sleptons are summed, as in previous figures. The values for the gaugino sector parameters are $\mu = \mu_{\text{eff}} = 170$ GeV, $\tan\beta = 30$, and $M_1 = M_2 = 500$ GeV, leading to $m_{\tilde{\chi}_1^0} \approx 157$ GeV, $m_{\tilde{\chi}_2^0} \approx 176$ GeV, and $m_{\tilde{\chi}_1^\pm} \approx 164$ GeV. The trilinear couplings read as $A_t|_{\text{eff}} = A_t = A_b = -A_\nu = -A_{\ell^\pm} = -500$ GeV. The 4D soft masses are $\tilde{m}_L^q = 170$ GeV, $\tilde{m}_R^q = 500$ GeV, $\tilde{m}_L^\ell = 180$ GeV, and $\tilde{m}_R^\ell = 500$ GeV, which give $m_{\tilde{\nu}_{\mu 1}} \approx m_{\tilde{\nu}_{\tau 1}} \approx 168$ GeV, $m_{\tilde{\mu}_1} \approx m_{\tilde{\tau}_1} \approx 185$ GeV, $m_{\tilde{t}_1} \approx 160$ GeV, and $m_{\tilde{b}_1} \approx 177$ GeV. In RS SUSY, the effective soft masses are $\tilde{m}_L^q|_{\text{eff}} = 275$ GeV, $\tilde{m}_R^q|_{\text{eff}} = 1000$ GeV, $\tilde{m}_L^\ell|_{\text{eff}} = 130$ GeV, and $\tilde{m}_R^\ell|_{\text{eff}} = 500$ GeV, giving $m_{\tilde{\nu}_{\mu 1}} \approx m_{\tilde{\nu}_{\tau 1}} \approx 172$ GeV, $m_{\tilde{\mu}_1} \approx m_{\tilde{\tau}_1} \approx 165$ GeV, and $m_{\tilde{t}_1} \approx m_{\tilde{b}_1} \approx 219$ GeV, while the 5D parameters are $c_{\tilde{q}_{L/R}} = 0.2$ and $c_{\tilde{\ell}_{L/R}} = -0.5$.

parameters (for smaller $c_{\tilde{q}_{L/R}}$, one would recover branching profiles similar to those in 4D SUSY). This leads, in particular, to an increase of $B(H \rightarrow \tilde{\chi}^\pm \tilde{\chi}^\mp, \tilde{\chi}^0 \tilde{\chi}^0)$. Finally, for a better understanding of Fig. 19, we remark

that in RS the slepton masses are mainly generated through large TeV-brane soft masses (reduced to the EWSB scale by wave function overlap factors) since the masses induced by Yukawa-type couplings to the Higgs VEV are

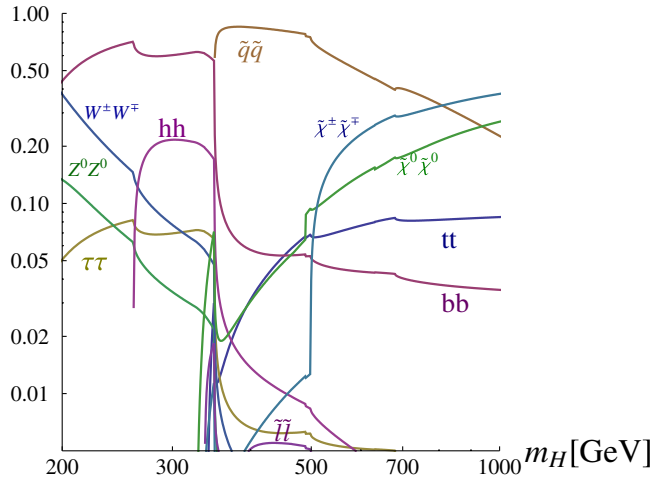
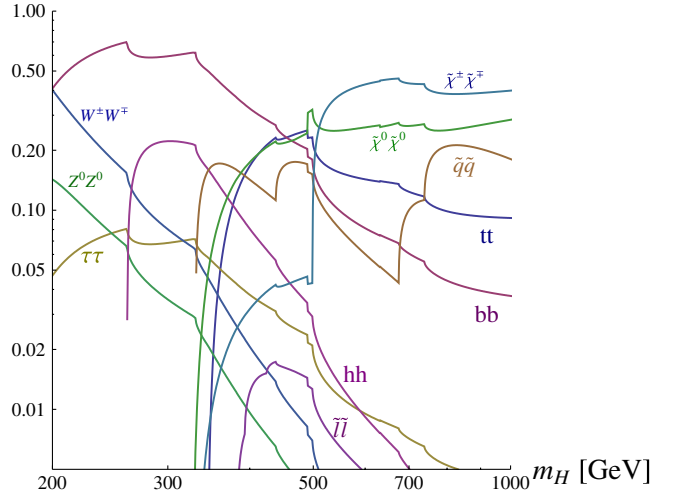
 $B(H \rightarrow XX)$  $B(H \rightarrow XX)$ 

FIG. 19 (color online). Branching ratios for the H boson decays as a function of m_H (in GeV) within pure SUSY [left] and RS SUSY [right]. The types of final states are indicated directly on the plot. The parameters in the Higgsino or gaugino sector, the scalar trilinear couplings, and the soft masses in 4D SUSY are the same as in Fig. 17 so that the left plot here is identical to the left plot of Fig. 17. In RS SUSY, the effective soft masses are $\tilde{m}_L^q|_{\text{eff}} = 500$ GeV, $\tilde{m}_R^q|_{\text{eff}} = 250$ GeV, $\tilde{m}_L^\ell|_{\text{eff}} = 1000$ GeV, and $\tilde{m}_R^\ell|_{\text{eff}} = 800$ GeV, giving $m_{\tilde{\nu}_{\mu 1}} \approx m_{\tilde{\nu}_{\tau 1}} \approx 197$ GeV, $m_{\tilde{\mu}_1} \approx m_{\tilde{\tau}_1} \approx 169$ GeV, $m_{\tilde{t}_1} \approx 165$ GeV, and $m_{\tilde{b}_1} \approx 219$ GeV, while the 5D parameters are $c_{\tilde{q}_L} = c_{\tilde{b}_R} = 0$, $c_{\tilde{t}_R} = 0.3$, and $c_{\tilde{\ell}_{L/R}} = +0.49$.

suppressed by the present high $c_{\tilde{\ell}_{L/R}}$ values. For comparison, within 4D SUSY, the soft masses in Fig. 19 are smaller (roughly at the EWSB scale) since those are not suppressed by overlap factors, while the masses induced by Yukawa coupling constants are negligible due to the tiny lepton masses.

Let us summarize this part on Higgs decays and conclude. In order to maximize the H couplings to sleptons in 4D SUSY, the A terms have been taken of the order of the TeV and not at zero. The slepton masses have also been taken close to their lower experimental limits to maximize the branching ratios of the slepton channel in 4D SUSY. However, we have found that even in these optimal cases the slepton channel branchings cannot reach amounts above $\sim 5\%$ (in agreement with Ref. [66]) while important slepton branchings can arise in RS—where $B(H \rightarrow \tilde{\ell} \tilde{\ell})$ can reach up to $\sim 60\%$ [even larger ratios are accessible, for instance, by decreasing again $c_{\tilde{\ell}_{L/R}}$ with respect to present values or by introducing a right-handed (s)neutrino]. Besides, the other way to try to increase the slepton channel branching ratio in 4D SUSY is to decrease the other branching ratios: For that purpose, we have explored—keeping trilinear couplings at the TeV scale—the main typical domains of 4D SUSY(-breaking) parameter space characterized by different types of dominant H decay channels. The conclusion was still that the slepton channel rate can never be as important as it can be in RS. Furthermore, the case of a dominant slepton channel can occur in RS (see, e.g., Fig. 17), whereas it is impossible in 4D SUSY. This is due to the fact that in 4D SUSY slepton-Higgs couplings are severely constrained by the small Yukawa coupling constants of SM leptons. Therefore, the experimental observation of either a dominant slepton channel or a slepton channel with, e.g., $B(H \rightarrow \tilde{\ell} \tilde{\ell}) \simeq 50\%$ would exclude the 4D pMSSM and indicate the possible existence of a warped version of the pMSSM. Such a potential test should, in principle, be doable at colliders; a four-momentum reconstruction of slepton

cascade decays based on measured slepton masses could allow one to identify the decay channel $H \rightarrow \tilde{\ell} \tilde{\ell}$, which is necessary to estimate its branching ratio—or (it would be sufficient here) a lower bound on this ratio. This kinematics approach being experimentally challenging, one could also use the clean leptonic event topology to identify the slepton channel. Indeed, the decay $H \rightarrow \tilde{\ell} \tilde{\ell}$ would lead to final states with an higher lepton multiplicity due to the decay $\tilde{\ell} \rightarrow \ell \tilde{\chi}_1^0$ (recall that $\tilde{\chi}_1^0$ is the LSP).

D. Top squark pair production at the ILC

In this part we consider the particularly clean environment of the future leptonic collider, the ILC, and we focus on the squark pair production which occurs only through s -channel exchanges. In 4D SUSY, as is well known, the top squark can be especially light due to its large left-right mass mixing terms favored by strong Yukawa coupling constants. We will first provide the theoretical tools needed for computing the more general cross section of the sfermion pair production through neutral SM gauge boson exchanges, namely, $e^+ e^- \rightarrow \tilde{f}_i \tilde{f}_j$ ($i, j = \{1, 2\}$ labeling the mass eigenstates), in the 4D pMSSM. Then, after a discussion on the KK squark mixing effects, we will analyze numerically the obtained cross sections in the two RS SUSY-breaking frameworks discussed previously (see the discussion on Fig. 13): with and without brane soft terms. Note that we concentrate here on the top squark $\tilde{t}_{1,2}$ states and do not specify the structure of the sector made of the first generations of sfermions.

1. Formal cross section

Let us describe the cross section for the reaction $e^+ e^- \rightarrow \tilde{f}_i \tilde{f}_j$ [$i, j = \{1, 2\}$] proceeding via the exchanges of the EW neutral gauge bosons—photon (γ) and Z boson—in the s channel. For polarized electron and positron beams, this cross section has the following form at tree level (it can be found with more details in Ref. [113]):

$$\begin{aligned} \sigma(e^+ e^- \rightarrow \tilde{f}_i \tilde{f}_j) &= \frac{\pi \alpha^2 \kappa_{ij}^3}{s^4} \left((Q_{e.m.}^f)^2 \delta_{ij} (1 - \mathcal{P}_- \mathcal{P}_+) - \frac{Q_{e.m.}^f c_{ij} \delta_{ij}}{2c_W^2 s_W^2} [v_e (1 - \mathcal{P}_- \mathcal{P}_+) - a_e (\mathcal{P}_- - \mathcal{P}_+)] \mathbf{D}_{\gamma Z} \right. \\ &\quad \left. + \frac{c_{ij}^2}{16s_W^4 c_W^4} [(v_e^2 + a_e^2)(1 - \mathcal{P}_- \mathcal{P}_+) - 2a_e v_e (\mathcal{P}_- - \mathcal{P}_+)] \mathbf{D}_{ZZ} \right), \end{aligned} \quad (71)$$

where $s_W \equiv \sin \theta_W$, $c_W \equiv \cos \theta_W$, $v_e = 4s_W^2 - 1$, and $a_e = -1$ are the vector and axial-vector couplings of the electron to the Z boson, whereas $Q_{e.m.}^f$ is the electric charge of the sfermion supersymmetric partner f . \mathcal{P}_\pm denote the degree of polarization of the e^\pm beams, with the convention $\mathcal{P}_\pm = -1, 0, +1$ for the left-polarized, unpolarized, and right-polarized e^\pm beams, respectively (e.g., $\mathcal{P}_- = -0.9$ means that 90% of the electrons are left-polarized

and the rest are unpolarized). c_{ij} is the $Z \tilde{f}_i \tilde{f}_j$ coupling matrix (up to a factor $1/c_W$)

$$c_{ij} = \begin{pmatrix} I_{3L}^f \cos^2 \theta_{\tilde{f}} - Q_{e.m.}^f s_W^2 & -\frac{1}{2} I_{3L}^f \sin 2\theta_{\tilde{f}} \\ -\frac{1}{2} I_{3L}^f \sin 2\theta_{\tilde{f}} & I_{3L}^f \sin^2 \theta_{\tilde{f}} - Q_{e.m.}^f s_W^2 \end{pmatrix}, \quad (72)$$

where $\theta_{\tilde{f}}$ is the sfermion mixing angle defined by

$$\tilde{f}_1 \equiv \cos\theta_{\tilde{f}}\tilde{f}_{L} + \sin\theta_{\tilde{f}}\tilde{f}_{R}, \quad \tilde{f}_2 \equiv \cos\theta_{\tilde{f}}\tilde{f}_{R} - \sin\theta_{\tilde{f}}\tilde{f}_{L}. \quad (73)$$

In the 4D pMSSM, this mixing angle is calculated from the diagonalization of the pMSSM top squark mass matrix previously given in Eq. (64). In the RS SUSY setup, it is obtained from the mass matrix derived in Eq. (46) [possibly including mixings with KK modes]. Finally, in Eq. (71), \sqrt{s} is the center-of-mass energy, $\kappa_{ij} = [(s - m_{\tilde{f}_i}^2 - m_{\tilde{f}_j}^2)^2 - 4m_{\tilde{f}_i}^2 m_{\tilde{f}_j}^2]^{1/2}$, and

$$\mathbf{D}_{ZZ} = \frac{s^2}{(s - m_Z^2)^2 + \Gamma_Z^2 m_Z^2}, \quad (74)$$

$$\mathbf{D}_{\gamma Z} = \frac{s(s - m_Z^2)}{(s - m_Z^2)^2 + \Gamma_Z^2 m_Z^2},$$

$\Gamma_Z = 2.4952 \pm 0.0023$ GeV [50] being the full decay width of the Z boson.

2. On the difficulty to distinguish 4D and RS SUSY in custodial realizations

In our previous studies of Secs. III B and III C, the KK sfermion mixing effects were subleading relatively to the studied structural effects on scalar masses and couplings. In the RS realization with a gauge custodial symmetry in the bulk, having specific BC KK states (the so-called ‘‘custodians’’) with theoretically possible low masses in the particle spectrum [114], there is *a priori* a hope that KK mixings bring other potential signatures of the warped SUSY version. In this section we thus study the RS version with an implementation of the $SU(2)_L \times SU(2)_R \times U(1)_X$ gauge custodial symmetry in the bulk (introduced in Sec. II A). The custodians are the new fermions—without zero modes—filling the $SU(2)_R$ representations to which matter (MS)SM (super)fields are promoted. Being in a SUSY context, we thus have to embed the custodians into superfields which leads to the theoretical prediction of the existence of custodian superpartners: Let us call them the ‘‘scustodians’’ (those are scalar fields). Since we do not consider a SUSY breaking à la Scherk-Schwarz, the custodians and their associated scustodians possess the same BC and hence identical 5D profiles and KK mass spectra. For instance, in complement to the top squark squark states $\tilde{t}_{L/R}$ and to a possible t' custodian [with the same electric charge as the SM top quark t of which it can be an $SU(2)_R$ partner], we would now have associated scustodians that we denote as $\tilde{t}'_{L/R}$. In RS, it is known that the mixing—induced by the localized Higgs VEV—of the t quark with, e.g., a t' partner is favored since the 5D c_t parameter, expected to be rather small for this third generation, tends to decrease the t' mass $m_{(-+)}^{(1)}(c_t)$ [115] and thus to make it closer to m_t . The t - t' mixing is expected to be larger than the t - $t^{(1)}$ mixing [not characteristic of the bulk gauge custodial realization] because $m_{(-+)}^{(1)}$

can be significantly smaller than $t^{(1)}$ masses [masses of the first KK excitation of SM top quarks which have $(++)$ BC] being above ~ 3 TeV typically from EW precision constraints. More generally, the small $c_{b,t}$ parameters of the third quark generation (b and t) tend to increase the b and t wave function overlaps with the TeV-brane which is the Higgs, a feature which also favors the t - t' or b - b' mixing. One may expect similar effects in the third-generation squark sector (by virtue of the same 5D profiles and KK masses) giving rise possibly to a significant mixing between the top squark squarks $\tilde{t}_{L/R}$ and some light scustodians $\tilde{t}'_{L/R}$ [116]. In our SUSY-breaking scenario where $c_{\tilde{t}} \neq c_t$, the $c_{\tilde{t}}$ parameter would be related to the top squark mass only (no more to the precisely known top quark mass), a freedom that could even reinforce the \tilde{t} - \tilde{t}' mixing. This mixing can affect the $Z\tilde{t}\tilde{t}'$ coupling since the Z charge of the \tilde{t}' , $Q_Z^{\tilde{t}'}$, can be different from the \tilde{t} one, $Q_Z^{\tilde{t}}$ (it is not the case for the photon and gluon couplings). Studying the top squark pair production via the Z exchange is more appropriate at the ILC since the top squark pair production is dominated by the gluon exchange at the LHC. The reaction $e^+e^- \rightarrow \tilde{t}_i\tilde{t}_j$ has also the interest to not involve the W boson nor gaugino contributions.

However, this task of generating significant corrections to the $Z\tilde{t}\tilde{t}'$ vertex, through \tilde{t} - \tilde{t}' mixings and a large difference $Q_Z^{\tilde{t}'} - Q_Z^{\tilde{t}}$, has revealed itself to be quite difficult to realize for the two following reasons. First, strong theoretical constraints hold on the choices of group representations and hence on the Z charge of the \tilde{t}' , $Q_Z^{\tilde{t}'} = I_{3L}^{\tilde{t}'} - (2/3)s_W^2$, due to the gauge structure of Yukawa couplings which has to be invariant under the $SU(2)_L \times SU(2)_R \times U(1)_X$ symmetry (and also allowed by the orbifold symmetry). For example, scalar couplings between \tilde{t} (left or right) and some \tilde{t}' scustodians can be realized only for scustodians with an $SU(2)_L$ isospin equal to $I_{3L}^{\tilde{t}'}/2 \pm 1/2$. Having this, their $Q_Z^{\tilde{t}'}$ cannot be very different from $Q_Z^{\tilde{t}L/R} = Q_Z^{\tilde{t}L/R}$. Second, another (related) origin of suppression in the variation of $Q_Z^{\tilde{t}'}$ is the compensation between various scustodians, e.g., between effects from a $\tilde{t} - \tilde{t}'$ mixing (with $Q_Z^{\tilde{t}'} = Q_Z^{\tilde{t}} + 1/2$) and a $\tilde{t} - \tilde{t}''$ mixing (with $Q_Z^{\tilde{t}''} = Q_Z^{\tilde{t}} - 1/2$). Moreover, the dominant mixing between the \tilde{t}_L and \tilde{t}_R states tends to reduce the mixing effect of scustodians.

Based on an exploration of the parameter space and models, we have found numerically that, even for optimal group representations and scustodian masses set at $\sim 10^2$ GeV [117], the deviations $\delta\sigma_{th}$ induced by the scustodian mixings on the cross section $\sigma(e^+e^- \rightarrow \tilde{t}_i\tilde{t}_j)$ in 4D SUSY cannot be significant in regard to the experimental precision on this cross section measurement one can reasonably expect at the ILC: $\delta\sigma_{exp} \sim 5\%$ [113] ($\sim 1\%$ at most [118]). Hence we must conclude that testing

4D SUSY against RS SUSY, by measuring precisely the cross section $\sigma(e^+e^- \rightarrow \tilde{t}_i \tilde{t}_j)$, is not realistic.

Since the RS SUSY signature of KK top squark (partner) mixing effects on the $\tilde{t}_i \tilde{t}_j$ production is too difficult, one could think of studying off-shell exchanges or mixing effects of KK gauge bosons [119], but then the simpler fermion production, like the top pair production, would probably be more fruitful to consider as no supersymmetric cascade decays should be reconstructed there. Nevertheless, it has already been shown that detecting a resonance tail [our work hypothesis being that no KK (gauge boson) states have been produced on-shell] of KK gluon in $t\bar{t}$ production at the LHC appears to be challenging due to small realistic cross sections [120] (see Ref. [121] for other KK gauge bosons). The indirect effects of such virtual KK mode exchanges in $t\bar{t}$ production at the ILC are more promising [122] but would be polluted by the SUSY background ($\tilde{t}\tilde{t}$ production followed by $\tilde{t} \rightarrow t\tilde{\chi}_1^0$, $t\bar{t}$ at loop level, etc.).

3. Discriminating between RS versions: Bulk versus brane SUSY breaking

In our framework with tree-level SUSY-breaking squark and slepton masses and trilinear A couplings, where we do not specify the mechanism at the origin of SUSY breaking (our phenomenological approach is more “bottom-up-like”), we will show that the top squark pair production at the ILC can be studied in order to differentiate between different variants of RS SUSY: the scenarios with or without soft scalar mass and trilinear A terms on the TeV-brane.

The KK (s)fermion mixings cannot be significant in the top squark pair production—the scustodian mixing is irrelevant (as shown in the previous subsection), and *a fortiori* the same conclusion holds for usual KK top squarks—so that such effects are not considered in this part. The heavy (at least at ~ 3 TeV) KK gauge boson

effects are also neglected in favor of the studied low-energy structural effects in scenarios with and without brane soft mass terms.

In Fig. 20, we present the cross sections for the reaction $e^+e^- \rightarrow \tilde{t}_1 \tilde{t}_1$ as a function of the lightest top squark mass $m_{\tilde{t}_1}$ within the 4D pMSSM and RS pMSSM with(out) soft terms [i.e., top squark masses and trilinear coupling] on the TeV-brane.

Those results are derived from scans on the parameters $c_{\tilde{t}_{L/R}}$, $\tan\beta$, μ (or μ_{eff} [see Eq. (22)], $\tilde{m}_{L/R}$ [$\tilde{m}_{L/R}|_{\text{eff}} = (\tilde{m}_{L/R}k)^{1/2}e^{-k\pi R_c}$ in RS SUSY], and A_t (or $A_t|_{\text{eff}} = A_t k e^{-k\pi R_c}$). As before, the allowed ranges in our scan for each parameter are $\tan\beta \in [2; 50]$, $\mu, \mu_{\text{eff}} \in [100; 1000]$ GeV, $c_{\tilde{t}_{L/R}} \in [-1, 1]$, $\tilde{m}_{L/R}, \tilde{m}_{L/R}|_{\text{eff}} \in [0; 1000]$ GeV, and $A_t, A_t|_{\text{eff}} \in [0; 1000]$ GeV. The experimental constraint on the top squark mass, $m_{\tilde{t}_1} > 95.7$ GeV [50,102], is respected on the plots. Once again, the signs of A_t ($A_t|_{\text{eff}}$) and μ (μ_{eff}) do not affect the present analysis.

The scanned points on the three plots of this figure never cross the drawn lines. The reason is that these lower and upper lines, obtained analytically, correspond, respectively, to the cross sections for the extremal $Z\tilde{t}_1\tilde{t}_1$ couplings $c_{11} = Q_Z^{tR}$ and $c_{11} = Q_Z^{tL}$ associated to $\cos\theta_{\tilde{t}} = 0$ and $\cos\theta_{\tilde{t}} = 1$, as shown in Eq. (72). We also observe that the obtained regions in the plots end up at the kinematic limit as expected.

Finally, Fig. 20 was obtained at a center-of-mass energy $\sqrt{s} = 500$ GeV and for some polarizations of the two beams, $\mathcal{P}_{\pm} = \pm 0.6$, which are realistic for an ILC prospect. Changing these experimental inputs \sqrt{s} and \mathcal{P}_{\pm} , changes the production amplitudes as well as kinematic limits, but these inputs do not affect the main shape of the obtained scans and are thus not really relevant for our study. This can be observed by comparing Fig. 20 with Fig. 21, where the same scans have been done for $\sqrt{s} = 800$ GeV and $\mathcal{P}_{\pm} = \pm 0.9$. One can thus freely adjust the

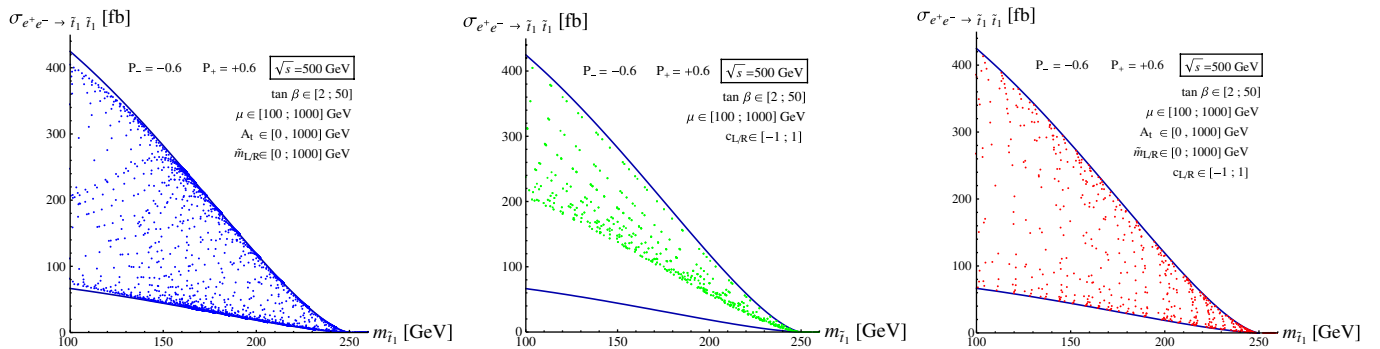


FIG. 20 (color online). Cross section for the reaction $e^+e^- \rightarrow \tilde{t}_1 \tilde{t}_1$ (in fb), at a center-of-mass energy $\sqrt{s} = 500$ GeV and with the polarizations \mathcal{P}_{\pm} [see Eq. (71)] indicated on the plot, as a function of $m_{\tilde{t}_1}$ (in GeV) within the 4D pMSSM [left plot], RS pMSSM without brane soft terms [middle], and RS pMSSM with brane soft terms [right]. All points presented here are obtained from a scan inside the ranges given on the plots for the parameters $c_{L/R} = c_{\tilde{t}_{L/R}}$, $\tan\beta$, and μ (and μ_{eff} in RS), the soft top squark masses $\tilde{m}_{L/R}$ (and brane masses $\tilde{m}_{L/R}|_{\text{eff}}$), and the soft trilinear coupling A_t (and brane coupling $A_t|_{\text{eff}}$). The limiting thick blue lines correspond to the analytically obtained cross sections for an extremal $Z\tilde{t}_1\tilde{t}_1$ coupling: $c_{11} = Q_Z^{tR}$ [lower limit] and $c_{11} = Q_Z^{tL}$ [upper limit].

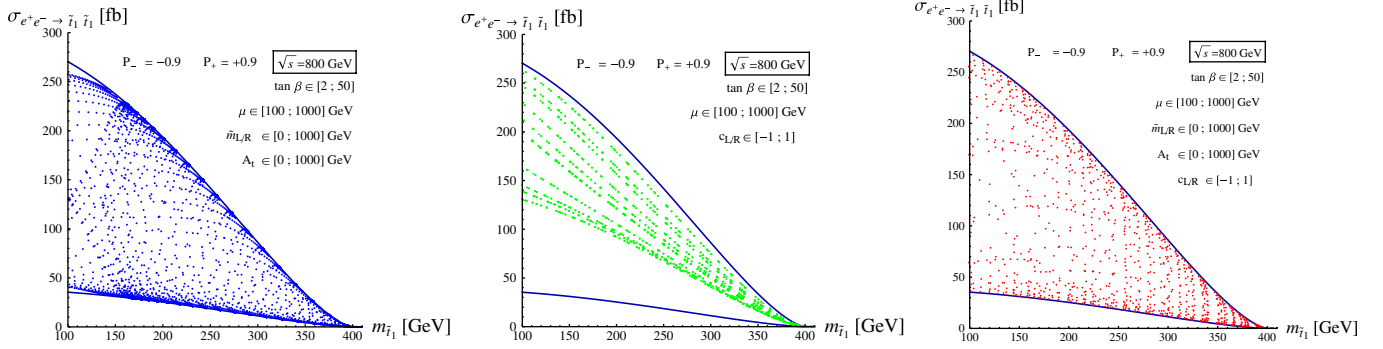


FIG. 21 (color online). The same as in Fig. 20 for $\sqrt{s} = 800$ GeV and $\mathcal{P}_{\pm} = \pm 0.9$.

center-of-mass energy and beam polarizations to get an optimal ratio of signal over backgrounds.

Now that we have described the way Figs. 20 and 21 were obtained, we can compare the three plots of, say, Fig. 20. The first conclusion is that the whole shapes of the scans within the 4D and 5D SUSY frameworks do not offer distinctive features (typically in both cases the entire domain in between the upper and lower analytical limits can be filled), forbidding us thus from developing a new test of discrimination between these two SUSY realizations.

Comparing the middle and right plots of Fig. 20, we observe that in the case without brane soft terms only cross section values roughly in the higher half of the theoretically allowed region are reached. This means that the relevant Z charge c_{11} of the \tilde{t}_1 squark [cf. Eq. (72)] is close to Q_Z^L ($c_{11} = Q_Z^L$ corresponds to the upper limit in scans) and hence that \tilde{t}_1 is never too far from being mainly composed by the \tilde{t}_L state; i.e., $\cos\theta_{\tilde{t}}$ is constrained (depending on $m_{\tilde{t}_1}$) to be relatively close to unity accordingly to Eq. (73). This result has to be enlightened with the previously explained upper bound (depending on $m_{\tilde{t}_1}$) on the highest top squark mass eigenvalue $m_{\tilde{t}_2}$ exhibited in

Fig. 13 [left plot] in the absence of brane soft terms. The presence of an upper bound on $m_{\tilde{t}_2}$ reflects the existence of an upper limit on the amplitude of mixing between the two \tilde{t}_L and \tilde{t}_R squark states. More formally, the mixing angle $\theta_{\tilde{t}} \in [0, \pi/2]$ in the 4D pMSSM [see Eq. (73)] is constrained to a smaller range $[0, \theta_{RS}]$ (with $\theta_{RS} < \pi/2$) in the warped pMSSM without brane soft terms. So we recover the conclusion from the middle plot of Fig. 20. Starting from the case of the middle plot of Fig. 20 and adding, in particular, a soft trilinear top squark coupling on the TeV-brane has the virtue of enlarging the mixing between \tilde{t}_L and \tilde{t}_R after EWSB. Doing so, the scanned points now fill the whole allowed theoretical region as can be seen in the right plot of Fig. 20.

In Fig. 22, we further illustrate the $e^+e^- \rightarrow \tilde{t}_2\tilde{t}_2$ reaction as a function of $m_{\tilde{t}_2}$, with $\sqrt{s} = 500$ GeV. The scanned points on plots never cross the drawn lines corresponding, respectively, to the cross sections for the extremal $Z\tilde{t}_2\tilde{t}_2$ couplings $c_{22} = Q_Z^{LR}$ and $c_{22} = Q_Z^L$ associated to $\cos\theta_{\tilde{t}} = 1$ and $\cos\theta_{\tilde{t}} = 0$ [see Eq. (72)]. We observe that in the 4D pMSSM case [left plot], there is a theoretical lower limit on $m_{\tilde{t}_2}$ around m_t as we have already described when discussing Figs. 13 and 14 [see also Eq. (69)].

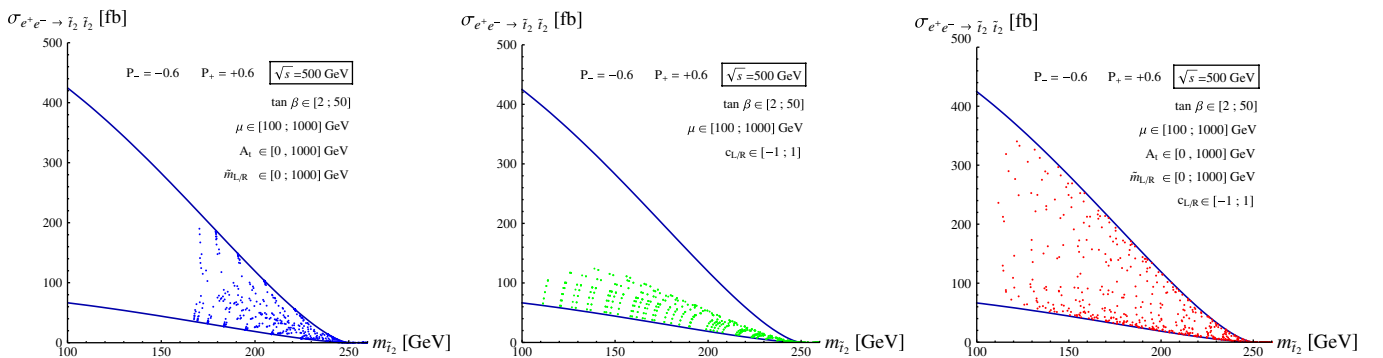


FIG. 22 (color online). Cross section for the reaction $e^+e^- \rightarrow \tilde{t}_2\tilde{t}_2$ (in fb), at a center-of-mass energy $\sqrt{s} = 500$ GeV and with the polarizations \mathcal{P}_{\pm} indicated on the plot, as a function of $m_{\tilde{t}_2}$ (in GeV) within the 4D pMSSM [left plot], RS pMSSM without brane soft terms [middle], and RS pMSSM with brane soft terms [right]. All points presented here are obtained from a scan inside the ranges given on the plots for the parameters $c_{L/R} = c_{\tilde{t}_{L/R}}$, $\tan\beta$, and μ (and μ_{eff} in RS), the soft top squark masses $\tilde{m}_{L/R}$ (and brane masses $\tilde{m}_{L/R}|_{\text{eff}}$), and the soft trilinear coupling A_t (and brane coupling $A_t|_{\text{eff}}$). The limiting thick blue lines correspond to the analytically obtained cross sections for an extremal $Z\tilde{t}_2\tilde{t}_2$ coupling: $c_{22} = Q_Z^{LR}$ [lower limit] and $c_{22} = Q_Z^L$ [upper limit].

In the middle plot of Fig. 22, without brane soft terms, only cross section values in a lower part of the theoretical region are reached; that is to say that the relevant Z charge c_{22} of the \tilde{t}_2 squark [cf. Eq. (72)] is close to $Q_Z^{\tilde{t}_R}$ ($c_{22} = Q_Z^{\tilde{t}_R}$ corresponds to the lower limit in the scan) and thus that \tilde{t}_2 is never too far from being mainly composed by the \tilde{t}_R state. This is consistent with the analysis of the middle plot of Fig. 20, which has revealed that \tilde{t}_1 is never too far from being mainly composed by the \tilde{t}_L .

In Fig. 23, we finally illustrate the $e^+e^- \rightarrow \tilde{t}_1\tilde{t}_2$ reaction as a function of $m_{\tilde{t}_2}$, with $\sqrt{s} = 800$ GeV. Now the scanned points on plots never cross the line corresponding to the cross section for the extremal $Z\tilde{t}_1\tilde{t}_2$ coupling $c_{12} = -(1/2) \times I_{3L}^{\tilde{t}_1} = -1/4$ [unique line drawn on the three plots] associated to $\sin 2\theta_{\tilde{t}} = 1$ [see Eq. (72)].

In the middle plot of Fig. 23, without brane soft terms, the reason why the cross section values never reach the analytical line at $c_{12} = -1/4$ is that $\sin 2\theta_{\tilde{t}}$ never reaches unity. Indeed, we have seen that, in the warped pMSSM without brane soft terms, the mixing angle $\theta_{\tilde{t}}$ is constrained from above.

For instance, a measurement of the cross section $\sigma(e^+e^- \rightarrow \tilde{t}_1\tilde{t}_1)$ and mass $m_{\tilde{t}_1}$ at the ILC could allow one to distinguish between the two RS scenarios of SUSY breaking. Indeed, the case where the experimental values of $\sigma(e^+e^- \rightarrow \tilde{t}_1\tilde{t}_1)$ and $m_{\tilde{t}_1}$ would fall outside the theoretically predicted domain in the middle plot of Fig. 20 would exclude the scenario without soft scalar mass and trilinear A terms on the TeV-brane. Such measurements would be compatible with the other RS version (presence of brane soft terms) if they belong to the theoretical region in the right plot of Fig. 20 [otherwise, these experimental data would conflict with both 4D and 5D SUSY].

The same kind of test could be investigated with measurements of $\sigma(e^+e^- \rightarrow \tilde{t}_2\tilde{t}_2)$ and $m_{\tilde{t}_2}$ [see Fig. 22]

or by reconstructing $\sigma(e^+e^- \rightarrow \tilde{t}_1\tilde{t}_2)$ and, e.g., $m_{\tilde{t}_2}$ [see Fig. 23]. It is interesting to note that performing the three above tests together at the ILC could even lead to correlated indications for the RS model with brane soft terms.

Such tests are possible if the predicted theoretical regions have fixed conservative limits. Now we have seen when discussing Fig. 13 that the theoretical region was limited (from above) by the minimal $c_{\tilde{t}_{L/R}}$ values. It is thus [see the above discussion] the case also for the theoretical domains obtained in the middle plots of Figs. 20–23—not speaking about the absolute limits (blue lines) induced by the extremal Z couplings. However, in the case of a bulk gauge custodial symmetry, one should impose typically $c_{\tilde{t}_{L/R}} \gtrsim -0.5$ [69] to avoid the existence of too light scustodians, which would have been observed at colliders. There would thus be fixed limits to the theoretically allowed domains. By the way, the above constraint, more strict than the one we have imposed: $c_{\tilde{t}_{L/R}} > -1$, would lead to an even more restricted area of spread scanned points. Furthermore, some information (and hence constraints) can be obtained on the $c_{\tilde{t}_{L/R}}$ parameters from top squark mass related measurements.

Concerning the experimental feasibility of such tests, a reasonable precision expected at the ILC for the $\sigma(e^+e^- \rightarrow \tilde{t}_i\tilde{t}_j)$ measurement is $\delta\sigma_{\text{exp}} \sim 5\%$ [113] ($\sim 1\%$ at most [118]), while it was shown in Ref. [123] that $m_{\tilde{t}}$ reconstructions at the ILC with an accuracy around 1% can be obtained by using 20 fb^{-1} of data. The exact uncertainties reachable at the ILC depend on the methods used and SUSY(-breaking) parameters. Stating on the above uncertainties at the percent level is realistic and sufficient for the realizations of the proposed tests, given the large sizes of theoretically forbidden regions in the middle plots of Figs. 20–23.

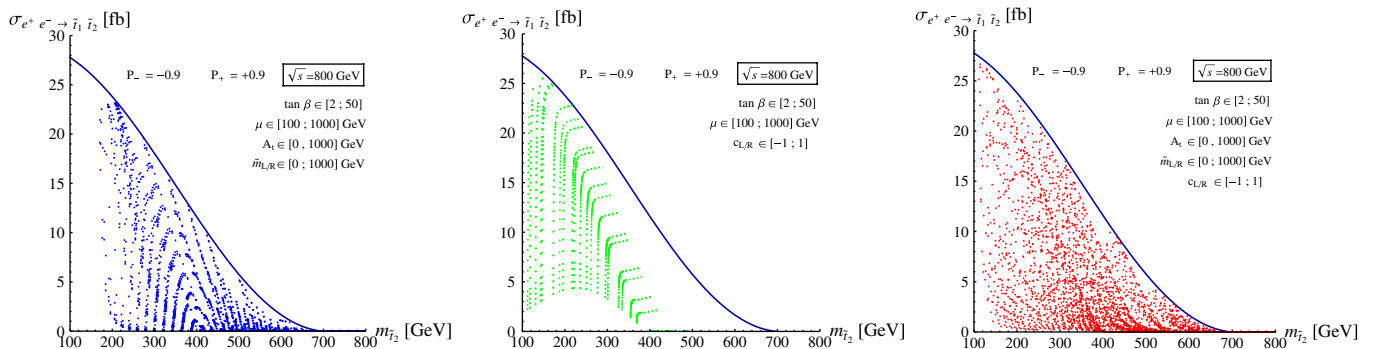


FIG. 23 (color online). Cross section for the reaction $e^+e^- \rightarrow \tilde{t}_1\tilde{t}_2$ (in fb) at a center-of-mass energy $\sqrt{s} = 800$ GeV as a function of $m_{\tilde{t}_2}$ (in GeV) within the 4D pMSSM [left plot], RS pMSSM without brane soft terms [middle], and RS pMSSM with brane soft terms [right]. All points presented here are obtained from a scan inside the ranges given on the plots for the parameters $c_{L/R} = c_{\tilde{t}_{L/R}}$, $\tan\beta$, and μ (and μ_{eff} in RS), the soft top squark masses $\tilde{m}_{L/R}$ (and brane masses $\tilde{m}_{L/R}|_{\text{eff}}$), and the soft trilinear coupling A_t (and brane coupling $A_t|_{\text{eff}}$). The limiting thick blue line corresponds to the analytically obtained cross section for an extremal $Z\tilde{t}_1\tilde{t}_2$ coupling: $c_{12} = -(1/2) \times I_{3L}^{\tilde{t}_1} = -1/4$.

IV. CONCLUSION

If the fundamental theory of nature is of the string theory kind, the effective low-energy model manifesting itself at present and future particle colliders would probably be a higher-dimensional SUSY model. In this paper, we have studied the theory and phenomenology of such models entering the class of particularly well-motivated frameworks with a warped space-time.

First, we have derived in a consistent analytical way, within the realistic 5D pMSSM context, the effective 4D Lagrangian for the brane-Higgs interactions as well as the complete sfermion mass matrices (illustrating explicitly the example of the top squark quark) induced partially by such interactions.

Those theoretical investigations have provided us with the necessary tools to perform concrete phenomenological studies of the RS SUSY models. In this respect, we have first demonstrated that the cancellation of quadratic divergences in the one-loop corrections to the Higgs mass is deeply related to the 5D anomaly cancellation (similarly to 4D). We have also found that the quadratic divergence cancellation occurs for any 5D cutoff, which means possibly for a “truncated” 5D SUSY theory (as it must be due to its nonrenormalizable aspect). In these loop calculations, the accent was also put on the justification of the infinite KK summation required in the KK regularization which opened up a rich debate in the literature a decade ago. Possible perspectives are the extensions of these calculations to the sfermion masses.

Concerning collider physics, there is a crucial question: In the hypothetical situation where some superpartners were discovered whereas all KK modes were outside the reach of direct detection (at the LHC and/or the ILC), how could one distinguish experimentally between a pure 4D SUSY scenario and a warped 5D SUSY model? In particular, the virtual effects of KK gluon excitations on the top squark pair production at the LHC might certainly be at least as tricky to detect as the similar effects for the top pair final state [120]. We have developed some tests that could help distinguishing, specifically, the RS pMSSM (with bulk SUSY-breaking sfermion masses and brane-Higgs bosons) from the 4D pMSSM. For instance, we have shown that the heaviest top squark eigenstate can reach lower mass values in the RS pMSSM than in the 4D pMSSM. Other clear 4D-RS pMSSM differences, that may be used for data-based discriminations, are those arising from the slepton mass sector of mSUGRA scenarios where larger mass splittings can occur in 5D setups. Finally, in the same philosophy applied to the SUSY Higgs sector, it has been shown, in particular, that branching ratios of H decay channels into sleptons can reach dominant levels in the RS pMSSM, a feature absent from the 4D pMSSM. In the future, it will be interesting to explore a related direction: The search at hadron colliders for the SM Higgs boson—or the lightest neutral 4D SUSY Higgs field h —could be

affected by new significant contributions to the gluon-fusion mechanism induced by 5D effects [if not too much constrained by present experimental data], effects representing other potential distinctive signatures of 5D SUSY scenarios. We conclude our phenomenological analysis with the suggestion of complementary methods for pinning down the presence of soft terms on the IR boundary by using top squark pair production at the ILC, which is more related to the discrimination between various RS pMSSM versions.

ACKNOWLEDGMENTS

The authors are grateful to Aldo Deandrea, Abdelhak Djouadi, Ulrich Ellwanger, Gero v. Gersdorff, Christophe Grojean, Swarup K. Majee, François Richard, and James D. Wells for useful discussions as well as to Marc Besançon for motivating conversations at early stages of this work. We also thank M. Calvet for her contribution to the manuscript. This work is supported by the European network HEPTOOLS and the A.N.R. *CPV-LFV-LHC* under Project No. NT09-508531 as well as the A.N.R. *TAPDMS* under Project No. 09-JCJC-0146.

APPENDIX A: THE SUPERSYMMETRIC 5D LAGRANGIAN

We consider the usual warped space-time based on the 5D metric G_{AB} :

$$ds^2 = G_{AB} dx^A dx^B = e^{-2\sigma(y)} \eta_{\mu\nu} dx^\mu dx^\nu - dy^2, \quad (A1)$$

$$y \in [-\pi R_c; +\pi R_c],$$

$$\sqrt{+G} \equiv \sqrt{\det[G_{AB}]} = \sqrt{(-1)^4 (e^{-2\sigma(y)})^4} = e^{-4\sigma(y)}, \quad (A2)$$

where capital Latin letters A and B are 5D Lorentz indices, $\eta_{\mu\nu}$ is the 4D flat (+, −, −, −) Minkowski metric, and x^μ denote the usual coordinates ($\mu = 0, 1, 2, 3$), while y parametrizes the fifth dimension.

1. Superfield content

Writing higher-dimensional SUSY Lagrangians with ordinary $N = 1$ 4D superfields only allows one to make the $N = 1$ 4D SUSY invariance manifest, and it prevents from explicitly covariant forms. In spite of these limitations, it allows for a more compact form than when using the component fields themselves and also to easily get the bulk-boundary couplings. We thus adopt this formalism. This approach was first developed for theories with 10 dimensions [124] and then extended to other dimensions [125] and to incorporate the radion superfield [39].

In this appendix, we derive explicitly in terms of the fields, within the RS SUSY framework with a bulk $U(1)$ gauge symmetry, the whole Lagrangian encoding the Yukawa and gauge couplings of the two $N = 1$ 5D (or $N = 2$ 4D) bulk hypermultiplets $\{\Phi_L, \Phi_L^-\}$ and $\{\Phi_L^c, \Phi_L^{c-}\}$ to

two $N = 1$ 4D complex chiral superfields localized on the TeV-brane called H_u^0 (as it will play the role of the ‘‘up-type’’ neutral Higgs superfield when extending this toy model to the pMSSM) and H_d^0 (for ‘‘down-type’’). The $N = 1$ chiral superfield Φ_L (the subscript L corresponds to the chirality of the contained fermion field once promoted to a four-component spinor: See just below [126]) with Neumann BC at $y = 0$, πR_c [denoted as $(++)$ in the main text] reads as

$$\begin{aligned} \Phi_L(x^\mu, y; \theta, \bar{\theta}) &\equiv \phi_L(x^\mu, y) + \sqrt{2}\theta\zeta_L(x^\mu, y)e^{-(1/2)\sigma(y)} \\ &\quad - \theta\theta F_L(x^\mu, y) + i\theta\sigma^\mu\bar{\theta}\partial_\mu\phi_L(x^\mu, y) \\ &\quad + \frac{i}{\sqrt{2}}\theta\theta\bar{\theta}\bar{\sigma}^\mu\partial_\mu\zeta_L(x^\mu, y)e^{-(1/2)\sigma(y)} \\ &\quad - \frac{1}{4}\theta\theta\bar{\theta}\bar{\theta}\partial_\mu\partial^\mu\phi_L(x^\mu, y), \end{aligned} \quad (\text{A3})$$

ζ_L being the two-component spinorial field, ϕ_L its scalar superpartner, and F_L the auxiliary field, whereas its complex conjugated expands according to

$$\begin{aligned} \bar{\Phi}(x^\mu, y; \theta, \bar{\theta}) &\equiv \bar{\phi}_L(x^\mu, y) + \sqrt{2}\bar{\theta}\bar{\zeta}_L(x^\mu, y)e^{-(1/2)\sigma(y)} \\ &\quad - \bar{\theta}\bar{\theta}\bar{F}_L(x^\mu, y) - i\theta\sigma^\mu\bar{\theta}\partial_\mu\bar{\phi}_L(x^\mu, y) \\ &\quad + \frac{i}{\sqrt{2}}\bar{\theta}\bar{\theta}\theta\sigma^\mu\partial_\mu\bar{\zeta}_L(x^\mu, y)e^{-(1/2)\sigma(y)} \\ &\quad - \frac{1}{4}\bar{\theta}\bar{\theta}\theta\theta\partial_\mu\partial^\mu\bar{\phi}_L(x^\mu, y), \end{aligned} \quad (\text{A4})$$

and its charge conjugated superfield with Dirichlet BC at $y = 0$, πR_c [denoted as $(--)$] is

$$\begin{aligned} \Phi_L^{--}(x^\mu, y; \theta, \bar{\theta}) &\equiv \phi_L^c(x^\mu, y) + \sqrt{2}\theta\chi_L(x^\mu, y)e^{-(1/2)\sigma(y)} \\ &\quad - \theta\theta F_L^c(x^\mu, y) + i\theta\sigma^\mu\bar{\theta}\partial_\mu\phi_L^c(x^\mu, y) \\ &\quad + \frac{i}{\sqrt{2}}\theta\theta\bar{\theta}\bar{\sigma}^\mu\partial_\mu\chi_L(x^\mu, y)e^{-(1/2)\sigma(y)} \\ &\quad - \frac{1}{4}\theta\theta\bar{\theta}\bar{\theta}\partial_\mu\partial^\mu\phi_L^c(x^\mu, y). \end{aligned} \quad (\text{A5})$$

We define another superfield Φ_L^c through its charge conjugated state [this will allow us to introduce only left-handed chiral superfields, as usually in the 4D pMSSM]:

$$\begin{aligned} \Phi_L^c(x^\mu, y; \theta, \bar{\theta}) &\equiv \phi_R(x^\mu, y) + \sqrt{2}\theta\chi_R(x^\mu, y)e^{-(1/2)\sigma(y)} \\ &\quad - \theta\theta F_R(x^\mu, y) + i\theta\sigma^\mu\bar{\theta}\partial_\mu\phi_R(x^\mu, y) \\ &\quad + \frac{i}{\sqrt{2}}\theta\theta\bar{\theta}\bar{\sigma}^\mu\partial_\mu\chi_R(x^\mu, y)e^{-(1/2)\sigma(y)} \\ &\quad - \frac{1}{4}\theta\theta\bar{\theta}\bar{\theta}\partial_\mu\partial^\mu\phi_R(x^\mu, y), \end{aligned} \quad (\text{A6})$$

and the opposite BC superfield is

$$\begin{aligned} \Phi_L^{c--}(x^\mu, y; \theta, \bar{\theta}) &\equiv \phi_R^c(x^\mu, y) + \sqrt{2}\theta\zeta_R(x^\mu, y)e^{-(1/2)\sigma(y)} \\ &\quad - \theta\theta F_R^c(x^\mu, y) + i\theta\sigma^\mu\bar{\theta}\partial_\mu\phi_R^c(x^\mu, y) \\ &\quad + \frac{i}{\sqrt{2}}\theta\theta\bar{\theta}\bar{\sigma}^\mu\partial_\mu\zeta_R(x^\mu, y)e^{-(1/2)\sigma(y)} \\ &\quad - \frac{1}{4}\theta\theta\bar{\theta}\bar{\theta}\partial_\mu\partial^\mu\phi_R^c(x^\mu, y). \end{aligned} \quad (\text{A7})$$

In our notations, the four-component fermions $\psi_{L/R}$ (L/R indicating the Lorentz chirality) read in terms of the two-component fields as

$$\psi^l \equiv (\zeta, \bar{\chi}), \quad \psi_L^l \equiv (\zeta, 0), \quad \psi^{cl} \equiv (\chi, \bar{\zeta}).$$

We consider a U(1) gauge symmetry whose $N = 1$ 5D (or $N = 2$ 4D) gauge supermultiplet is known to have the same field content as *one* $N = 1$ vector supermultiplet with $(++)$ BC, for which we write the decomposition as (in the Wess-Zumino gauge)

$$\begin{aligned} V(x^\mu, y; \theta, \bar{\theta}) &\equiv \theta\sigma^\mu\bar{\theta}A_\mu(x^\mu, y) - i\bar{\theta}\theta\lambda_1(x^\mu, y)e^{-(3/2)\sigma(y)} \\ &\quad + i\theta\theta\bar{\theta}\bar{\lambda}_1(x^\mu, y)e^{-(3/2)\sigma(y)} + \frac{1}{2}\theta\theta\bar{\theta}\bar{\theta}D(x^\mu, y), \end{aligned} \quad (\text{A8})$$

A_μ denoting the gauge boson, λ_1 the Weyl gaugino field, and D the complex auxiliary field, plus *one* $(--)$ $N = 1$ chiral superfield, that we write as

$$\begin{aligned} \Omega(x^\mu, y; \theta, \bar{\theta}) &\equiv \frac{1}{\sqrt{2}}[\Sigma(x^\mu, y) - iA_5(x^\mu, y)] - i\sqrt{2}\theta\lambda_2(x^\mu, y)e^{-(1/2)\sigma(y)} - \theta\theta F_\Omega(x^\mu, y) + i\theta\sigma^\mu\bar{\theta}\partial_\mu\frac{1}{\sqrt{2}}[\Sigma(x^\mu, y) - iA_5(x^\mu, y)] \\ &\quad + \frac{1}{\sqrt{2}}\theta\theta\bar{\theta}\bar{\sigma}^\mu\partial_\mu\lambda_2(x^\mu, y)e^{-(1/2)\sigma(y)} - \frac{1}{4}\theta\theta\bar{\theta}\bar{\theta}\partial_\mu\partial^\mu\frac{1}{\sqrt{2}}[\Sigma(x^\mu, y) - iA_5(x^\mu, y)], \end{aligned} \quad (\text{A9})$$

Σ being a real scalar field.

2. Superfield action

The field content described in the previous subsection together with the following action \mathcal{S}_{5D} define the toy model analyzed in this part. This action is given by $\mathcal{S}_{5D} = \mathcal{S}_{\text{gauge}} + \mathcal{S}_{\text{Higgs}}|_{\text{brane}} + \mathcal{S}_{\text{matter}}$ with, following the formalism of Ref. [39],

$$\begin{aligned} \mathcal{S}_{\text{gauge}} &= \frac{1}{4} \int d^5x \int d^2\theta (W^\alpha W_\alpha + \text{H.c.}) \\ &\quad + \int d^5x \int d^4\theta e^{-2\sigma(y)} \left(\partial_y V - \frac{1}{\sqrt{2}} (\Omega + \bar{\Omega}) \right)^2, \end{aligned} \quad (\text{A10})$$

$$\begin{aligned} \mathcal{S}_{\text{matter}} &= \int d^5x \int d^4\theta e^{-2\sigma(y)} (\bar{\Phi}_L e^{-2gq_L V} \Phi_L + \bar{\Phi}_L^- e^{2gq_L V} \bar{\Phi}_L^- \\ &\quad + \bar{\Phi}_L^c e^{-2gq_R V} \Phi_L^c + \bar{\Phi}_L^{c-} e^{2gq_R V} \bar{\Phi}_L^{c-}) \\ &\quad + \int d^5x \int d^2\theta e^{-3\sigma(y)} (\Phi_L^- [D_5 - \sqrt{2}gq_L \Omega] \Phi_L \\ &\quad + \Phi_L^{c-} [D_5 - \sqrt{2}gq_R \Omega] \Phi_L^c) + \text{H.c.}, \end{aligned} \quad (\text{A11})$$

$$\begin{aligned} \mathcal{S}_{\text{Higgs|brane}} &= \int d^5x \int d^4\theta e^{-2\sigma(y)} (\bar{H}_u^0 e^{-(2gq_u^0)V} H_u^0 \\ &\quad + \bar{H}_d^0 e^{-(2gq_d^0)V} H_d^0) \delta(y - \pi R_c) \\ &\quad + \int d^5x \int d^2\theta e^{-3\sigma(y)} (\mu H_u^0 H_d^0 + \mathcal{Y} H_u^0 \Phi_L \Phi_L^c) \delta(y - \pi R_c) \\ &\quad + \text{H.c.}, \end{aligned} \quad (\text{A12})$$

where g (\mathcal{Y}) is the 5D gauge (Yukawa) coupling constant, $D_5 = \partial_y - (\frac{3}{2} - c_{L/R})\sigma'$ [with $\sigma' = \partial_y \sigma(y) = \text{sgn}(y) \times k$, $\text{sgn}(y)$ being a step function], and the U(1) charges of the

$$\begin{aligned} \mathcal{L}_F &= e^{-2\sigma} (\bar{F}_L F_L + F_L^c \bar{F}_L^c + \bar{F}_R F_R + F_R^c \bar{F}_R^c) - e^{-3\sigma} (F_L^c D_5 \phi_L - F_L D_5' \phi_L^c + F_R^c D_5 \phi_R - F_R D_5' \phi_R^c) + \text{H.c.} \\ &\quad + e^{-3\sigma} 2g (q_L (\phi_L^c F_L + F_L^c \phi_L) + q_R (\phi_R^c F_R + F_R^c \phi_R)) \Sigma + \text{H.c.} \\ &\quad - e^{-3\sigma} \mathcal{Y} (\phi_{H_u^0} \phi_R F_L + \phi_{H_u^0} \phi_L F_R) \delta(y - \pi R_c) + \text{H.c.}, \end{aligned} \quad (\text{A15})$$

where $D_5' = \partial_y - (\frac{3}{2} + c_{L/R})\sigma'$. This Lagrangian is obtained after integrating by part (for convenience).

The 5D Lagrangian for the Higgs auxiliary fields $F_{H_u^0}$ and $F_{H_d^0}$ is given by

$$\begin{aligned} \mathcal{L}_H &= e^{-2\sigma} (\bar{F}_{H_u^0} F_{H_u^0} + \bar{F}_{H_d^0} F_{H_d^0}) \delta(y - \pi R_c) \\ &\quad - e^{-3\sigma} (\mu F_{H_u^0} \phi_{H_d^0} + \mu \phi_{H_u^0} F_{H_d^0} \\ &\quad + \mathcal{Y} F_{H_u^0} \phi_L \phi_R) \delta(y - \pi R_c) + \text{H.c.} \end{aligned} \quad (\text{A16})$$

4. Auxiliary field solutions

The solutions of the equations of motion for the auxiliary fields are the following ones:

$$\begin{aligned} D &= -e^{-2\sigma} \{ (\partial_y - 2\sigma') \Sigma - g (q_L (\bar{\Phi}_L \phi_L - \phi_L^c \bar{\Phi}_L^c) \\ &\quad + q_R (\bar{\Phi}_R \phi_R - \phi_R^c \bar{\Phi}_R^c)) - g (q_{H_u^0} \bar{\Phi}_{H_u^0} \phi_{H_u^0} \\ &\quad + q_{H_d^0} \phi_{H_d^0} \bar{\Phi}_{H_d^0}) \delta(y - \pi R_c) \}, \end{aligned} \quad (\text{A17})$$

superfields $H_{u,d}^0$, Φ_L , and Φ_L^c must obey $q_{H_u^0} + q_L + q_R = 0$, $q_{H_u^0} + q_{H_d^0} = 0$. The above $c_{L/R}$ terms represent 5D mass terms in the superpotential of the superfields Φ_L/Φ_L^c that will lead to 5D fermion and 5D scalar mass terms, as will appear soon. In the above action, the fundamental parameter μ is of the order of k .

3. Auxiliary field Lagrangians

The 5D Lagrangian for the gauge auxiliary field D is given by [from now on, σ stands for $\sigma(y)$]

$$\begin{aligned} \mathcal{L}_D &= \frac{1}{2} D^2 + e^{-2\sigma} D (\partial_y - 2\sigma') \Sigma \\ &\quad - g e^{-2\sigma} D (q_L (\bar{\Phi}_L \phi_L - \phi_L^c \bar{\Phi}_L^c) + q_R (\bar{\Phi}_R \phi_R - \phi_R^c \bar{\Phi}_R^c)) \\ &\quad - g e^{-2\sigma} D (q_{H_u^0} \bar{\Phi}_{H_u^0} \phi_{H_u^0} + q_{H_d^0} \bar{\Phi}_{H_d^0} \phi_{H_d^0}) \delta(y - \pi R_c), \end{aligned} \quad (\text{A13})$$

$\phi_{H_u^0}$ and $\phi_{H_d^0}$ being the scalar field components of the superfields H_u^0 and H_d^0 , respectively.

The 5D Lagrangian for the auxiliary field F_Ω is given by

$$\begin{aligned} \mathcal{L}_\Omega &= e^{-2\sigma} \bar{F}_\Omega F_\Omega \\ &\quad - \sqrt{2} g e^{-3\sigma} ((q_L \phi_L^c \phi_L + q_R \phi_R^c \phi_R) F_\Omega + \text{H.c.}). \end{aligned} \quad (\text{A14})$$

The 5D Lagrangian for the matter auxiliary fields, namely, F_L , F_R , F_L^c , and F_R^c , is given by

$$F_\Omega = -\sqrt{2} g e^{-\sigma} (q_L \bar{\Phi}_L^c \bar{\Phi}_L + q_R \bar{\Phi}_R^c \bar{\Phi}_R), \quad (\text{A18})$$

$$\begin{aligned} F_L &= -e^{-\sigma} ((D_5' + g\Sigma) \bar{\Phi}_L^c - \bar{\mathcal{Y}} \delta(y - \pi R_c) \bar{\Phi}_{H_u^0} \bar{\Phi}_R), \\ \bar{F}_L^c &= e^{-\sigma} (D_5 - g\Sigma) \phi_L, \end{aligned} \quad (\text{A19})$$

$$\begin{aligned} F_R &= -e^{-\sigma} ((D_5' + g\Sigma) \bar{\Phi}_R^c - \bar{\mathcal{Y}} \delta(y - \pi R_c) \bar{\Phi}_{H_u^0} \bar{\Phi}_L), \\ \bar{F}_R^c &= e^{-\sigma} (D_5 - g\Sigma) \phi_R, \end{aligned} \quad (\text{A20})$$

$$F_{H_u^0} = e^{-\sigma} (\bar{\mu} \bar{\Phi}_{H_u^0} + \bar{\mathcal{Y}} \bar{\Phi}_L \bar{\Phi}_R), \quad F_{H_d^0} = e^{-\sigma} \bar{\mu} \bar{\Phi}_{H_d^0}. \quad (\text{A21})$$

Plugging those back into the above Lagrangians, we get

$$\mathcal{L}_D = -\frac{1}{2} D^2, \quad \mathcal{L}_\Omega = -e^{-2\sigma} \bar{F}_\Omega F_\Omega, \quad (\text{A22})$$

$$\mathcal{L}_F = -e^{-2\sigma} (\bar{F}_L F_L + F_L^c \bar{F}_L^c + \bar{F}_R F_R + F_R^c \bar{F}_R^c), \quad (\text{A23})$$

$$\mathcal{L}_H = -e^{-2\sigma} (\bar{F}_{H_u^0} F_{H_u^0} + \bar{F}_{H_d^0} F_{H_d^0}) \delta(y - \pi R_c). \quad (\text{A24})$$

5. Scalar field Lagrangian

The whole 5D Lagrangian—all SUSY Lagrangians given in terms of 5D fields in this appendix are provided before field redefinition through warp factors—for scalar fields $\mathcal{L}_{\text{kin}} + \mathcal{L}_{\text{scalar}}$, with $\mathcal{L}_{\text{scalar}} = \mathcal{L}_D + \mathcal{L}_\Omega + \mathcal{L}_F + \mathcal{L}_H$, can be rewritten in explicit forms as

$$\begin{aligned} \mathcal{L}_{\text{kin}} = & e^{-2\sigma} \partial_\mu \bar{\phi}_{H_u^0} \partial^\mu \phi_{H_u^0} \delta(y - \pi R_c) + e^{-2\sigma} \partial_\mu \bar{\phi}_{H_d^0} \partial^\mu \phi_{H_d^0} \delta(y - \pi R_c) + e^{-2\sigma} \partial_\mu \bar{\phi}_L \partial^\mu \phi_L \\ & + e^{-2\sigma} \partial_\mu \bar{\phi}_L^c \partial^\mu \phi_L^c + e^{-2\sigma} \partial_\mu \bar{\phi}_R \partial^\mu \phi_R + e^{-2\sigma} \partial_\mu \bar{\phi}_R^c \partial^\mu \phi_R^c, \end{aligned} \quad (\text{A25})$$

$$\begin{aligned} -\sqrt{G}^{-1} \mathcal{L}_{\text{scalar}} = & D_5 \bar{\phi}_L D_5 \phi_L + D_5 \bar{\phi}_R D_5 \phi_R + |\mu|^2 \bar{\phi}_{H_u^0} \phi_{H_u^0} \delta(y - \pi R_c) + |\mathcal{Y} \delta(y - \pi R_c) \phi_{H_u^0} \phi_L - D_5' \phi_R^c|^2 \\ & + |\mathcal{Y} \delta(y - \pi R_c) \phi_{H_u^0} \phi_R - D_5' \phi_L^c|^2 + |\mu \phi_{H_d^0} + \mathcal{Y} \phi_L \phi_R|^2 \delta(y - \pi R_c) + 2g^2 |q_L \phi_L^c \phi_L + q_R \phi_R^c \phi_R|^2 \\ & + \frac{1}{2} |(\partial_y - 2\sigma') \Sigma - g(q_L \Delta_{\phi_L} + q_R \Delta_{\phi_R} + [q_{H_d^0} \bar{\phi}_{H_d^0} \phi_{H_d^0} + q_{H_u^0} \bar{\phi}_{H_u^0} \phi_{H_u^0}] \delta(y - \pi R_c))|^2, \end{aligned} \quad (\text{A26})$$

where, e.g., $\Delta_{\phi_R} \equiv \bar{\phi}_R \phi_R - \phi_R^c \bar{\phi}_R^c$. By developing the $|D_5 \phi|^2$, $|D_5' \phi|^2$, and $|(\partial_y - 2\sigma') \Sigma|^2$ terms from above, one finds the 5D scalar masses:

$$m_{\phi_{L/R}, \phi_{L/R}^c}^2 \equiv (c_{L/R}^2 \pm c_{L/R} - \frac{15}{4})k^2 + (\frac{3}{2} \mp c_{L/R}) \partial_y (\partial_y \sigma), \quad m_\Sigma^2 \equiv -4k^2 + 2\partial_y (\partial_y \sigma). \quad (\text{A27})$$

If one now develops the last two lines proportional to the g gauge coupling in the above Lagrangian, one finds (after a few simplifications)

$$\begin{aligned} -\sqrt{G}^{-1} \mathcal{L}_{\text{scalar}} = & D_5 \bar{\phi}_L D_5 \phi_L + D_5 \bar{\phi}_R D_5 \phi_R + |\mu|^2 \bar{\phi}_{H_u^0} \phi_{H_u^0} \delta(y - \pi R_c) + |\mathcal{Y} \delta(y - \pi R_c) \phi_{H_u^0} \phi_L - D_5' \phi_R^c|^2 \\ & + |\mathcal{Y} \delta(y - \pi R_c) \phi_{H_u^0} \phi_R - D_5' \phi_L^c|^2 + |\mu \phi_{H_d^0} + \mathcal{Y} \phi_L \phi_R|^2 \delta(y - \pi R_c) + \frac{1}{2} |D_5^k \Sigma|^2 \\ & - g(q_L (\bar{\phi}_L \phi_L - \phi_L^c \bar{\phi}_L^c) + q_R (\bar{\phi}_R \phi_R - \phi_R^c \bar{\phi}_R^c)) + \delta(y - \pi R_c) (q_{H_u^0} \bar{\phi}_{H_u^0} \phi_{H_u^0} + q_{H_d^0} \bar{\phi}_{H_d^0} \phi_{H_d^0}) D_5^k \Sigma \\ & + \frac{g^2}{2} (q_L^2 (|\phi_L|^4 + |\phi_L^c|^4) + q_R^2 (|\phi_R|^4 + |\phi_R^c|^4) + \delta^2(y - \pi R_c) (q_{H_u^0}^2 |\phi_{H_u^0}|^4 + q_{H_d^0}^2 |\phi_{H_d^0}|^4)) \\ & + g^2 (q_L^2 |\phi_L^c \phi_L|^2 + q_R^2 |\phi_R^c \phi_R|^2 + q_{H_u^0} q_{H_d^0} \delta^2(y - \pi R_c) |\phi_{H_u^0} \phi_{H_d^0}|^2) + g^2 q_L q_R (|\phi_L \phi_R|^2 \\ & - |\phi_L \phi_R^c|^2 - |\phi_L^c \phi_R|^2 + |\phi_L^c \phi_R^c|^2 + 2(\phi_L^c \phi_L \bar{\phi}_R^c \bar{\phi}_R + \phi_R^c \phi_R \bar{\phi}_L^c \bar{\phi}_L)) \\ & + g^2 (q_L (q_{H_u^0} |\phi_L \phi_{H_u^0}|^2 + q_{H_d^0} |\phi_L \phi_{H_d^0}|^2) + q_R (q_{H_u^0} |\phi_R \phi_{H_u^0}|^2 + q_{H_d^0} |\phi_R \phi_{H_d^0}|^2)) \delta(y - \pi R_c), \end{aligned} \quad (\text{A28})$$

with $D_5^k = \partial_y - 2\sigma'$.

One can also simply add the soft bilinear terms for the Higgs fields on the TeV-brane, and having, as usual in RS, soft squared Higgs masses and $B\mu$ (Higgs mixing) scales of the order of k squared leads to 4D effective soft terms with a scale at the TeV. The soft scalar trilinear A couplings are discussed in detail in the main text.

6. Fermion field Lagrangian

We now derive the fermionic part of the 5D Lagrangian issued from the actions in Eqs. (A10)–(A12):

$$\begin{aligned} \mathcal{L}_{\text{fermion}} = & -e^{-4\sigma} (\chi_L D_5'' \zeta_L + \bar{\chi}_L D_5'' \bar{\zeta}_L + \chi_R D_5'' \zeta_R + \bar{\chi}_R D_5'' \bar{\zeta}_R) - ie^{-3\sigma} (\zeta_L \sigma^\mu \partial_\mu \bar{\zeta}_L + \zeta_R \sigma^\mu \partial_\mu \bar{\zeta}_R) \\ & - ie^{-3\sigma} (\chi_L \sigma^\mu \partial_\mu \bar{\chi}_L + \chi_R \sigma^\mu \partial_\mu \bar{\chi}_R) - ie^{-3\sigma} (\zeta_{H_u^0} \sigma^\mu \partial_\mu \bar{\zeta}_{H_u^0} + \zeta_{H_d^0} \sigma^\mu \partial_\mu \bar{\zeta}_{H_d^0}) \delta(y - \pi R_c) \\ & - e^{-4\sigma} (\lambda_2 (\partial_y - \frac{3}{2}k) \lambda_1 + \bar{\lambda}_2 (\partial_y - \frac{3}{2}k) \bar{\lambda}_1) - ie^{-3\sigma} (\lambda_1 \sigma^\mu \partial_\mu \bar{\lambda}_1 + \lambda_2 \sigma^\mu \partial_\mu \bar{\lambda}_2) \\ & - e^{-4\sigma} (\mu \zeta_{H_u^0} \zeta_{H_d^0} + \mathcal{Y} \phi_{H_u^0} \zeta_L \zeta_R + \mathcal{Y} \phi_L \zeta_{H_u^0} \zeta_R + \mathcal{Y} \phi_R \zeta_{H_u^0} \zeta_L) \delta(y - \pi R_c) \\ & - i\sqrt{2} e^{-4\sigma} g (q_{H_u^0} (\bar{\phi}_{H_u^0} \lambda_1 \zeta_{H_u^0} - \phi_{H_u^0} \bar{\zeta}_{H_u^0} \bar{\lambda}_1) + q_{H_d^0} (\bar{\phi}_{H_d^0} \lambda_1 \zeta_{H_d^0} - \phi_{H_d^0} \bar{\zeta}_{H_d^0} \bar{\lambda}_1)) \delta(y - \pi R_c) \\ & - i\sqrt{2} e^{-4\sigma} g (q_L (\bar{\phi}_L \lambda_1 \zeta_L - \phi_L \bar{\zeta}_L \bar{\lambda}_1) + q_R (\bar{\phi}_R \lambda_1 \zeta_R - \phi_R \bar{\zeta}_R \bar{\lambda}_1)) \\ & + i\sqrt{2} e^{-4\sigma} g (q_L (\bar{\phi}_L^c \lambda_1 \chi_L - \phi_L^c \bar{\chi}_L \bar{\lambda}_1) + q_R (\bar{\phi}_R^c \lambda_1 \chi_R - \phi_R^c \bar{\chi}_R \bar{\lambda}_1)) \\ & - i\sqrt{2} e^{-4\sigma} g (q_L (\phi_L^c \lambda_2 \zeta_L + \phi_L \chi_L \lambda_2) + q_R (\phi_R^c \lambda_2 \zeta_R + \phi_R \chi_R \lambda_2)) + \text{H.c.}, \end{aligned} \quad (\text{A29})$$

where $D_5'' = \partial_y - (2 - c_{L/R})\sigma'$ and $\zeta_{H_{u,d}^0}$ are the Higgsino two-component spinors.

7. Gauge field Lagrangian

Finally, the gauge interactions encoded in the superfield actions of Eqs. (A10)–(12) read in terms of the 5D gauge fields as

$$\begin{aligned}
\mathcal{L}_{\text{gauge}} = & -\frac{1}{4}F_{\mu\nu}F^{\mu\nu} + \frac{1}{2}e^{-2\sigma}\partial_y A_\mu\partial_y A^\mu + \frac{1}{2}e^{-2\sigma}\partial_\mu\Sigma\partial^\mu\Sigma \\
& + e^{-2\sigma}(\overline{D_\mu\phi_L}D^\mu\phi_L + \overline{D_\mu\phi_L^c}D^\mu\phi_L^c + \overline{D_\mu\phi_R}D^\mu\phi_R + \overline{D_\mu\phi_R^c}D^\mu\phi_R^c) \\
& - e^{-3\sigma}(i\zeta_L\sigma^\mu D_\mu\bar{\zeta}_L + i\chi_L\sigma^\mu D_\mu\bar{\chi}_L + i\zeta_R\sigma^\mu D_\mu\bar{\zeta}_R + i\chi_R\sigma^\mu D_\mu\bar{\chi}_R) \\
& + e^{-2\sigma}(\overline{D_\mu\phi_{H_u^0}}D^\mu\phi_{H_u^0} + \overline{D_\mu\phi_{H_d^0}}D^\mu\phi_{H_d^0})\delta(y - \pi R_c) \\
& - e^{-3\sigma}(i\zeta_{H_u^0}\sigma^\mu D_\mu\bar{\zeta}_{H_u^0} + i\zeta_{H_d^0}\sigma^\mu D_\mu\bar{\zeta}_{H_d^0})\delta(y - \pi R_c),
\end{aligned} \tag{A30}$$

where

$$\begin{aligned}
D_\mu & \equiv \partial_\mu + ig_{QL/R}A_\mu/\partial_\mu + ig_{QH_{u,d}}A_\mu\overline{D_\mu\phi}D^\mu\phi \\
& \equiv \partial_\mu\bar{\phi}\partial^\mu\phi + igq(\phi\partial_\mu\bar{\phi} - \bar{\phi}\partial_\mu\phi)A^\mu \\
& \quad + g^2q^2\bar{\phi}\phi A_\mu A^\mu i\zeta\sigma^\mu D_\mu\bar{\zeta} \\
& \equiv i\zeta\sigma^\mu\partial_\mu\bar{\zeta} - gq\zeta\sigma^\mu\bar{\zeta}A_\mu.
\end{aligned}$$

To compare with another parametrization often found in literature, one can rewrite the second term of Eq. (A30) in terms of the new coordinate $z = \frac{e^{\sigma(y)}}{k}$ ($y = 0 \Leftrightarrow z = \frac{1}{k} \equiv R$ and $y = \pi R_c \Leftrightarrow z = \frac{e^{k\pi R_c}}{k} \equiv R'$):

$$\frac{1}{2}e^{-2\sigma}(\partial_y A_\mu)^2 = -\frac{1}{2}A_\mu\left(\partial_z^2 - \frac{1}{z}\partial_z\right)A^\mu. \tag{A31}$$

APPENDIX B: WAVE FUNCTIONS

1. Generic relations

Any wave function $f_n(y)$, for an n th KK state along the fifth dimension y , satisfies the orthonormalization condition (after the usual RS field redefinition)

$$\int_{-\pi R_c}^{\pi R_c} \bar{f}_n(y)f_m(y)dy = \delta_{nm}, \tag{B1}$$

showing that $f_n(y)$ has dimension 1/2, and the completeness relation (see, for instance, Ref. [127])

$$\sum_{n=0}^{\infty} \bar{f}_n(y)f_n(y') = \delta(y - y'). \tag{B2}$$

2. Solutions for free vectorial fields

For the equations of motion in the warped SUSY background, the solutions for the wave functions along the fifth dimension of the free 5D vectorial field in Eq. (A8), with KK decomposition

$$A_\mu(x^\mu, y) = \sum_{n=0}^{\infty} A_\mu^{(n)}(x^\mu)g_n^{++}(y),$$

are [7] for $n \geq 1$

$$\begin{aligned}
g_n^{++}(y) = & \frac{1}{\sqrt{2\pi R_c}}\frac{e^\sigma}{N_n}\left[J_1\left(\frac{M^{(n)}e^\sigma}{k}\right)\right. \\
& \left. + b_1^{++}(M^{(n)})Y_1\left(\frac{M^{(n)}e^\sigma}{k}\right)\right],
\end{aligned} \tag{B3}$$

$$b_1^{++}(M^{(n)}) = -\frac{J_1(M^{(n)}/k) + (M^{(n)}/k)J_1'(M^{(n)}/k)}{Y_1(M^{(n)}/k) + (M^{(n)}/k)Y_1'(M^{(n)}/k)},$$

where $\sigma = \sigma(y) = k|y|$, $J_1, Y_1(J_1', Y_1')$ are the (differentiated) Bessel functions, $M^{(n)} = M_{\text{KK}}^{(n)}$ is the n th KK gauge mass, and N_n is the normalization constant. Note that these wave functions are given here before the field redefinition usually done in the RS model. The solutions for the wave functions of the associated 5D scalar field in Eq. (A9), with KK decomposition

$$\Sigma(x^\mu, y) = \sum_{n=1}^{\infty} \Sigma^{(n)}(x^\mu)g_n^{--}(y), \tag{B4}$$

are [7] for $n \geq 1$

$$\begin{aligned}
g_n^{--}(y) = & \text{sgn}(y)\frac{1}{\sqrt{2\pi R_c}}\frac{e^{2\sigma}}{N_n}\left[J_0\left(\frac{M^{(n)}e^\sigma}{k}\right)\right. \\
& \left. + b_0^{--}(M^{(n)})Y_0\left(\frac{M^{(n)}e^\sigma}{k}\right)\right],
\end{aligned} \tag{B5}$$

$$b_0^{--}(M^{(n)}) = -\frac{J_0(M^{(n)}/k)}{Y_0(M^{(n)}/k)} = b_1^{++}(M^{(n)}).$$

For completeness, we present the wave functions of the would-be A_5 component, even if we work in the gauge where $A_5 = 0$ together with the constraint $\partial^\mu A_\mu = 0$:

$$A_5(x^\mu, y) = \sum_{n=1}^{\infty} A_5^{(n)}(x^\mu)a_n^{--}(y),$$

with, for $n \geq 1$,

$$a_n^{--}(y) = e^{-\sigma}g_n^{--}(y). \tag{B6}$$

Using the various relations on Bessel function derivatives, one obtains the useful following relation:

$$(\partial_y - 2\sigma')g_n^{--}(y) = -M^{(n)}e^{2\sigma}g_n^{++}(y). \tag{B7}$$

There is also a term $-(\sigma''/\sigma')g_n^{--}$, but this term gives rise to a vanishing contribution when replaced in couplings and

integrated over y because $\sigma'' = 2k[\delta(y) - \delta(y - \pi R_c)]$ and g_n^{--} vanishes at $y = 0, \pi R_c$. One finds also the relation

$$\partial_y g_n^{++}(y) = M^{(n)} g_n^{--}(y). \quad (\text{B8})$$

Equations (B7) and (B8) allow one to recover the differential equations [128]

$$\partial_y \left(\frac{1}{e^{2\sigma}} \partial_y g_n^{++}(y) \right) = -(M^{(n)})^2 g_n^{++}(y) \quad (\text{B9})$$

and [7]

$$-e^{-4\sigma} \partial_y \left(\frac{1}{e^{4\sigma}} \partial_y g_n^{--}(y) \right) - 4k^2 g_n^{--}(y) = (M^{(n)})^2 e^{2\sigma} g_n^{--}(y). \quad (\text{B10})$$

for the unique zero mode and as [defining $\alpha_{L/R}^\pm = |c_{L/R} \pm 1/2|$]

$$f_n^{++}(c_{L/R}; y) = \frac{1}{\sqrt{2\pi R_c}} \frac{e^{2\sigma}}{\mathcal{N}_n} \left[J_{\alpha_{L/R}^+} \left(\frac{m_{L/R}^{(n)} e^\sigma}{k} \right) + b_{\alpha_{L/R}^+}^{++}(m_{L/R}^{(n)}) Y_{\alpha_{L/R}^+} \left(\frac{m_{L/R}^{(n)} e^\sigma}{k} \right) \right], \quad (\text{B14})$$

$$b_{\alpha_{L/R}^+}^{++}(m_{L/R}^{(n)}) = - \frac{[2 - (3/2 - c_{L/R})] J_{\alpha_{L/R}^+}(m_{L/R}^{(n)}/k) + (m_{L/R}^{(n)}/k) J'_{\alpha_{L/R}^+}(m_{L/R}^{(n)}/k)}{[2 - (3/2 - c_{L/R})] Y_{\alpha_{L/R}^+}(m_{L/R}^{(n)}/k) + (m_{L/R}^{(n)}/k) Y'_{\alpha_{L/R}^+}(m_{L/R}^{(n)}/k)},$$

$$f_n^{--}(c_{L/R}; y) = \text{sgn}(y) \frac{1}{\sqrt{2\pi R_c}} \frac{e^{2\sigma}}{\mathcal{N}_n} \left[J_{\alpha_{L/R}^-} \left(\frac{m_{L/R}^{(n)} e^\sigma}{k} \right) + b_{\alpha_{L/R}^-}^{--}(m_{L/R}^{(n)}) Y_{\alpha_{L/R}^-} \left(\frac{m_{L/R}^{(n)} e^\sigma}{k} \right) \right], \quad (\text{B15})$$

$$b_{\alpha_{L/R}^-}^{--}(m_{L/R}^{(n)}) = - \frac{J_{\alpha_{L/R}^-}(m_{L/R}^{(n)}/k)}{Y_{\alpha_{L/R}^-}(m_{L/R}^{(n)}/k)}$$

for KK modes ($n \geq 1$), where $m_{L/R}^{(n)} = m_{\text{KK}}^{(n)}(c_{L/R})$ is the n th KK scalar mass (the KK fermion spectrum is identical as we do not consider Sherk-Schwarz-like mechanisms of SUSY breaking) and \mathcal{N}_n is the normalization constant. At this level, the field redefinition has not been performed for the n th wave functions.

From the above wave function expressions, we deduce the useful relations

$$(\partial_y - (c_{L/R} + \frac{3}{2})\sigma') f_n^{--}(c_{L/R}; y) = -m_{\text{KK}}^{(n)}(c_{L/R}) e^\sigma f_n^{++}(c_{L/R}; y), \quad (\text{B16})$$

$$(\partial_y - (-c_{L/R} + \frac{3}{2})\sigma') f_n^{++}(c_{L/R}; y) = m_{\text{KK}}^{(n)}(c_{L/R}) e^\sigma f_n^{--}(c_{L/R}; y). \quad (\text{B17})$$

Concerning fermions, an example of KK decomposition is (in the two-component notation)

$$\zeta_L(x^\mu, y) = \sum_{n=0}^{\infty} \zeta_L^{(n)}(x^\mu) \omega_n^{++}(c_L; y), \quad (\text{B18})$$

3. Scalar and fermion fields and SUSY breaking

Similarly, the solutions for the wave functions along the fifth dimension of the 5D scalar fields introduced in Appendix A, with KK decomposition

$$\phi_{L/R}(x^\mu, y) = \sum_{n=0}^{\infty} \phi_{L/R}^{(n)}(x^\mu) f_n^{++}(c_{L/R}; y), \quad (\text{B11})$$

$$\phi_{L/R}^c(x^\mu, y) = \sum_{n=1}^{\infty} \phi_{L/R}^{c(n)}(x^\mu) f_n^{--}(c_{L/R}; y), \quad (\text{B12})$$

read as [7]

$$f_0^{++}(c_{L/R}; y) = \sqrt{\frac{k}{2}} \sqrt{\frac{1 - 2c_{L/R}}{1 - e^{-(1-2c_{L/R})k\pi R_c}}} e^{k((1/2) - c_{L/R})(y - \pi R_c)} \quad (\text{B13})$$

$$\chi_L(x^\mu, y) = \sum_{n=1}^{\infty} \chi_L^{(n)}(x^\mu) \omega_n^{--}(c_L; y), \quad (\text{B19})$$

where c_L parametrizes the 5D mass of the Φ_L superfield in Eq. (A11). The wave function $\omega_n^{++}(c_L; y)$ [respectively, $\omega_n^{--}(c_L; y)$] is exactly equal [after the RS field redefinition] to the scalar superpartner wave function $f_n^{++}(c_L; y)$ [respectively, $f_n^{--}(c_L; y)$] as imposed by SUSY. This remains true as long as the SUSY breaking does not occur through the Scherk-Schwarz mechanism. In fact, these scalar wave functions $f_n^{++/--}$ depend on the scalar bulk mass a and boundary mass b , which are imposed by 5D SUSY to be the following functions of the fermionic superpartner bulk mass $c_L \sigma'$ [cf. Eq. (A29)]: $a(c_L) = c_L^2 \pm c_L - 15/4$ and $b(c_L) = 3/2 \mp c_L$ [cf. Eq. (A27)], relations rendering the scalar and fermion wave functions identical in terms of the c_L parameter. Analog remarks hold for the c_R case as well as for the KK masses $m_{\text{KK}}^{(n)}(c_{L/R})$.

A possible SUSY-breaking framework—that we consider in this paper without specifying the underlying

breaking mechanism—is that additional bulk or brane masses arise for the scalar fields, encoded, e.g., in $a(c_L) + \delta a$ and $b(c_L) + \delta b$: These corrective masses spoil the SUSY relations between scalar and fermion bulk or brane masses and in turn break SUSY. It is more convenient for the numerical calculation parts to define, e.g., a new c_L^s parameter for scalars such that $a(c_L) + \delta a = a(c_L^s)$ and $b(c_L) + \delta b = b(c_L^s)$, c_L^s being different from the fermion (or superfield) mass parameter c_L in this framework. Then the fermion wave functions can still be written $\omega_n^{+/-}(c_L; y)$, while the scalar wave functions $f_n^{+/-}(c_L^s; y)$ are now controlled by an independent mass parameter related to the amount of SUSY breaking.

Note that such a SUSY-breaking framework resembles the situation where additional (with respect to the pure 5D SUSY Lagrangian) bulk masses, e.g., $\delta c_L \sigma'$ would appear for fermions. Indeed, the SUSY bulk masses for fermions $c_L \sigma'$ would be shifted to $c_L^f \sigma' = (c_L + \delta c_L) \sigma'$, a new mass independent from the scalar ones depending on $a(c_L)$, $b(c_L)$ [one would deal here with $\omega_n^{+/-}(c_L^f; y)$ and $f_n^{+/-}(c_L; y)$]. This framework would be quantitatively equivalent to the previous one for final physical masses but would lead to an interesting alternative to usual SUSY-breaking frameworks (4D or 5D): Here typically both fermions and their scalar superpartners would be initially heavy (mainly due to their large and identical effective Yukawa couplings generated by equal wave functions), i.e., respecting the lower bounds on scalar masses, while the fermions would become lighter (reduced down to their measured masses) because of the effect of their arising SUSY-breaking bulk masses [$\delta c_{L/R} > 0$] on wave functions.

APPENDIX C: 4D VERSUS 5D PROPAGATORS

For a generic bulk field (expressed in terms of $z = \frac{e^{\sigma(y)}}{k}$)

$$\Phi(x^\mu, z) = \sum_n \phi^{(n)}(x^\mu) S_a^{(n)}(z)$$

satisfying the orthonormalization condition

$$\int_R^{R'} dz \left(\frac{R}{z}\right)^3 S_a^{(n)}(z) S_a^{(m)}(z) = \delta_{nm},$$

the 5D action and the corresponding KK decomposed 4D action are given by

$$\begin{aligned} \mathcal{S}_5 = & -\frac{1}{2} \int d^4x \int_R^{R'} dz \left(\frac{R}{z}\right)^3 \bar{\Phi}(x^\mu, z) \\ & \times \left[\eta^{\mu\nu} \partial_\mu \partial_\nu - \partial_z^2 + \frac{3}{z} \partial_z + \frac{a^2}{z^2} \right] \Phi(x^\mu, z), \end{aligned} \quad (\text{C1})$$

$$\mathcal{S}_4 = -\frac{1}{2} \int d^4x \sum_n \bar{\phi}^{(n)}(x^\mu) (\eta^{\mu\nu} \partial_\mu \partial_\nu + m_n^2) \phi^{(n)}(x^\mu). \quad (\text{C2})$$

The equation of motion reads as

$$\left[-\partial_z^2 + \frac{3}{z} \partial_z + \frac{a^2}{z^2} \right] S_a^{(n)}(z) = m_n^2 S_a^{(n)}(z),$$

and the 2-point functions are defined as follows:

$$\text{From } \mathcal{S}_5: \left[p^2 + \partial_z^2 - \frac{3}{z} \partial_z - \frac{a^2}{z^2} \right] G_5^{S_a}(p^2; z, z') = \delta(z - z'), \quad (\text{C3})$$

$$\text{from } \mathcal{S}_4: [p^2 - m_n^2] G_4^{(n)}(p^2) = 1. \quad (\text{C4})$$

From above, one can find the relation between the 4D and 5D propagators:

$$\begin{aligned} G_5^{S_a}(p^2; z, z') &= \sum_{n=0}^{\infty} G_4^{(n)}(p^2) S_a^{(n)}(z) S_a^{(n)}(z') \\ &= \sum_{n=0}^{\infty} \frac{S_a^{(n)}(z) S_a^{(n)}(z')}{p^2 - m_n^2} \end{aligned} \quad (\text{C5})$$

$$= \frac{S_a^{(0)}(z) S_a^{(0)}(z')}{p^2} + \sum_{n \geq 1} \frac{S_a^{(n)}(z) S_a^{(n)}(z')}{p^2 - m_n^2}. \quad (\text{C6})$$

Indeed, one can check that

$$\begin{aligned} & \left[p^2 + \partial_z^2 - \frac{3}{z} \partial_z - \frac{a^2}{z^2} \right] G_5^{S_a}(p^2; z, z') \\ &= \left[p^2 + \partial_z^2 - \frac{3}{z} \partial_z - \frac{a^2}{z^2} \right] \sum_n G_4^{(n)}(p^2) S_a^{(n)}(z) S_a^{(n)}(z') \\ &= \sum_n G_4^{(n)}(p^2) \left[p^2 + \partial_z^2 - \frac{3}{z} \partial_z - \frac{a^2}{z^2} \right] S_a^{(n)}(z) S_a^{(n)}(z') \\ &= \sum_n G_4^{(n)}(p^2) [p^2 - m_n^2] S_a^{(n)}(z) S_a^{(n)}(z') \\ &= \sum_n S_a^{(n)}(z) S_a^{(n)}(z') = \delta(z - z'). \end{aligned} \quad (\text{C7})$$

[1] L. Randall and R. Sundrum, *Phys. Rev. Lett.* **83**, 3370 (1999); see also M. Gogberashvili, *Int. J. Mod. Phys. D* **11**, 1635 (2002).

[2] The RS scenarios with a fundamental Higgs boson on the so-called TeV-brane, the alternative models of gauge-Higgs unification [3], and the Higgsless models [4] can be thought of as warped extra-dimension models constituting dual descriptions—through the

AdS/CFT correspondence [5]—of four-dimensional (4D) strongly coupled gauge theories (in the limit of a large number of colors) predicting the effective Higgs scalar field as a composite state (see, e.g., Ref. [6]).

[3] See, e.g., M. Carena, E. Ponton, J. Santiago, and C. E. M. Wagner, *Nucl. Phys.* **B759**, 202 (2006); *Phys. Rev. D* **76**, 035006 (2007).

- [4] C. Csáki, C. Grojean, H. Murayama, L. Pilo, and J. Terning, *Phys. Rev. D* **69**, 055006 (2004); C. Csáki, C. Grojean, L. Pilo, and J. Terning, *Phys. Rev. Lett.* **92**, 101802 (2004); G. Cacciapaglia, C. Csáki, C. Grojean, and J. Terning, *Phys. Rev. D* **70**, 075014 (2004).
- [5] J. M. Maldacena, *Adv. Theor. Math. Phys.* **2**, 231 (1998); *Int. J. Theor. Phys.* **38**, 1113 (1999); S. S. Gubser, I. R. Klebanov, and A. M. Polyakov, *Phys. Lett. B* **428**, 105 (1998); E. Witten, *Adv. Theor. Math. Phys.* **2**, 253 (1998); N. Arkani-Hamed, M. Porrati, and L. Randall, *J. High Energy Phys.* **08** (2001) 017.
- [6] R. Contino, Y. Nomura, and A. Pomarol, *Nucl. Phys.* **B671**, 148 (2003); K. Agashe, R. Contino, and A. Pomarol, *Nucl. Phys.* **B719**, 165 (2005); K. Agashe and R. Contino, *Nucl. Phys.* **B742**, 59 (2006); R. Contino, L. Da Rold, and A. Pomarol, *Phys. Rev. D* **75**, 055014 (2007).
- [7] T. Gherghetta and A. Pomarol, *Nucl. Phys.* **B586**, 141 (2000).
- [8] I. Antoniadis, *Phys. Lett. B* **246**, 377 (1990); G. Dvali and M. Shifman, *Nucl. Phys.* **B504**, 127 (1997).
- [9] A. Delgado and M. Quirós, *Nucl. Phys.* **B607**, 99 (2001).
- [10] For lecture notes, see M. Quirós, [arXiv:hep-ph/0302189](https://arxiv.org/abs/hep-ph/0302189)
- [11] E. A. Mirabelli and M. E. Peskin, *Phys. Rev. D* **58**, 065002 (1998); W. D. Goldberger, Y. Nomura, and D. R. Smith, *Phys. Rev. D* **67**, 075021 (2003); H. P. Nilles, in *Supersymmetry, Supergravity and Supercolliders*, edited by J. A. Bagger (World Scientific, Singapore, 1997).
- [12] It has been shown recently that, in the limit of an infinite Majorana mass term on the infrared brane [13], the gaugino mediation mechanism through the bulk is comparable to a SUSY breaking with twisted boundary conditions.
- [13] S. Abel and T. Gherghetta, *J. High Energy Phys.* **12** (2010) 091.
- [14] T. Gherghetta and A. Pomarol, *Nucl. Phys.* **B602**, 3 (2001).
- [15] J. Scherk and J. H. Schwarz, *Phys. Lett.* **82B**, 60 (1979); *Nucl. Phys.* **B153**, 61 (1979).
- [16] I. Antoniadis, *Phys. Lett. B* **246**, 377 (1990).
- [17] E. Dudas and C. Grojean, *Nucl. Phys.* **B507**, 553 (1997).
- [18] In this context of extra dimensions, other new scenarios of SUSY breaking have arisen [8].
- [19] J. Casas, J. R. Espinosa, and I. Navarro, *Nucl. Phys.* **B620**, 195 (2002); R. C. Myers and O. Tafjord, *J. High Energy Phys.* **11** (2001) 009.
- [20] C. Schmidhuber, *Nucl. Phys.* **B585**, 385 (2000); **B619**, 603 (2001).
- [21] K. R. Dienes, E. Dudas, and T. Gherghetta, *Phys. Lett. B* **436**, 55 (1998); *Nucl. Phys.* **B537**, 47 (1999).
- [22] P. K. Townsend, *Phys. Rev. D* **15**, 2802 (1977); S. Deser and B. Zumino, *Phys. Rev. Lett.* **38**, 1433 (1977).
- [23] E. Shuster, *Nucl. Phys.* **B554**, 198 (1999).
- [24] J. A. Bagger, D. Nemeschansky, and R.-J. Zhang, *J. High Energy Phys.* **08** (2001) 057; M. Eto, N. Maru, and N. Sakai, *Phys. Rev. D* **70**, 086002 (2004); J. A. Bagger and M. Redi, *J. High Energy Phys.* **04** (2004) 031; N. Maru and N. Okada, *Phys. Rev. D* **70**, 025002 (2004); [arXiv:hep-th/0408182](https://arxiv.org/abs/hep-th/0408182); [arXiv:hep-th/0508113](https://arxiv.org/abs/hep-th/0508113); S. Ichinose and A. Murayama, *Phys. Lett. B* **625**, 106 (2005); H. Davoudiasl and E. Ponton, *J. High Energy Phys.* **10** (2010) 102.
- [25] R. Altendorfer, J. A. Bagger, and D. Nemeschansky, *Phys. Rev. D* **63**, 125025 (2001); N. Alonso-Alberca, P. Meessen, and T. Ortin, *Phys. Lett. B* **482**, 400 (2000).
- [26] M. A. Luty and R. Sundrum, *Phys. Rev. D* **65**, 066004 (2002); Z. Lalak and R. Matyszkiewicz, [arXiv:hep-th/0211043](https://arxiv.org/abs/hep-th/0211043); P. Brax and N. Chatillon, *J. High Energy Phys.* **12** (2003) 026; J. A. Bagger and M. Redi, *Phys. Lett. B* **582**, 117 (2004); K. Choi, D. Y. Kim, I.-W. Kim, and T. Kobayashi, *Eur. Phys. J. C* **35**, 267 (2004); L. J. Hall, Y. Nomura, T. Okui, and S. J. Oliver, *Nucl. Phys.* **B677**, 87 (2004); N. Maru, N. Sakai, and N. Uekusa, *Phys. Rev. D* **74**, 045017 (2006); A. Katz, M. Redi, Y. Shadmi, and Y. Shirman, *J. High Energy Phys.* **06** (2006) 048; M. Gabella, T. Gherghetta, and J. Giedt, *Phys. Rev. D* **76**, 055001 (2007); H. Abe and Y. Sakamura, *J. High Energy Phys.* **03** (2007) 106; M. R. Douglas, J. Shelton, and G. Torroba, [arXiv:0704.4001](https://arxiv.org/abs/hep-th/07044001); C. P. Burgess *et al.*, *J. High Energy Phys.* **04** (2008) 053; N. Uekusa, *Mod. Phys. Lett. A* **23**, 603 (2008); F. Benini *et al.*, *J. High Energy Phys.* **12** (2009) 031.
- [27] A. Pomarol, *Phys. Rev. Lett.* **85**, 4004 (2000); W. D. Goldberger, Y. Nomura, and D. R. Smith, *Phys. Rev. D* **67**, 075021 (2003); Y. Nomura and D. R. Smith, *Phys. Rev. D* **68**, 075003 (2003); K.-W. Choi, H. Do Kim, and I.-W. Kim, *J. High Energy Phys.* **03** (2003) 034; H.-Y. Guo, C.-G. Huang, Z. Xu, and B. Zhou, *Phys. Lett. A* **331**, 1 (2004); O. Saremi and A. W. Peet, *Phys. Rev. D* **70**, 026008 (2004); Y. Nomura and D. Tucker-Smith, *Nucl. Phys.* **B698**, 92 (2004); Y. Nomura, D. Tucker-Smith, and B. Tweedie, *Phys. Rev. D* **71**, 075004 (2005); T. Gherghetta, *Phys. Rev. D* **71**, 065001 (2005).
- [28] A. Falkowski, Z. Lalak, and S. Pokorski, *Phys. Lett. B* **491**, 172 (2000); **509**, 337 (2001); T. Gherghetta and A. Pomarol, *Phys. Lett. B* **536**, 277 (2002); Z. Lalak and R. Matyszkiewicz, [arXiv:hep-th/0310161](https://arxiv.org/abs/hep-th/0310161); J. A. Bagger and D. V. Belyaev, *J. High Energy Phys.* **06** (2003) 013; T. Gregoire, R. Rattazzi, C. A. Scrucca, A. Strumia, and E. Trincherini, *Nucl. Phys.* **B720**, 3 (2005).
- [29] J. E. Kim and B. Kyae, *Phys. Lett. B* **500**, 313 (2001); M. A. Luty and R. Sundrum, *Phys. Rev. D* **64**, 065012 (2001); M. A. Luty, *Phys. Rev. Lett.* **89**, 141801 (2002); P. Salgado, S. del Campo, and M. Cataldo, *Phys. Rev. D* **68**, 024021 (2003); H. Abe, T. Kobayashi, N. Maru, and K. Yoshioka, *Phys. Rev. D* **67**, 045019 (2003); J. A. Bagger and D. V. Belyaev, *Phys. Rev. D* **67**, 025004 (2003); K. Choi, D. Y. Kim, I.-W. Kim, and T. Kobayashi, [arXiv:hep-ph/0301131](https://arxiv.org/abs/hep-ph/0301131); Z. Lalak and R. Matyszkiewicz, *Phys. Lett. B* **562**, 347 (2003); **583**, 364 (2004); J.-P. Derendinger, C. Kounnas, and F. Zwirner, *Nucl. Phys.* **B691**, 233 (2004); H.-S. Goh, M. A. Luty, and S.-P. Ng, *J. High Energy Phys.* **01** (2005) 040; R. Sundrum, *J. High Energy Phys.* **01** (2011) 062; C. Csáki, Y. Shirman, and J. Terning, [arXiv:1106.3074](https://arxiv.org/abs/1106.3074); J. A. Bagger and C. Xiong, [arXiv:1105.4852](https://arxiv.org/abs/1105.4852).
- [30] T. Gherghetta, [arXiv:hep-ph/0601213](https://arxiv.org/abs/hep-ph/0601213); [arXiv:1008.2570](https://arxiv.org/abs/1008.2570).
- [31] P. Breitenlohner and D. Z. Freedman, *Phys. Lett.* **115B**, 197 (1982); L. Mezincescu, P. K. Townsend, and P. van Nieuwenhuizen, *Phys. Lett.* **143B**, 384 (1984); Y. Igarashi and T. Nonoyama, *Phys. Rev. D* **34**, 1928 (1986);

- D. Z. Freedman, S. S. Gubser, K. Pilch, and N. P. Warner, *Adv. Theor. Math. Phys.* **3**, 363 (1999); M. Blau, *J. High Energy Phys.* **11** (2000) 023; K. Behrndt and M. Cvetič, *Phys. Rev. D* **61**, 101901 (2000); E. Bergshoeff, R. Kallosh, and A. Van Proeyen, *Fortschr. Phys.* **49**, 625 (2001); V. Balasubramanian, E. G. Gimon, D. Minic, and J. Rahmfeld, *Phys. Rev. D* **63**, 104009 (2001); M. Zucker, *Phys. Rev. D* **64**, 024024 (2001); T. Kugo and K. Ohashi, *Prog. Theor. Phys.* **108**, 203 (2002); H. Abe and Y. Sakamura, *J. High Energy Phys.* **10** (2004) 013; F. P. Correia, M. G. Schmidt, and Z. Tavartkiladze, *Nucl. Phys.* **B709**, 141 (2005); R. S. Garavuso, *Nucl. Phys.* **B750**, 73 (2006); O. Miskovic, R. Troncoso, and J. Zanelli, *Phys. Lett. B* **637**, 317 (2006); J. P. Gauntlett and O. Varela, *Phys. Rev. D* **76**, 126007 (2007); O. A. P. Mac Conamhna and E. Ó Colgáin, *J. High Energy Phys.* **03** (2007) 115; R. S. Garavuso and F. Toppan, *Nucl. Phys.* **B796**, 320 (2008); A. J. Amsel and G. Compère, *Phys. Rev. D* **79**, 085006 (2009); A. J. Amsel and D. Marolf, *Classical Quantum Gravity* **26**, 025010 (2009).
- [32] B. de Wit and I. Herger, *Lect. Notes Phys.* **541**, 79 (2000); E. D'Hoker and D. Z. Freedman, arXiv:hep-th/0201253.
- [33] H. Verlinde, *Nucl. Phys.* **B580**, 264 (2000); A. Bacchetta and P. J. Mulders, *Phys. Rev. D* **62**, 114004 (2000); E. Bergshoeff, R. Kallosh, and A. Van Proeyen, *J. High Energy Phys.* **10** (2000) 033; M. Cvetič *et al.*, *Nucl. Phys.* **B605**, 141 (2001); J. R. Pelaez and A. G. Nicola, *AIP Conf. Proc.* **602**, 34 (2001); M. J. Duff, J. T. Liu, and K. S. Stelle, *J. Math. Phys. (N.Y.)* **42**, 3027 (2001); R. N. Faustov and A. P. Martynenko, *Yad. Fiz.* **65**, 291 (2002) [*Phys. At. Nucl.* **65**, 265 (2002)]; T. W. Kephart and H. Päs, *Phys. Rev. D* **70**, 086009 (2004); G. A. Diamandis, B. C. Georgalas, P. Kouroumalou, and A. B. Lahanas, *Phys. Lett. B* **602**, 112 (2004); F. Marchesano, P. McGuirk, and G. Shiu, *J. High Energy Phys.* **04** (2009) 095.
- [34] I. R. Klebanov and M. J. Strassler, *J. High Energy Phys.* **08** (2000) 052.
- [35] S. B. Giddings, S. Kachru, and J. Polchinski, *Phys. Rev. D* **66**, 106006 (2002).
- [36] S. Kachru, R. Kallosh, A. D. Linde, and S. P. Trivedi, *Phys. Rev. D* **68**, 046005 (2003).
- [37] J. A. Strathdee, *Int. J. Mod. Phys. A* **2**, 273 (1987).
- [38] We use a $N = 1$ 4D superfield formalism as in Ref. [39].
- [39] D. Martí and A. Pomarol, *Phys. Rev. D* **64**, 105025 (2001).
- [40] E. Sharpe, *Nucl. Phys.* **B523**, 211 (1998).
- [41] M. McGarrie and R. Russo, *Phys. Rev. D* **82**, 035001 (2010); M. McGarrie and D. C. Thompson, *Phys. Rev. D* **82**, 125034 (2010); S. Ichinose and A. Murayama, arXiv:hep-th/0606167.
- [42] A. Delgado, G. v. Gersdorff, P. John, and M. Quirós, *Phys. Lett. B* **517**, 445 (2001); G. Grignani, M. Orselli, and G. W. Semenoff, *J. High Energy Phys.* **07** (2001) 004.
- [43] G. Bhattacharyya, S. K. Majee, and A. Raychaudhuri, *Nucl. Phys.* **B793**, 114 (2008); G. Bhattacharyya, S. K. Majee, and T. S. Ray, *Phys. Rev. D* **78**, 071701 (2008); G. Bhattacharyya and T. S. Ray, *J. High Energy Phys.* **05** (2010) 040.
- [44] J. L. Hewett and D. Sadri, *Phys. Rev. D* **69**, 015001 (2004).
- [45] Let us insist on the fact that there exists a wide variety of 5D warped SUSY models and we claim here *only* that there are possible experimental tests for distinguishing between a uniquely defined 5D warped SUSY model—the RS MSSM with bulk SUSY-breaking sfermion masses and brane-Higgs bosons—and the 4D MSSM.
- [46] “Minimal” here means that the SUSY-breaking masses and couplings are universal at the GUT scale.
- [47] Strictly speaking, $\tilde{\mu}_{1,2}$ denote the two lightest mass eigenstates which are generally mainly composed of the left and right [with respect to gauge group $SU(2)_L$] smuon zero modes, while the heavier eigenstates are mainly made of their KK modes.
- [48] H. P. Nilles, *Phys. Rep.* **110**, 1 (1984).
- [49] No deep modifications are expected for the branching ratios of the lightest neutral Higgs boson h , since its decays into two squarks or sleptons ($\tilde{q}/\tilde{\ell}$) are kinematically closed due to the upper theoretical mass bound on m_h GeV combined with the lower direct experimental bounds $m_{\tilde{q}/\tilde{\ell}} \gtrsim 10^2$ GeV [50].
- [50] Particle Data Group, *Phys. Lett. B* **667**, 1 (2008); *J. Phys. G* **37**, 075021 (2010).
- [51] A. Delgado and M. Quirós, *Phys. Lett. B* **484**, 355 (2000).
- [52] A. Deandrea, P. Hosteins, M. Oertel, and J. Welzel, *Phys. Rev. D* **75**, 113005 (2007).
- [53] K. R. Dienes, E. Dudas, and T. Gherghetta, *Phys. Lett. B* **436**, 55 (1998); *Nucl. Phys.* **B537**, 47 (1999); G. Altarelli and F. Feruglio, *Phys. Lett. B* **511**, 257 (2001); G. Bhattacharyya and K. Sridhar, *J. Phys. G* **29**, 993 (2003); Y. Nomura, D. Poland, and B. Tweedie, *J. High Energy Phys.* **12** (2006) 002.
- [54] F. Brümmer, S. Fichtel, A. Hebecker, and S. Kraml, *J. High Energy Phys.* **08** (2009) 011; F. Brümmer, S. Fichtel, S. Kraml, and R. K. Singh, *J. High Energy Phys.* **08** (2010) 096.
- [55] M. Redi and B. Gripaios, *J. High Energy Phys.* **08** (2010) 116.
- [56] A. Knochel and T. Ohl, *Phys. Rev. D* **78**, 045016 (2008); **81**, 036013 (2010); A. Knochel, arXiv:1005.2103.
- [57] M. Masip and I. Mastromatteo, *Phys. Rev. D* **73**, 015007 (2006).
- [58] A. Djouadi and S. Rosier-Lees, arXiv:hep-ph/9901246.
- [59] S. J. Huber and Q. Shafi, *Phys. Lett. B* **498**, 256 (2001); **512**, 365 (2001); **544**, 295 (2002); **583**, 293 (2004); S. Chang *et al.*, *Phys. Rev. D* **73**, 033002 (2006); G. Moreau and J. I. Silva-Marcos, *J. High Energy Phys.* **01** (2006) 048; **03** (2006) 090; K. Agashe *et al.*, *Phys. Rev. D* **71**, 016002 (2005); *Phys. Rev. Lett.* **93**, 201804 (2004); *Phys. Rev. D* **75**, 015002 (2007); **74**, 053011 (2006).
- [60] T. Lari *et al.*, *Eur. Phys. J. C* **57**, 183 (2008); M. Raidal *et al.*, *Eur. Phys. J. C* **57**, 13 (2008).
- [61] We will not discuss the type of possibility suggested in Ref. [62], which is characteristic of the Scherk-Schwarz mechanism not considered here. A related approach based on twisted BC for the Higgs fields was proposed in Ref. [63].
- [62] A. Delgado, A. Pomarol, and M. Quirós, *Phys. Rev. D* **60**, 095008 (1999).
- [63] T. Gherghetta and A. Pomarol, *Phys. Rev. D* **67**, 085018 (2003).

- [64] We use the conventional notations for the pMSSM Higgs scalar fields: $\phi_{H^0} = (v_{u/d} + \phi_{h^0} + i\phi_{p^0})/\sqrt{2}$ (ϕ_{p^0} denoting the pseudoscalars) with $\tan\beta = v_{u/d}/v_d$ and the squared VEV given by $v^2 = v_u^2 + v_d^2 \simeq (246 \text{ GeV})^2$.
- [65] M. Drees and K. Hagiwara, *Phys. Rev. D* **42**, 1709 (1990).
- [66] A. Djouadi, *Phys. Rep.* **459**, 1 (2008).
- [67] C. Csáki *et al.*, *Phys. Rev. D* **66**, 064021 (2002); G. Burdman, *Phys. Rev. D* **66**, 076003 (2002); J. Hewett, F. Petriello, and T. Rizzo, *J. High Energy Phys.* **09** (2002) 030.
- [68] C. Bouchart and G. Moreau, *Nucl. Phys.* **B810**, 66 (2009); *Phys. Rev. D* **80**, 095022 (2009); A. Djouadi, G. Moreau, and F. Richard, *Nucl. Phys.* **B773**, 43 (2007).
- [69] K. Agashe, A. Delgado, M.J. May, and R. Sundrum, *J. High Energy Phys.* **08** (2003) 050; A. Delgado and A. Falkowski, *J. High Energy Phys.* **05** (2007) 097.
- [70] Note that the $\phi_L^{c(n)}$ fields, whose presence reflects the vectorial aspect of the 5D theory (like for the $\Sigma^{(n)}$ fields), enter indirectly—via some exchanges—the couplings in the 4D chiral Lagrangian.
- [71] The 5D Yukawa coupling constant \mathcal{Y} has dimension -1 in energy for the simplified scheme with $\hbar = c = 1$, while \mathcal{Y}_{4D} is dimensionless.
- [72] A. Abada, C. Biggio, F. Bonnet, M.B. Gavela, and T. Hambye, *J. High Energy Phys.* **12** (2007) 061.
- [73] Note that taking purely real wave functions and Yukawa coupling constants simplifies the approach by avoiding a *bi-diagonalization*, as it renders the mass matrix fully real and symmetric.
- [74] G. Moreau, *Eur. Phys. J. C* **40**, 539 (2005).
- [75] D. Ghilencea and H.P. Nilles, *Phys. Lett. B* **507**, 327 (2001); E.M. Prodanov, *Phys. Lett. B* **530**, 210 (2002).
- [76] H. Do Kim, [arXiv:hep-ph/0106072](https://arxiv.org/abs/hep-ph/0106072); B. Morariu and A.P. Polychronakos, *J. High Energy Phys.* **07** (2001) 006.
- [77] I. Antoniadis, S. Dimopoulos, A. Pomarol, and M. Quirós, *Nucl. Phys.* **B544**, 503 (1999); A. Delgado, A. Pomarol, and M. Quirós, *Phys. Rev. D* **60**, 095008 (1999); N. Arkani-Hamed, L.J. Hall, Y. Nomura, D. Smith, and N. Weiner, *Nucl. Phys.* **B605**, 81 (2001); R. Barbieri, L.J. Hall, and Y. Nomura, *Phys. Rev. D* **63**, 105007 (2001).
- [78] In fact, within our approach we do not have to make *abnormally* an infinite KK summation before a loop integration.
- [79] T. Kobayashi and H. Terao, *Prog. Theor. Phys.* **107**, 785 (2002); Sunil Mukhi, *Pramana* **58**, 21 (2002).
- [80] The approach developed in Ref. [42] also shows that the Higgs mass corrections at higher order (two loops) potentially give rise to linear divergences which are in fact cancelled by linear threshold effects of Yukawa and gauge couplings [81].
- [81] A. Delgado, G.V. Gersdorff, and M. Quirós, *Nucl. Phys.* **B613**, 49 (2001); M. Giovannini, *Phys. Rev. D* **64**, 124004 (2001).
- [82] Hence, our approach to the cutoff problem (with respect to divergence cancellations) is different from Refs. [42,79]: We do not deal with the kind of cutoff that is applied, but instead we justify why this cutoff must not be applied systematically on KK sums.
- [83] R. Contino and L. Pilo, *Phys. Lett. B* **523**, 347 (2001); T. Fujita and K. Ohashi, *Prog. Theor. Phys.* **106**, 221 (2001); A. Masiero, C.A. Scrucca, M. Serone, and L. Silvestrini, *Phys. Rev. Lett.* **87**, 251601 (2001); A. Nayeri and A. Reynolds, [arXiv:hep-ph/0107201](https://arxiv.org/abs/hep-ph/0107201); V. Di Clemente, S.F. King, and D.A.J. Rayner, *Nucl. Phys.* **B617**, 71 (2001).
- [84] K. Goeke, M.V. Polyakov, and M. Vanderhaeghen, *Prog. Part. Nucl. Phys.* **47**, 401 (2001); R. Emparan, D. Mateos, and P. Townsend, *J. High Energy Phys.* **07** (2001) 011; T. Ueda, T. Uematsu, and K. Sasaki, *Phys. Lett. B* **640**, 188 (2006); E. Álvarez and A.F. Faedo, *Phys. Rev. D* **74**, 124029 (2006); G.F. Giudice, R. Rattazzi, and J.D. Wells, *Nucl. Phys.* **B630**, 293 (2002); R. Contino and A. Gambassi, *J. Math. Phys. (N.Y.)* **44**, 570 (2003).
- [85] S.L. Adler and W.A. Bardeen, *Phys. Rev.* **182**, 1517 (1969); R. Jackiw, *Lectures on Current Algebra and its Applications* (Princeton University, Princeton, NJ, 1972).
- [86] A. Djouadi, G. Moreau, and R.K. Singh, *Nucl. Phys.* **B797**, 1 (2008).
- [87] T. Hirayama and K. Yoshioka, *J. High Energy Phys.* **01** (2004) 032.
- [88] C.T. Hill, *Phys. Rev. D* **73**, 085001 (2006); P. Anastasopoulos, M. Bianchi, E. Dudas, and E. Kiritsis, *J. High Energy Phys.* **11** (2006) 057.
- [89] B. Gripaos, *Phys. Lett. B* **663**, 419 (2008).
- [90] This Chern-Simons term has anyway no effects on the quadratic divergences of the Higgs mass.
- [91] See, e.g., L. Senatore, *Phys. Rev. D* **71**, 103510 (2005); D.A. Demir, [arXiv:hep-ph/0410056](https://arxiv.org/abs/hep-ph/0410056).
- [92] A. Djouadi, *Phys. Lett. B* **435**, 101 (1998).
- [93] KK contributions to this gluon-gluon-fusion mechanism have been studied, e.g., in Ref. [94].
- [94] A. Djouadi and G. Moreau, *Phys. Lett. B* **660**, 67 (2008).
- [95] L. Scodellaro (CDF and D0 Collaboration), [arXiv:0905.2554](https://arxiv.org/abs/0905.2554).
- [96] Tevatron New Phenomena, Higgs working group, for the CDF Collaboration, and D0 Collaboration, [arXiv:0903.4001](https://arxiv.org/abs/0903.4001).
- [97] J. Baglio and A. Djouadi, *Phys. Lett. B* **699**, 372 (2011).
- [98] J.-M. Frère, D.R.T. Jones, and S. Raby, *Nucl. Phys.* **B222**, 11 (1983); L. Alvarez-Gaumé, J. Polchinski, and M. Wise, *Nucl. Phys.* **B221**, 495 (1983); M. Claudson, L. Hall, and I. Hinchliffe, *Nucl. Phys.* **B228**, 501 (1983).
- [99] U. Ellwanger and C. Hugonie, *Phys. Lett. B* **457**, 299 (1999).
- [100] H. Komatsu, *Phys. Lett. B* **215**, 323 (1988).
- [101] A. Strumia, *Nucl. Phys.* **B482**, 24 (1996); T. Falk, K.A. Olive, L. Koszkowski, A. Singh, and M. Srednicki, *Phys. Lett. B* **396**, 50 (1997).
- [102] CDF and D0 experiment Web pages: <http://www-cdf.fnal.gov/> and <http://www-d0.fnal.gov/>.
- [103] See last results and references at <http://lepewwg.web.cern.ch/LEPEWWG/>.
- [104] *ATLAS Detector and Physics Performance*, Technical Design Report, Vol. II, 1999; *Physics Performance*, CMS Physics TDR: Vol. II (PTDR2), 2006.
- [105] We use the standard renormalization group equation evolution to the weak scale at one loop for the studied smuon masses.
- [106] CMS Collaboration, *Phys. Lett. B* **698**, 196 (2011); ATLAS Collaboration, *Phys. Rev. Lett.* **106**, 131802 (2011); *Phys. Lett. B* **701**, 186 (2011); [arXiv:1103.6214](https://arxiv.org/abs/1103.6214); Report No. ATLAS-CONF-2011-039; Report

- No. ATLAS-CONF-2011-064; Report No. ATLAS-CONF-2011-086.
- [107] More precisely, we will take only $\tan\beta = 6$ and $\tan\beta = 30$ in order to illustrate the main characteristic behaviors.
- [108] The mass constraints obtained recently at the LHC in non-SUGRA scenarios assume specific conditions [109], like a gravitino LSP [110], a gluino mass smaller than [111] or equal [112] to squark ones, that we do not assume here.
- [109] ATLAS Collaboration, [arXiv:1103.6208](https://arxiv.org/abs/1103.6208).
- [110] CMS Collaboration, [arXiv:1103.0953](https://arxiv.org/abs/1103.0953).
- [111] ATLAS Collaboration, [arXiv:1103.4344](https://arxiv.org/abs/1103.4344).
- [112] CMS Collaboration, *J. High Energy Phys.* **06** (2011) 093.
- [113] A. Bartl *et al.*, *Eur. Phys. J. direct C* **2**, 6 (2000).
- [114] FCNC and EW precision tests constrain such masses from below.
- [115] Strictly speaking, $m_{(-+)}^{(1)}(c_t)$ is the mass of the first KK mode with $(-+)$ [and $(+-)$] BC.
- [116] For scalar fields, the $\tilde{t}-\tilde{t}'$ mass mixing terms come from the μ and A mass terms.
- [117] Those low masses could maybe even be excluded by FCNC and EW precision constraints.
- [118] F. Richard (private communication).
- [119] Maybe even KK gaugino effects or KK top mixings.
- [120] K. Agashe *et al.*, *Phys. Rev. D* **77**, 015003 (2008); B. Lillie, J. Shu, and T.M.P. Tait, *Phys. Rev. D* **76**, 115016 (2007); B. Lillie, L. Randall and L.-T. Wang, *J. High Energy Phys.* **09** (2007) 074; M. Guchait, F. Mahmoudi, and K. Sridhar, *Phys. Lett. B* **666**, 347 (2008); A. Djouadi, G. Moreau, and R.K. Singh, *Nucl. Phys.* **B797**, 1 (2008).
- [121] K. Agashe *et al.*, *Phys. Rev. D* **81**, 096002 (2010); **80**, 075007 (2009); **76**, 115015 (2007); F. Ledroit, G. Moreau, and J. Morel, *J. High Energy Phys.* **09** (2007) 071.
- [122] E. De Pree and M. Sher, *Phys. Rev. D* **73**, 095006 (2006).
- [123] J. L. Feng and D. E. Finnell, *Phys. Rev. D* **49**, 2369 (1994).
- [124] N. Marcus, A. Sagnotti, and W. Siegel, *Nucl. Phys.* **B224**, 159 (1983).
- [125] N. Arkani-Hamed, T. Gregoire, and J. Wacker, *J. High Energy Phys.* **03** (2002) 055; A. Hebecker, *Nucl. Phys.* **B632**, 101 (2002).
- [126] Note that L/R would be seen as a gauge index within the pMSSM, corresponding to a doublet or singlet under $SU(2)_L$.
- [127] A. Falkowski, *Phys. Rev. D* **77**, 055018 (2008).
- [128] S. Chang *et al.*, *Phys. Rev. D* **62**, 084025 (2000).